Science and Technology of Nuclear Installations

Lessons Learned from the Fukushima Accident: An Integrated Perspective

Guest Editors: Inn Seock Kim, Akira Omoto, Enrico Zio, Joon-Eon Yang, and Yanko Yanev

Lessons Learned from the Fukushima Accident: An Integrated Perspective

Science and Technology of Nuclear Installations

Lessons Learned from the Fukushima Accident: An Integrated Perspective

Guest Editors: Inn Seock Kim, Akira Omoto, Enrico Zio, Joon-Eon Yang, and Yanko Yanev

Editorial Board

Contents

Hindawi Publishing Corporation
Science and Technology of Nuclear Installations
Volume 2014, Article ID 213919, 2 pages
http://dx.doi.org/10.1155/2014/213919

Editorial

Lessons Learned from the Fukushima Accident: An Integrated Perspective

Inn Seock Kim,[1] Akira Omoto,[2] Enrico Zio,[3] Joon-Eon Yang,[4] and Yanko Yanev[5]

[1] *ISSA Technology, Germantown, MD 20876, USA*
[2] *Tokyo Institute of Technology, Tokyo, Japan*
[3] *Ecole Centrale Paris and Supelec and Energy Department, Polytechnic University of Milan, Milan, Italy*
[4] *Korea Atomic Energy Research Institute, Daejeon, Republic of Korea*
[5] *Nuclear Knowledge Management Institute, Gersthofer Straße, 1180 Vienna, Austria*

Correspondence should be addressed to Inn Seock Kim; isk@issatechinc.com

Received 17 July 2014; Accepted 17 July 2014; Published 23 July 2014

The unprecedented damage and radiological release at the Fukushima Dai-ichi Nuclear Power Station, which were brought about by the extreme natural disaster including earthquake and subsequent tsunami, exposed a number of potential nuclear plant vulnerabilities. This special issue is aimed at the lessons learned from the Fukushima accident of March 11, 2011, in Japan so that they can be applied to further improve nuclear plant safety.

Management of nuclear plant safety, that is, "safety management," can be accomplished through an integrated approach consisting of three elements: (1) by managing risk before an accident occurs, that is, risk management; (2) by preventing an abnormality from escalating into an accident or mitigating the consequence of an accident, that is, accident management; and (3) by minimizing the impacts of the radiological accident on the public, critical social infrastructures, and environment, that is, emergency management. The articles included in this special issue can also be viewed from a perspective of safety management in the light of the lessons from the Fukushima accident.

The articles by S. Park et al. and J.-Y. Kim et al. address the element of "risk management." The former shows a novel approach to prioritize accident precursors using the techniques of analytic hierarchy process (AHP) and Bayesian belief network (BBN). A case study was conducted by applying this approach to the Fukushima lessons as identified in the accident analysis report by the Korean Nuclear Society. The latter article analyzes the anomalous behavior of fuel pellets and claddings following loss of coolant accidents (LOCAs) under various conditions, such as partial malfunctions of control rods resulting in different levels of heat generation and failure of the emergency core cooling system (ECCS).

The element of "accident management" is touched upon by four articles, including a couple by S.-W. Lee et al. The first article by S.-W. Lee et al. discusses the coping capability of APR1400 pressurized water nuclear power plants against an extended station blackout as experienced during the Fukushima accident, demonstrating the effectiveness of an external water injection strategy for steam generators. Another article by S.-W. Lee et al. investigates the effectiveness of a mitigating strategy to maintain containment integrity against overpressurization scenarios in a 1000 MWe PWR with large dry containment by use of a containment filtered venting system (CFVS).

As reliable information is essential for accident management, the article by M. Yoo et al. discusses the result of their pioneering research to develop an instrument transmitter protecting device against high-temperature condition during severe accidents. M. C. Kim reviews the beyond design basis events (BDBEs) at Fukushima with a focus on the accident information and systems operation, emphasizing the need for implementation of mitigating strategies to cope with BDBEs in a cost-effective manner, together with reliable information under harsh environment and development of operator support systems for extreme events.

Finally, "emergency management," which is oftentimes viewed as the last defense barrier among the three elements of safety management, is addressed by M. Hussain et al. in an article on intervention distances for urgent protective actions.

We believe that this special issue provides interesting information on each element of safety management but, even more, it points to the fact that more research is needed for further enhancement of nuclear safety especially against beyond-design basis accidents from external events.

As a final remark, we would like to acknowledge the outstanding contributions of all the authors and the accurate and timely collaboration of both the authors and the reviewers. To all of them goes our sincere professional appreciation and personal gratitude.

Inn Seock Kim
Akira Omoto
Enrico Zio
Joon-Eon Yang
Yanko Yanev

Hindawi Publishing Corporation
Science and Technology of Nuclear Installations
Volume 2014, Article ID 841895, 10 pages
http://dx.doi.org/10.1155/2014/841895

Research Article

Containment Depressurization Capabilities of Filtered Venting System in 1000 MWe PWR with Large Dry Containment

Sang-Won Lee, Tae-Hyub Hong, Yu-Jung Choi, Mi-Ro Seo, and Hyeong-Taek Kim

Korea Hydro and Nuclear Power, Central Research Institute, 70 Gil, Yuseong-Daero 1312, Yuseong-Gu, Daejeon 305-343, Republic of Korea

Correspondence should be addressed to Sang-Won Lee; sangwon@khnp.co.kr

Received 24 February 2014; Revised 26 May 2014; Accepted 29 May 2014; Published 22 June 2014

Academic Editor: Inn Seock Kim

After the Fukushima Daiichi nuclear power plant accident, the Korean government and nuclear industries performed comprehensive safety inspections on all domestic nuclear power plants against beyond design bases events. As a result, a total of 50 recommendations were defined as safety improvement action items. One of them is installation of a containment filtered venting system (CFVS) or portable backup containment spray system. In this paper, the applicability of CFVS is examined for OPR1000, a 1000 MWe PWR with large dry containment in Korea. Thermohydraulic analysis results show that a filtered discharge flow rate of 15 [kg/s] at 0.9 [MPa] is sufficient to depressurize the containment against representative containment overpressurization scenarios. Radiological release to the environment is reduced to 10^{-3} considering the decontamination factor. Also, this cyclic venting strategy reduces noble gas release by 50% for 7 days. The probability of maintaining the containment integrity in level 2 probabilistic safety assessment (PSA) initiating events is improved twofold, from 43% to 87%. So, the CFVS can further improve the containment integrity in severe accident conditions.

1. Introduction

After the Fukushima Daiichi nuclear power plant accident [1], the Korean government and industry performed comprehensive special safety inspections on all domestic nuclear power plants against beyond design bases external events. The major concerns of the inspection were protection against extreme natural hazards, prevention of severe accidents, mitigation of severe accidents, emergency preparedness, and design of structures and equipment against earthquakes and coastal flooding. As a result, a total of 50 recommendations were defined as safety improvement action items. These were classified into 5 categories, as shown in Table 1, and should be implemented.

One of the major action items in mitigation of severe accidents is to maintain containment integrity against overpressurization scenarios. Containment may lose its functional capability as last barrier of radioactive material release to the environment due to overpressurization as a consequence of long-term steam and noncondensable gas generation by molten core concrete interaction (MCCI) [2].

The possible means to mitigate overpressurization are internal decay heat removal, external cooling of the containment surface, and containment venting [3]. Internal heat removal is the most obvious concept that can be used to prevent steam generation inside the containment. However, in cases of severe accidents caused by station blackout (SBO) or loss of recirculation, independent overpressurization protection facilities, such as portable equipment or severe accident grade spray, should be designed to mitigate accidents. Also, external cooling of the containment surface requires steel containment for effective heat transfer to the atmosphere.

The basic idea of a filtered venting system is to open a controlled flow path to the external environment to relieve the steam and noncondensable gases that are generated inside the containment. By doing this, it is possible to delay or prevent structural failure of the containment. Also it provides additional time to mitigate the accident and reduces the offsite consequences compared to those produced by containment failure. Typically, the decontamination efficiency of an external filter against aerosol is required to be 99.9% in order

Table 1: Safety improvement action items in Korea after Fukushima accidents.

Categories	Major action item
(1) Design of structures and equipment against earthquakes	(i) Installing an automatic seismic trip system (ii) Improving seismic capability of the safe shutdown systems and MCR (iii) Reassessment of maximum potential earthquakes for nuclear plant sites
(2) Design of structures and equipment against coastal flooding	(i) Extension of the height of sea wall (ii) Installation of waterproof gates and discharge pump (iii) Investigation of the design basis sea water level of nuclear plant sites
(3) Integrity of electric power, cooling, and fire protection system upon inundation	(i) Securing availability of portable power generator vehicles and batteries (ii) Upgrading design basis of alternative AC diesel generators (iii) Ensuring countermeasure against loss of spent fuel pool cooling function (iv) Improving fire protection facilities and fire protection plan
(4) Countermeasures against severe accidents	(i) Installation of passive hydrogen removal equipment (ii) Installation of filtered vent system or backup spray system (iii) Revision of severe accident management guidelines to enhance effectiveness (iv) Installation of reactor injection flow path from external cooling source
(5) Emergency response	(i) Amending emergency plans to address concurrent events at multiple units (ii) Development of extensive damage mitigation guidelines

to prevent long-term ground contamination and 99% for elemental iodine to limit thyroid doses and the need for short-term evacuation [4].

Different kinds of filtered venting design were investigated in the 1980s, such as sand/gravel filters, scrubbing through a water pool, scrubbing through a bed of ice in the PWR ice condenser containment, scrubbing through a venturi scrubber in a water pool and a metallic mesh filter outside the containment, and dry filters [5]. Also, different containment filtered venting strategies were proposed [6]. After the Chernobyl accident, several European countries (France, Sweden, and Germany) installed containment filtered venting systems (CFVS). In Switzerland, all nuclear power plants had installed filtered venting systems and theirs design characteristics had been described [4]. However, the negative impacts of filtered venting systems, such as containment subatmospheric pressure, hydrogen buildup in the filtered venting system due to condensation in the subcooled water pool, and unnecessary release of radioactive material due to inadvertent opening, had been studied in the US [5, 7, 8]. Also, estimation of the risk reduction factor of filtered venting was found to vary from 2 to 100 based on plant design and assumptions but still has large uncertainties [9–11].

After the Fukushima Daiichi nuclear power plant accident, many countries reexamined the applicability of filtered venting as a mitigation measure for containment integrity [12, 13]. In Korea, four pressurized heavy water reactors (PHWR) will install the CFVS because their containment designs are vulnerable compared to that of a conventional PWR. In this paper, the depressurization capability and the effects on safety improvement of CFVS will be examined for a 1000 MWe PWR with large dry containment.

2. Severe Accident Analysis

To assess the severe accident mitigation effect of CFVS, analyses of containment overpressurization scenarios are performed using the MAAP4 computer code [14]. The MAAP code can analyze severe accidents following loss of coolant accidents (LOCAs), SBOs, and various general transients. Developed for the Electric Power Research Institute (EPRI) by Fauske et al., MAAP4.0.4 is used here. MAAP4 has a simplified thermohydraulic model and solves first-order differential equations for conservation of mass and energy. However, it has a reasonable prediction capability comparable to those of MELCOR and SCDAP [15]. Also, recently, technical justification of the MAAP4 code for post-Fukushima applications has been performed [16].

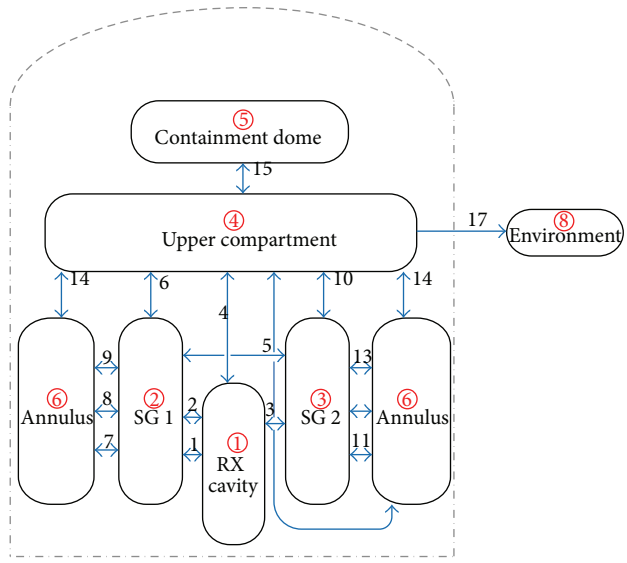

Figure 1: Containment noding diagram.

The reference plant is OPR1000, a 1000 MWe large dry PWR in Korea. A containment noding diagram for OPR1000 is shown in Figure 1. In OPR1000, ultimate containment failure pressure with 5% probability 95% confidence level is 1.01 MPa and it is used in hardened venting without an external filter in severe accident management guidelines [17].

Table 2: Initial and boundary conditions.

Parameter	Value
Rx power	2815 [MW_{th}]
CTMT net free volume	7.73×10^4 [m^3]
CTMT design pressure	0.5 [MPa]
CTMT ultimate pressure	1.01 [MPa]
CFVS opening/closing set-point	0.9/0.6 [MPa] 0.5/0.2 [MPa]
CFVS flow rate	17 kg/s @ 0.9 MPa 10 kg/s @ 0.5 MPa

CFVS is modelled as a junction connecting the containment upper compartment to the environment. Venting area is assumed to be 230 mm (9 inch) in diameter and flow resistance through the CFVS is considered. To activate the CFVS, the containment isolation valves should be opened either by the operator (active means) or by the rupture disc (passive means) when the set-point is reached. A decontamination factor of 1,000 for aerosol is assumed in this calculation. Representative containment venting strategies are divided into early venting (venting before core heat-up) and late venting (venting beyond containment design pressure). The disadvantage of the early venting strategy is that depressurization occurs at a time when the fission product level in the containment is high and aerosol deposition begins. So, the aerosol loading of the vent system is high in that period. However, late venting has some potential benefits in preventing a large amount of uncontrolled release of radioactive materials to the environment and no negative influence on the hydrogen explosion [6].

The containment pressure behavior is analyzed for three different cases: without venting, with cyclic venting at severe accident pressure of 0.9 MPa/0.6 MPa (CFVS-9 case), and with cyclic venting at containment design pressure of 0.5 MPa/0.2 MPa (CFVS-5 case). Without a closing set-point, the containment pressure reaches 0.1 MPa. Then, pressure becomes unstable and a small amount of steam condensation leads to subatmospheric pressure, especially in the ice condenser containment [3]. So, the cyclic venting strategy is assumed to prevent subatmospheric pressure concerns.

Initial and boundary conditions are summarized in Table 2. Major analysis scenarios are extended SBO and LBLOCA. These scenarios are chosen based on representative PSA initiating events that are expected to envelope the containment overpressurization accident [18].

2.1. Effect on SBO Scenarios. SBO is a representative high pressure scenario. In a SBO, molten debris and coolant discharged into containment are in a superheated condition and lead to rapid containment pressurization. The initiating event is a SBO concurrent with failure of the alternative AC. At 9.0 sec, the SG safety valve opens due to the primary to secondary heat transfer. The turbine driven auxiliary feedwater system is assumed to fail. So, the SG inventory is depleted at 50 min. Also, emergency core cooling system and containment spray system are not available. So the RCS

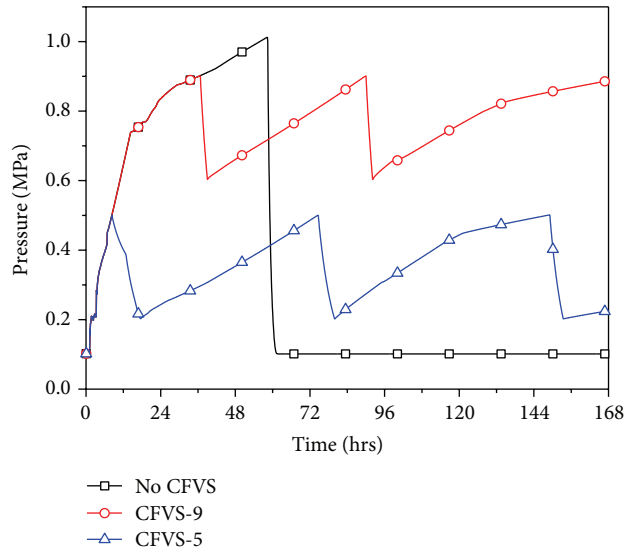

Figure 2: Containment pressure history in extended SBO.

inventory is continuously discharged into the containment via the pressurizer safety valve and the core starts to uncover at 1.6 hrs. Core exit temperature reaches severe accident management guideline entry condition of 922 K at 2.0 hrs. However, there are no mitigation measures available. Finally the reactor vessel fails at 3.3 hrs. Because high pressure is maintained before the RCS fail, a large amount of superheated steam and hydrogen are discharged into the containment. Also, interaction between the molten core material and the cavity water that is discharged from accumulator leads to a large amount of steam generation in the cavity. So, the containment pressure rapidly increases, so-called steam spike. After the cavity water is depleted, hydrogen and noncondensable gas are generated by molten core concrete interaction in the base-mat. After 58.4 hrs, the containment pressure reaches its ultimate pressure and leads to containment failure. Table 3 summarizes the sequence of events.

However, the CFVS-9 case shows that the CFVS starts to operate at 36.8 hrs as shown in Figure 2. Then, the containment pressure rapidly decreases to the closing set-point of 0.6 MPa within 2.2 hrs. On the other hand, the CFVS-5 case shows that the CFVS starts to operate at 8.4 hrs and maintains for 9.1 hrs due to the relatively large decay heat level and its limited venting flow-rate, which is due to small pressure difference, as shown in Figure 3.

Fractional releases of radioactive material without CFVS and that for the CFVS case are compared in Figures 4 and 5. Most of the radioactive material releases to the environment are reduced substantially due to the effect of the decontamination factor of 1,000 in the CFVS case. In addition, the cyclic venting strategy reduces the noble gas release to ~50% in the CFVS-9 case, as shown in Figure 6. With respect to the opening set-point, the CFVS-9 case is beneficial for radioactive releases to the environment because CFVS operating timing is delayed and operation duration is shorter compared to that of the CFVS-5 case. Also, aerosol loading is decreased due to the fact that the deposition inside

Table 3: Extended SBO sequence of event.

Event summary	No CFVS	CFVS @ 0.9 MPa	CFVS @ 0.5 MPa
SBO occurs Rx Scram No ECCS/spray/aux feed available	0.0 sec		
2nd safetyv cycling	9.0 sec		
SG dryout	50 min		
Primary safety valve cycling	50 min		
Core uncover	1.6 Hr		
CET > 1200 F (SAMG entry)	2.0 Hr		
Vessel failure	3.3 Hr		
CFVS opening/closing	—	36.8 Hrs/39.0 Hrs 90.1 Hrs/92.2 Hrs	8.4 Hrs/17.5 Hrs 74.6 Hrs/80.0 Hrs 149.2 Hrs/153.5 Hrs
Containment failure	58.4 Hrs	No fail	No fail
Calc. end	168 Hr		

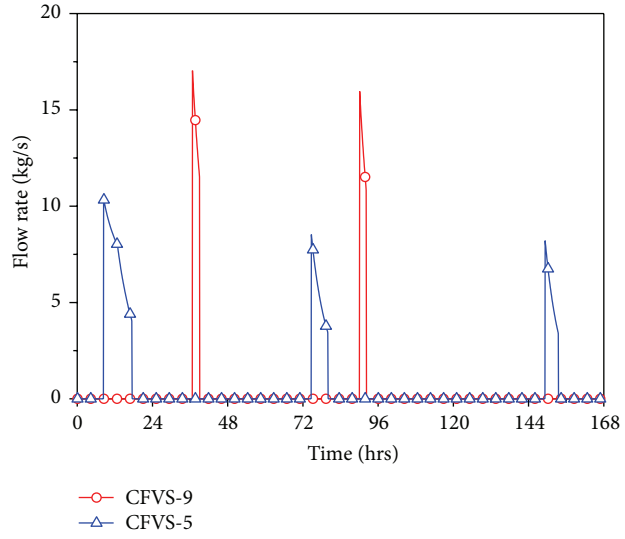

Figure 3: CFVS discharge flow rate in extended SBO.

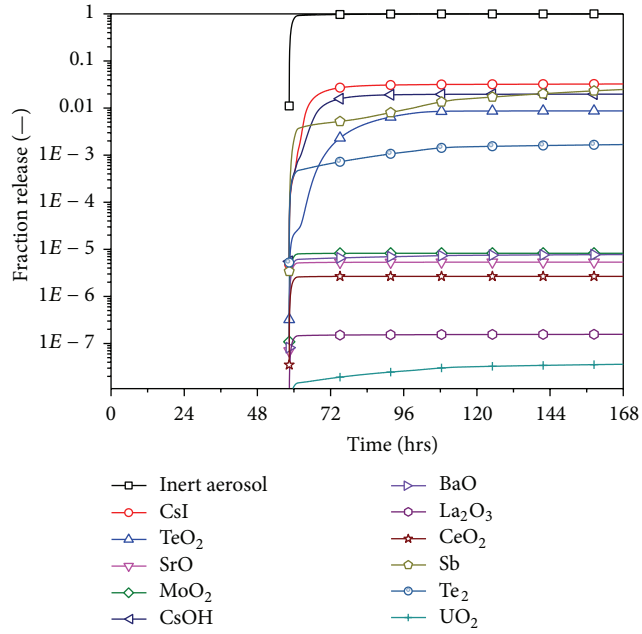

Figure 4: Fractional release of radioactive material without CFVS in extended SBO.

the containment occurs during delayed venting, as shown in Figure 7.

2.2. Effect on LBLOCA Scenarios. LBLOCA is the representative low pressure scenario. The initiating event is a cold leg double-ended guillotine break at 0.0 sec. After the blow-down phase, RCS depressurization leads to accumulator injection for initial core quenching. Due to the large amount of accumulator water, some of the spilled water is collected into the reactor cavity. The containment pressure decreases after its initial peak during the blow-down phase due to the passive heat sink in the containment. However, all of emergency core cooling systems fail to deliver when the injection signal occurs. Eventually, molten corium relocation to the lower head occurs at 1.4 hrs. During this time period, the containment pressure continuously increases due to the break steam flow rate to the containment. Finally, RCS fails at 2.4 hrs. Interaction between the molten core material and the cavity water leads to a large amount of steam generation in the cavity. So, the containment pressure reincreases. Also, hydrogen and noncondensable gas are steadily generated by the molten core concrete interaction in the base-mat. The containment pressure reaches its ultimate pressure at 53.8 hrs. Table 4 summarizes the sequence of events.

The CFVS-9 case shows that the CFVS starts to operate at 28.0 hrs as shown in Figure 8. Then, the containment pressure rapidly decreases to the closing set-point of 0.6 MPa within 2.3 hrs. On the other hand, the CFVS-5 case shows that the CFVS starts to operate at 4.4 hrs and maintains for 9.6 hrs. This activation time is just 2 hrs after the RCS fails. So, a relatively large amount of noble gas and CsI are released to the environment, as shown in Figures 9 and 10.

Table 4: LBLOCA sequence of event.

Event summary	No CFVS	CFVS @ 0.9 MPa	CFVS @ 0.5 MPa
Cold leg LBLOCA occurs Rx Scram No CTMT spray/aux feed available	0.0 sec		
PZR empty	7.0 sec		
Core uncovery	8.0 sec		
Accumulator empty	41.0 sec		
Relocation to lower head	1.4 Hrs		
Vessel failure	2.4 Hrs		
CFVS opening/closing		28 Hrs/30.3 Hrs 88.1 Hrs/90.2 Hrs 151.8 Hrs/153.8 Hrs	4.4 Hrs/14.0 Hrs 68.0 Hrs/73.3 Hrs 137.5 Hrs/141.9 Hrs
Containment failure	53.8 Hrs	No fail	No fail
Calc. end	168 Hr		

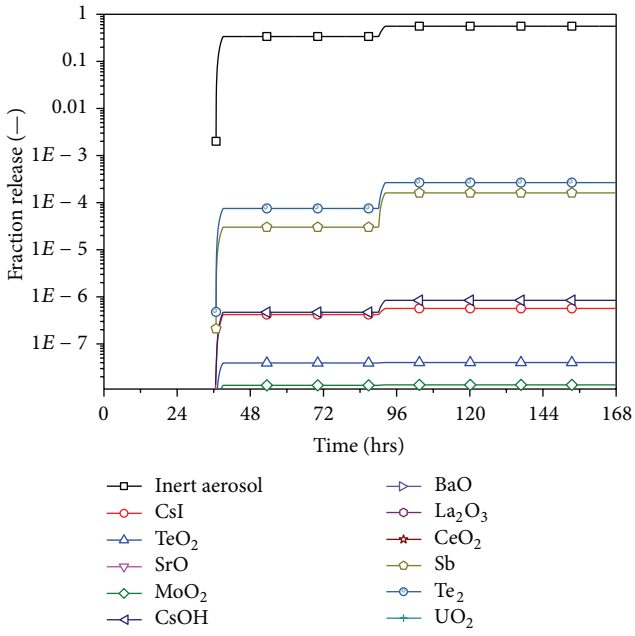

Figure 5: Fractional release of radioactive material with CFVS-9 case in extended SBO.

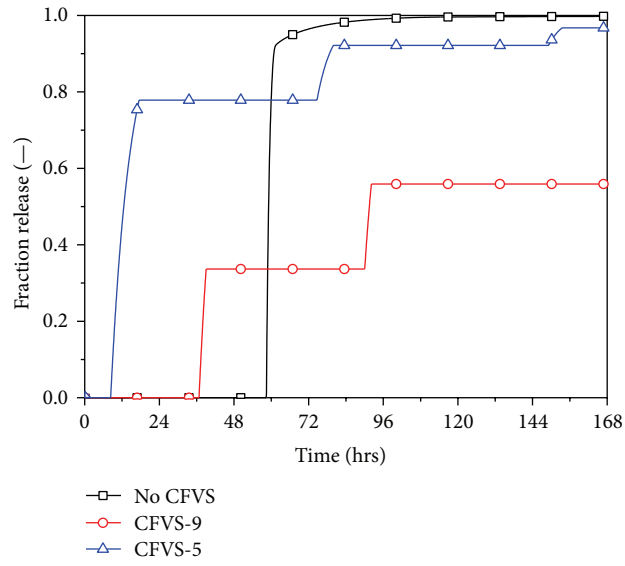

Figure 6: Comparison of fractional release of noble gas in extended SBO.

2.3. Analysis Results. Analysis results show that the OPR1000 could maintain its integrity against severe accident overpressurization scenarios for 2~3 days due to the design characteristic of sufficient free volume in the large dry containment. However, if operator recovery action for containment depressurization or cooling function using existing active system (i.e., containment spray system or fan cooler) is not successful within this time, the containment may lose its functional capability as the last barrier against fission product release into the environment.

When CFVS is in place, containment pressure reaches the CFVS set-point approximately 1~2 days after the initial event. Then, a filtered discharge flow rate of 17 [kg/s] at 0.9 MPa is sufficient to depressurize the containment in most of the late containment failure scenarios. Also 2~3 times of operation in a 7-day period are sufficient to control the containment pressure. Radiological release to the environment is reduced to 10^{-3} considering the decontamination factor. In addition, the cyclic venting strategy can reduce the noble gas release by 50% for 7 days. As for containment penetration, OPR1000 satisfies regulatory requirement 10CFR50.34(f) which requires 3 ft diameter containment penetration for venting provision. And a 17 [kg/s] flow rate is roughly equivalent to a penetration diameter of 9 inches.

3. PSA Assessment

To assess the safety improvement effects on PSA, the current OPR1000 level 2 PSA model is examined [18]. In level 2 PSA, the general containment failure modes can be divided into six categories [19].

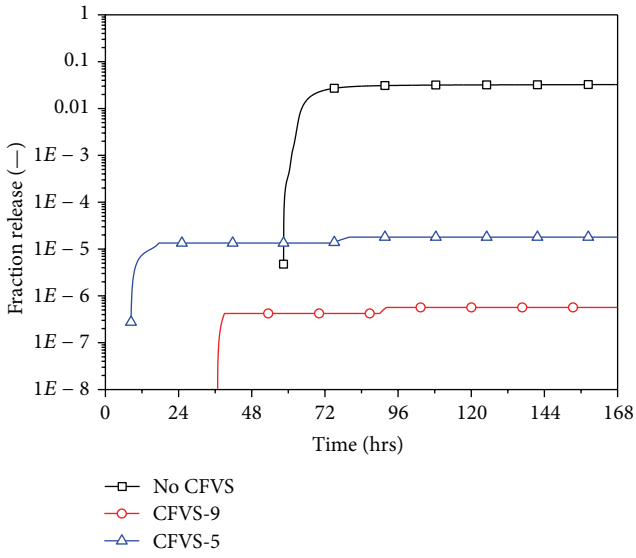

Figure 7: Comparison of fractional release of CsI in extended SBO.

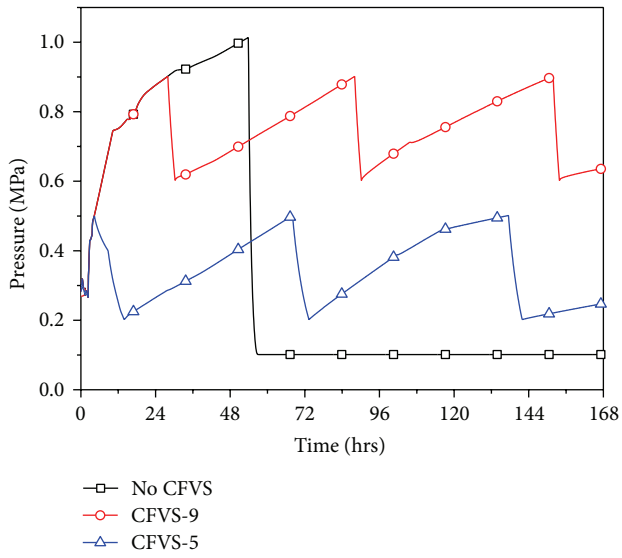

Figure 8: Containment pressure history in LBLOCA.

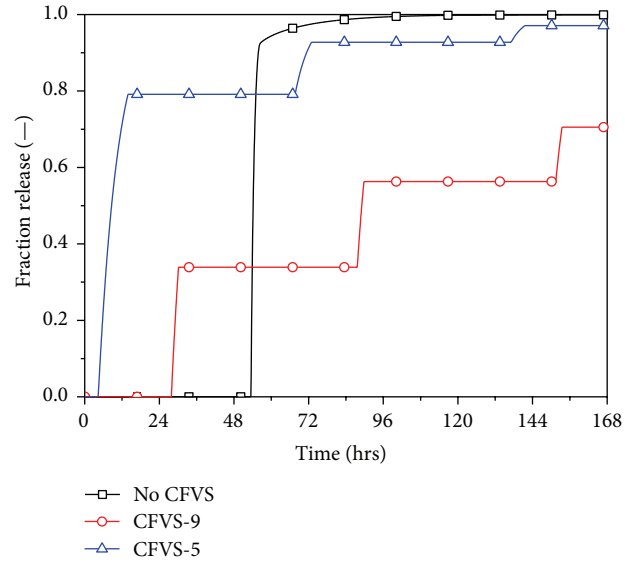

Figure 9: Comparison of fractional release of noble gas in LBLOCA.

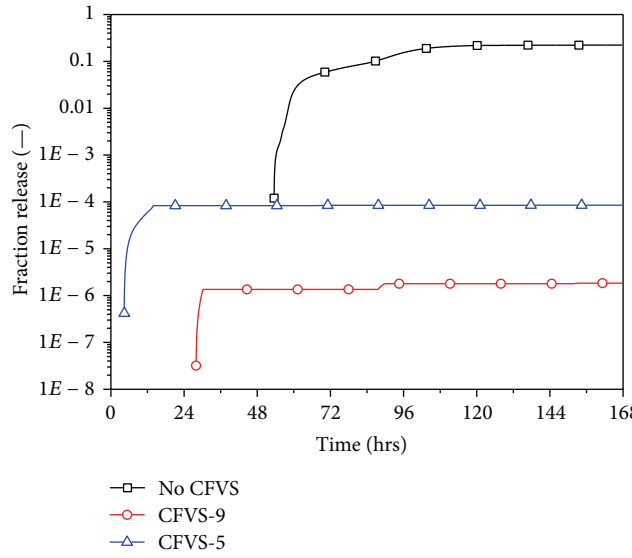

Figure 10: Comparison of fractional release of CsI in LBLOCA.

(i) No containment failure (NO CF): core damage occurs in the reactor vessel, but the molten corium does not penetrate the reactor vessel lower head. And containment integrity is maintained.

(ii) Early containment failure (ECF): containment failure occurs at a relatively early stage of the event. Major phenomena are violent hydrogen explosion, direct containment heating, steam explosion, and so forth.

(iii) Late containment failure (LCF): containment failure occurs 2~3 days after the reactor vessel failure by continuous overpressurization due to molten core concrete interaction and steam generation.

(iv) Base-mat melt-through (BMT): the molten corium interacts with the concrete floor of the reactor building and melts through the containment floor.

(v) Isolation failure (NOT ISO): Although the containment integrity is maintained, the containment pressure boundary is damaged by containment isolation failure and radioactive material is released to the outside containment.

(vi) Containment bypass (BYPASS): fission products generated in the core are released outside the containment directly through containment penetration. Steam generator tube rupture (SGTR) accident and interfacing system LOCA (ISLOCA) are included in this category.

3.1. Effectiveness of CFVS against Level 2 PSA Internal Event. To assess the overall beneficial impact of CFVS, several

Table 5: Containment event tree of OPR1000.

CET Heading	Definition	Subbranch	Effect on CFVS	Remark
RCSFAIL	RCS fail before RV fail	No fail HL Break SGTR	— — No	Bypass
MELTSTOP	Core melt progression Stopped before RV fail	Melt stop RV rupture CFBRB	— — Yes	
ALPHA	ALPHA mode containment failure	No fail Fail	— No	Early CTMT failure
CR-EJECT	Amount of corium ejected out of cavity	High, medium, low	—	
CF-EARLY	Early containment failure	No fail Leak/Rupture	— No	Early CTMT failure
CS-LATE	Recirculation spray failure	No fail, fail	—	
EXVCOOL	Debris cooled ex-vessel	No cooled, cooled	—	
CF-LATE	Late containment failure	No fail Leak/rupture	— Yes	

factors should be considered such as system unavailability due to component failure and inadvertent opening of CFVS [9, 10]. These failure probabilities depend on system design configuration. In this study, these failures are not considered because CFVS is simple and works passively. So, level 2 PSA internal events are examined with respect to conditional containment failure probability (CCFP) and containment failure frequency. The containment performance analysis estimates the failure probability of the containment for all of the core damage sequences using the containment event tree (CET), shown in Figure 11. To quantify CET, the decomposition of the event trees is performed for each of the CET headings in OPR1000. There are 9 representative CET headings and 95 sequences. The definition and subbranch of each CET heading that is related to the CFVS installation are summarized in Table 5. Qualitative assessment results show that 21 out of a total of 95 existing sequences are selected as scenarios that can be improved by installation of CFVS, as shown in Table 6. The total containment failure frequency that can be prevented by the installation of the CFVS is calculated as $7.295E-07$/yr. Current total containment failure frequency for the OPR1000 is $1.88E-06$/yr. So, the safety improvement effect of the CFVS is determined to be a 39% reduction in the containment failure frequency. Also, CCFP is reduced from 0.337 to 0.2.

3.2. Effectiveness of CFVS against Level 2 PSA External Event. In order to evaluate the overall effect of safety improvement by CFVS installation, external event PSA results, including those for earthquake and fire, are considered. So, a rough estimation of the overall safety improvement effect was determined based on each containment failure mode. The major assumption for external event scenarios is that late containment failure and containment failure before reactor breach (CFBRB) can be prevented by CFVS because the major factors of these failure modes are the loss of cooling and/or depressurization of the containment, such as containment spray or containment fan cooler [9]. Also, containment overpressurization occurs mostly 2~3 days after an initiating event. So, the operator has sufficient time to perform the proper action based on SAMG. Table 7 briefly shows the assessment results. As can be seen in the table, probability of maintaining containment integrity is improved from 43% to 87%.

4. Conclusions

After the Fukushima Daiichi nuclear power plant accident, one of the safety improvement action items in Korea is the installation of containment filtered venting systems. So, the applicability of CFVS is examined for OPR1000, a 1000 MWe PWR with large dry containment.

The following are the conclusions.

(i) OPR1000 could maintain its integrity against severe accident overpressurization scenarios for 2~3 days due to the sufficient free volume in large dry containment.

(ii) Filtered discharge flow rate of 15 [kg/s] at 0.9 [MPa] is sufficient to depressurize the containment during the overpressurization scenarios.

(iii) Radiological release to the environment is reduced to 10^{-3} using current filtered venting technology.

(iv) Late venting is beneficial for aerosol loading and compact design because operating timing is delayed and operation duration is shorter.

(v) Cyclic venting strategy reduces the possibility of noble gas release to the environment.

(vi) Probability of maintaining containment integrity in level 2 probabilistic safety assessment (PSA) initiating events is improved substantially.

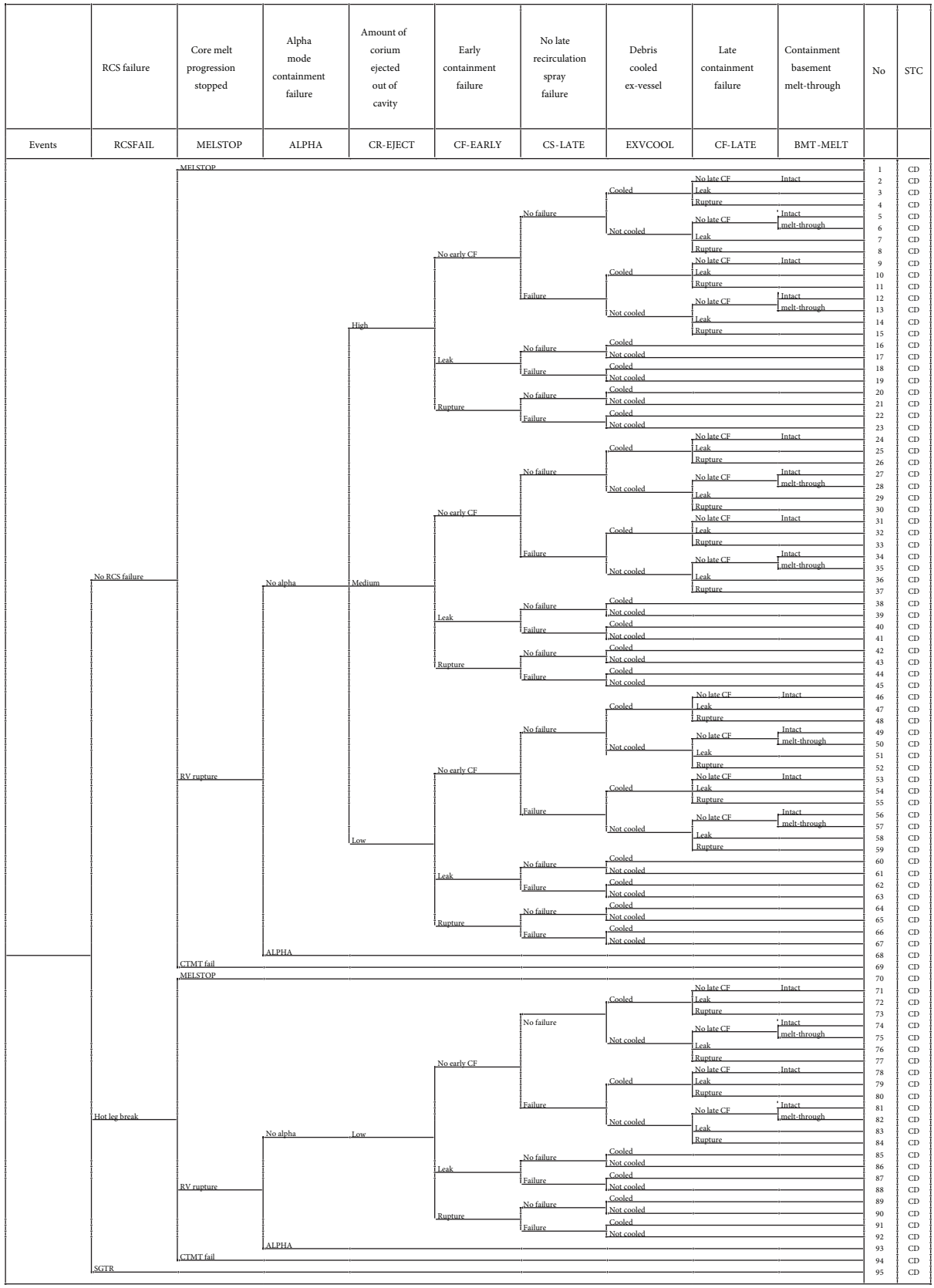

Figure 11: Representative containment event tree.

Table 6: Level 2 PSA internal event affected by CFVS.

RCSFAIL	MELTSTOP	ALPHA	CR-EJECT	CF-EARLY	CS-LATE	EXVCOOL	CF-LATE	Seq
No RCS failure	RV rupture	No alpha	High	No early CF	Failure	Cooled	Leak	10
No RCS failure	RV rupture	No alpha	High	No early CF	Failure	Cooled	Rupture	11
No RCS failure	RV rupture	No alpha	High	No early CF	Failure	Not cooled	Leak	14
No RCS failure	RV rupture	No alpha	High	No early CF	Failure	Not cooled	Rupture	15
No RCS failure	RV rupture	No alpha	Medium	No early CF	Failure	Cooled	Leak	32
No RCS failure	RV rupture	No alpha	Medium	No early CF	Failure	Cooled	Rupture	33
No RCS failure	RV rupture	No alpha	Medium	No early CF	Failure	Not cooled	Leak	36
No RCS failure	RV rupture	No alpha	Medium	No early CF	Failure	Not cooled	Rupture	37
No RCS failure	RV rupture	No alpha	Low	No early CF	No failure	Not cooled	Rupture	52
No RCS failure	RV rupture	No alpha	Low	No early CF	Failure	Cooled	Leak	54
No RCS failure	RV rupture	No alpha	Low	No early CF	Failure	Cooled	Rupture	55
No RCS failure	RV rupture	No alpha	Low	No early CF	Failure	Not cooled	Leak	58
No RCS failure	RV rupture	No alpha	Low	No early CF	Failure	Not cooled	Rupture	59
No RCS failure	CTMNT fail	—	—	—	—	—	—	60
Hot leg break	RV rupture	No alpha	Low	No early CF	No failure	Not cooled	Leak	76
Hot leg break	RV rupture	No alpha	Low	No early CF	No failure	Not cooled	Rupture	77
Hot leg break	RV rupture	No alpha	Low	No early CF	Failure	Cooled	Leak	79
Hot leg break	RV rupture	No alpha	Low	No early CF	Failure	Cooled	Rupture	80
Hot leg break	RV rupture	No alpha	Low	No early CF	Failure	Not cooled	Leak	83
Hot leg break	RV rupture	No alpha	Low	No early CF	Failure	Not cooled	Rupture	84
Hot leg break	CTMNT fail	—	—	—	—	—	—	94

Table 7: Overall safety improvement effect by the installation of the CFVS.

Category	Internal event	External event		Current design	w/CFVS
		Fire	Seismic		
No containment failure	66.3	40.0	39.3	43.1	87.3
Early containment failure	0.5	1.0	1.0	0.9	0.9
Late containment failure	12.5	46.1	48.2	43.1	0.0
Base-mat melt through	3.8	4.8	4.5	4.4	4.4
CFBRB	5.9	0.2	0.3	1.1	0.0
Isolation failure	1.5	6.9	5.4	4.9	4.9
Containment bypass	9.5	1.1	1.2	2.4	2.4
Sum	100	100	100	100	100

(vii) Overall, CFVS can further improve the containment integrity in severe accident conditions.

Conflict of Interests

The authors declare that there is no conflict of interests regarding the publication of this paper.

Acknowledgments

This work was supported by the Nuclear Research and Development of the Korea Institute of Energy Technology and Planning (KETEP) Grant funded by the Korean Government, Ministry of Trade, Industry, and Energy (20111510100020).

References

[1] TEPCO, "Overview of the Earthquake & Tsunami and Nuclear Accident : The Great East Japan Earthquake and Current Status of Nuclear Power Stations," 2011.

[2] B. De Boeck, "Prevention and mitigation measures to ensure containment integrity," *Nuclear Engineering and Design*, vol. 209, no. 1–3, pp. 147–154, 2001.

[3] H. Tuomisto, "Filtered venting considerations of an ice condenser containment," *Nuclear Engineering and Design*, vol. 117, no. 1, pp. 25–31, 1989.

[4] H. Rust, C. Tännler, W. Heintz, D. Haschke, M. Nuala, and R. Jakab, "Pressure release of containments during severe accidents in Switzerland," *Nuclear Engineering and Design*, vol. 157, no. 3, pp. 337–352, 1995.

[5] R. O. Schlueter and R. P. Schmitz, "Filtered vented containments," *Nuclear Engineering and Design*, vol. 120, no. 1, pp. 93–103, 1990.

[6] K. Bracht and M. Tiltmann, "Analysis of strategies for containment venting in case of severe accidents," *Nuclear Engineering and Design*, vol. 104, no. 3, pp. 235–240, 1987.

[7] R. Jack Dallman, W. J. Galyean, and K. C. Wagner, "Containment venting as an accident management strategy for BWRS with Mark I containments," *Nuclear Engineering and Design*, vol. 121, no. 3, pp. 421–429, 1990.

[8] D. L. Kelly, "Overview of containment venting as an accident mitigation strategy in US light water reactors," *Nuclear Engineering and Design*, vol. 131, no. 2, pp. 253–261, 1991.

[9] F. Gazzillo and W. E. Kastenberg, "Risk reduction by filtered venting in PWR large dry-containments," *Nuclear Engineering and Design*, vol. 77, no. 1, pp. 69–85, 1984.

[10] M. Gonzales-Cuesta, D. Okrent, and W. E. Kastenberg, "A study of risk reduction for some mitigation features for PWRs," *Nuclear Engineering and Design*, vol. 75, no. 1, pp. 13–22, 1983.

[11] R. Schechtman and C. D. Heising, "Risk assessment of the beneficial impact of a filtered venting containment system in a PWR with large, dry containment," *Annals of Nuclear Energy*, vol. 23, no. 8, pp. 641–661, 1996.

[12] G. Huang and L. Fang, "Feasibility research of containment venting for CANDU 6," *Nuclear Engineering and Design*, vol. 268, pp. 113–120, 2014.

[13] K. Yuan, D. Q. Guob, L. L. Tong, and X. W. Cao, "Evaluation of containment venting strategy via VFS path for advanced passive PWR NPP," *Progress in Nuclear Energy*, vol. 73, pp. 102–106, 2014.

[14] EPRI, "MAAP4-Modular Accident Analysis Program for LWR Power Plants," 1994.

[15] K. Vierow, Y. Liao, J. Johnson, M. Kenton, and R. Gauntt, "Severe accident analysis of a PWR station blackout with the MELCOR, MAAP4 and SCDAP/RELAP5 codes," *Nuclear Engineering and Design*, vol. 234, no. 1–3, pp. 129–145, 2004.

[16] EPRI, "Use of MAAP in support of Post-Fukushima Applications," 2013.

[17] PWROG, "Severe Accident Management Guideline," MUHP-2310, 1994.

[18] KHNP, "Probabilistic Safety Assessment for OPR1000 Containment Performance Analysis," 2004.

[19] NRC, "Reactor Safety Study," WASH-1400, 1975.

Hindawi Publishing Corporation
Science and Technology of Nuclear Installations
Volume 2014, Article ID 345729, 7 pages
http://dx.doi.org/10.1155/2014/345729

Research Article

Development of Instrument Transmitter Protecting Device against High-Temperature Condition during Severe Accidents

Min Yoo, Sung Min Shin, and Hyun Gook Kang

Nuclear Plant Reliability & Man-Machine Interface Design Laboratory, Korea Advanced Institute of Science and Technology, Daehak-ro 291, Yuseong-Gu, Daejeon 305-701, Republic of Korea

Correspondence should be addressed to Hyun Gook Kang; hyungook@kaist.ac.kr

Received 9 March 2014; Accepted 3 May 2014; Published 17 June 2014

Academic Editor: Inn Seock Kim

Reliable information through instrumentation systems is essential in mitigating severe accidents such as the one that occurred at the Fukushima Daiichi nuclear power plant. There are five elements which might pose a potential threat to the reliability of parameter detection at nuclear power plants during a severe accident: high temperature, high pressure, high humidity, high radiation, and missiles generated during the evolution of a severe accident. Of these, high temperature apparently poses the most serious threat, since thin shielding can get rid of pressure, humidity, radiation (specifically, alpha and beta radiations), and missile effects. In view of this fact, our study focused on designing an instrument transmitter protecting device that can eliminate the high-temperature effect on transmitters to maintain their functional integrity. We present herein a novel concept for designing such a device in terms of heat transfer model that takes into account various heat transfer mechanisms associated with the device.

1. Introduction

On March 11, 2011, one of the most serious accidents in nuclear power history took place at the Fukushima Daiichi nuclear power plant as a result of the extreme natural disaster caused by an earthquake and subsequent tsunami [1–3]. The emergency response manuals for severe accidents at the Tokyo Electric Power Company (TEPCO) were developed based on the assumption that the monitoring systems would be normally operating during the severe accidents. However, during the actual accidents at Fukushima they lost detectors and monitoring equipment, so that "the decisions and responses to the accident had to be made on the spot by operational staff at the site, with absent valid tools and manuals" [4]. Without the information on the plant operation, monitoring the process parameters such as temperature, pressure, water level, or radiation was extremely difficult.

There are some detectors that are needed in mitigating severe accidents. For instance, the following are referred to as requisite detectors in the severe accident management guidance (SAMG) for a pressurized water reactor (PWR): core exit thermocouple (CET), heated junction thermocouple (HJTC), resistance temperature detector (RTD), pressurizer manometer, safety injection flow meter, auxiliary feedwater flow meter, steam generator water level gauges, water level gauges for in-containment refueling water storage tank (IRWST), hydrogen sensor, radiation sensor, containment pressure sensor, containment temperature sensor, and containment spray flow meter [5]. Among requisite detectors, thermocouple, RTD, pressure sensor, and radiation sensor are exposed to high temperature. Thermocouple (TC) and RTD sensor do not need to be protected once the temperature is below melting point. TC, RTD, and radiation sensor are expected to lose their accuracy if they are protected by the device. Pressure sensor transmitter includes pressure sensing function. Pressure is directly put to the transmitter from the place where it should be measured through pipe; then transmitter produces electric signal. Thus the study aims to protect the transmitter (pressure sensor and RTD) from high temperature.

A transmitter in an instrumentation system converts analog signals from a sensor to a few mA electronic signals. Then, those signals can be transferred over long distance with little noise. Among the requisite detectors, manometer, flow meter, and water level gauges have a transmitter. In a severe accident, transmitters may be out of control in

harsh environment. They are not manufactured so that they can endure in harsh environmental conditions. One of the transmitters that supports pressure detectors endures (a) 1 hour at 157.8°C and 4.826 bar; (b) 7 hours at 150.5°C and 3.819 bar; and (c) 42 hours at 110°C and 0.414 bar steam exposure, with an accuracy within ±0.75% [6]. In the case of other transmitters, the long-term limitation of temperature over a few tens of hours is 80°C with some safety margin.

Based on the severe accident analysis for Shin Kori Units 3 and 4 PWRs, the temperature and pressure around the transmitters during severe accidents are too high to endure. One of the most harsh compartment temperatures reaches 600°C right after the accident occurrence and then decreases to 180°C during the first 10 minutes remaining around this temperature afterwards. Under this harsh environmental condition associated with high temperature, pressure, humidity, or radiation, the transmitters are not likely to perform their intended functions. In addition, they also may be subject to missiles generated during a severe accident. Each of these five elements poses a potential threat to the reliability of parameter detection at nuclear power plants.

Therefore, in order that instrument transmitters can properly send signals during a severe accident, they must be protected against such harsh environment as might be caused during the evolution of such an accident. Of the aforementioned five elements, this research focuses on protection of transmitters from high temperature. The reason for this focus is that high temperature is the most serious threat, since thin shielding can get rid of pressure, humidity, radiation (alpha and beta), and missile effects.

This research is specially aimed at maintaining the temperature of instrument transmitters below the long-term limitation temperature mentioned above, that is, 80°C, for at least 72 hours in the harsh environmental conditions. The duration of 72 hours is in line with a typical assumption that if the accident condition is managed for 72 hours, core damage is not likely to occur in a nuclear power plant [7, 8].

In the sequel, we present a novel concept to design a protecting device for instrument transmitters in high-temperature environmental condition. The structural design scheme of a cooler is first discussed along with the theoretical heat transfer model. Cooling methods are then described taking into account various factors affecting the protector performance, such as the protector thickness, material, size, environmental pressure, inside heat generation from the transmitter, and environmental temperature.

2. Design Concept for Instrument Transmitter Protecting Device

According to a study performed for APR1400 by Korea Hydro and Nuclear Power Company (KHNP), the temperature in some compartments at the APR1400 plant for accident scenarios such as loss of feedwater flow (LOFW), loss of coolant accident (LOCA), or station blackout (SBO) reaches as high as 600°C for 10 seconds into the initiating event, drops to around 180°C in 600 seconds, and then remains at 180°C [5]. Therefore, in order to protect the integrity of transmitters, we envision that the critical transmitters should be protected by a box-shaped protecting device for insulation.

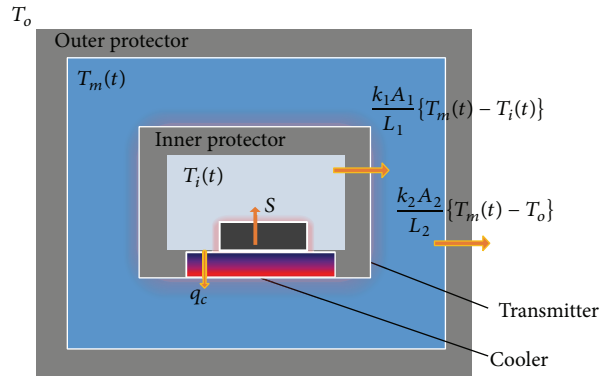

Figure 1: Instrument transmitter protecting device.

2.1. Cooler and Cooling Method. Figure 1 shows a schematic of the protecting device. The protection system consists of inner and outer protectors in the form of a double-box shape. Transmitters are placed in the interior of the inner protector surrounded by air. The space between the outer protector and the inner protector is filled with water. The outer protector shields heat from the outside, and the inner protector releases heat from inside heat source. The water contained between the two protectors stores heat from both the inside and the outside. A cooler is optionally installed. We derive an equation for the inner temperature from heat transfer relations with an aim to determine appropriate protector properties, sizes, amount of water, and so on.

$T_i(t)$ and $T_m(t)$ represent the temperature inside the inner protector and the intermediate water temperature, respectively. S is heat generation from the inside (i.e., transmitter), and $(kA/L)\Delta T$ represents the heat transfer by conduction due to temperature difference between the inside and the outside protectors. q_c represents heat removal by the cooler. Subscripts 1 and 2 refer to the inner and the outer protector, respectively.

There are a few cooling methods available based on use of heat conduction, refrigerant, vortex tube, and thermoelectric cooler (TEC). However, spatial limitation and harsh environmental condition should be taken into account in designing the instrument transmitter protecting device. Furthermore, the cooling method that will be applied to such devices ought to have high reliability. In consideration of these various constraints, only TEC was judged to be a feasible method in this research. The TEC is based on Peltier effect which is a thermoelectric phenomenon where current flows at junction of two different conductors; one side is heated and the other side is cooled. Figure 2 is a general structure of single stage TEC [9]. It consists of insulators (ceramics plates), soldering, semiconductors (pellets), and electric conductors [9, 10].

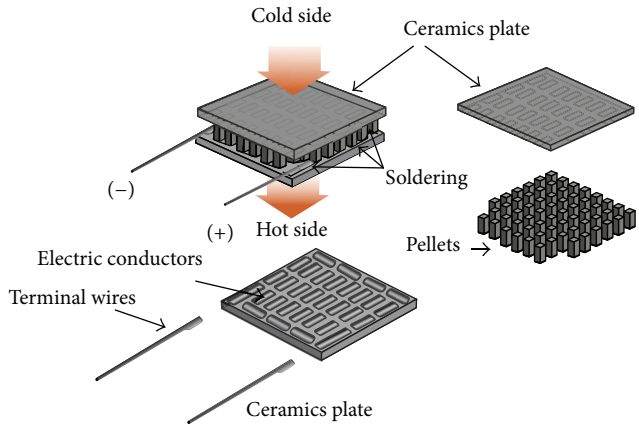

Figure 2: Structure of TEC.

The heat pumped at cold surface of the TEC can be expressed as

$$q_c = 2N\left[\alpha I T_c - \left(\frac{I^2\rho}{(2G)}\right) - k_c\left(T_h - T_c\right)G\right], \quad (1)$$

where N is the number of thermocouples, α is Seebeck coefficient, T_c and T_h are cold and hot side temperatures, I is current, G is the area divided by the length of the element, and k_c is thermal conductivity. α, G, and k_c are constants related to the TEC material properties [11].

In this study, the inner temperature of the protector system is derived based on the following assumptions.

(1) Convections are ignorable and, as a result, the surface temperature of the protector is assumed to equal the temperature of the fluid that it faces. Only conductive heat transfer works through the wall. That is, the heat transfer rate equals $(kA/L)\Delta T$.

(2) It is reasonable to assume that the ambient temperature T_o is constant. The initial thermal shock has a negligible impact on $T_i(t)$.

(3) The initial temperature of all materials and medium is $T(0) = 20^\circ\mathrm{C}$.

(4) The temperature of the protector wall changes linearly along the wall thickness. $T(0,t)$ is the outer surface temperature of the wall at time t, and $T(L,t)$ is inner surface temperature of the wall at time t. L is thickness of the wall, and with wall temperature along thickness x and time t, $T(x,t)$ equals $((T(L,t) - T(0,t))/L)x + T(0,t)$.

(5) The outside size of the inner protector is assumed to be $l_{11} \times l_{12} \times l_{13} = 0.3 \times 0.3 \times 0.4\,\mathrm{m}^3$.

(6) The width, length, and height of outer protector are $l_{21} = l_{11} + l$, $l_{22} = l_{12} + l$, and $l_{23} = l_{13} + l$, where l is length difference between the inner and outer protector edges.

(7) The temperature of the protector wall is a volumetric average temperature of $T(0,t)$ and $T(L,t)$. It means that average temperature is

$$\begin{aligned}
&T_{\text{avg}} \\
&= \frac{\int T(x,t)\,dV}{\text{wall volume } V} \\
&= \left(\int_0^L \left\{\frac{T(L,t) - T(0,t)}{L}x + T(0,t)\right\}\right. \\
&\qquad \times 2\left\{\left(l_1 - 2x\right)\left(l_2 - 2x\right)\right. \\
&\qquad\qquad + \left(l_2 - 2x\right)\left(l_3 - 2x\right) \\
&\qquad\qquad \left. \left. + \left(l_3 - 2x\right)\left(l_1 - 2x\right)\right\} dx\right) \\
&\qquad \times \left(l_1 l_2 l_3 - \left(l_1 - 2L\right)\left(l_2 - 2L\right)\left(l_3 - 2L\right)\right)^{-1} \\
&= \left(T(L,t)\left\{3L^2 - \frac{4}{3}\left(l_1 + l_2 + l_3\right)L + \frac{1}{2}\left(l_1 l_2 + l_2 l_3 + l_3 l_1\right)\right\}\right. \\
&\qquad \left. + T(0,t)\left\{L^2 - \frac{2}{3}\left(l_1 + l_2 + l_3\right)L + \frac{1}{2}\left(l_1 l_2 + l_2 l_3 + l_3 l_1\right)\right\}\right) \\
&\qquad \times \left(4L^2 - 2\left(l_1 + l_2 + l_3\right)L + \left(l_1 l_2 + l_2 l_3 + l_3 l_1\right)\right)^{-1} \\
&= \alpha T(0,t) + \beta T(L,t),
\end{aligned} \quad (2)$$

where

$$\alpha = \frac{L^2 - (2/3)\left(l_1 + l_2 + l_3\right)L + (1/2)\left(l_1 l_2 + l_2 l_3 + l_3 l_1\right)}{4L^2 - 2\left(l_1 + l_2 + l_3\right)L + \left(l_1 l_2 + l_2 l_3 + l_3 l_1\right)}, \quad (3)$$

$$\beta = \frac{3L^2 - (4/3)\left(l_1 + l_2 + l_3\right)L + (1/2)\left(l_1 l_2 + l_2 l_3 + l_3 l_1\right)}{4L^2 - 2\left(l_1 + l_2 + l_3\right)L + \left(l_1 l_2 + l_2 l_3 + l_3 l_1\right)}. \quad (4)$$

α and β are about 0.5 unless wall thickness is too thick.

2.2. Heat Transfer Model. Whether the instrument transmitter protection system successfully carries out its intended function or not depends on the inner temperature. That is, the maximum $T_i(t)$ should remain below 80°C for the period of 72 hours.

Equation (1) can be revised to (5) under the aforementioned assumptions and $e_1 = 2N(\alpha I + k_c G)$, $e_2 = 2Nk_c G$, and $e_3 = \rho I^2 N/G$.

Consider

$$q_c = e_1 T_i(t) - e_2 T_m(t) - e_3. \quad (5)$$

The first part of the derivation of inside the inner protector is about temperature change in the intermediate water:

$$\frac{k_1 A_1}{L_1}\left\{T_i(t) - T_m(t)\right\} + \frac{k_2 A_2}{L_2}\left\{T_o - T_m(t)\right\} + q_c = c_m m_m \dot{T}_m + c_2 m_2 \frac{d}{dx}\left(\frac{\int_0^{L_2} T_{2,\mathrm{avg}}(x,t)\,dV}{V_2}\right) = \left(c_m m_m + c_2 m_2\ \beta_2\right)\dot{T}_m, \quad (6)$$

where k is thermal conductivity, A the surface area, and L the thickness of the protector. c_m and m_m are the specific heat capacity and mass of water, respectively, and $\dot{T}_m$ is time derivative of water temperature. β_2 equals $(3L_2^2 - (4/3)(l_{21} + l_{22} + l_{23})L_2 + (1/2)(l_{21}l_{22} + l_{22}l_{23} + l_{23}l_{21}))$ / $(4L_2^2 - 2(l_{21} + l_{22} + l_{23})L_2 + (l_{21}l_{22} + l_{22}l_{23} + l_{23}l_{21}))$.

If

$$a_1 = \frac{k_1 A_1}{L_1}, \qquad a_2 = \frac{k_2 A_2}{L_2}, \qquad b_1 = \frac{a_1 + e_1}{c_m m_m + c_2 m_2 \beta_2}, \qquad b_2 = \frac{a_2 T_o - e_3}{c_m m_m + c_2 m_2 \beta_2}, \qquad p = \frac{a_1 + a_2 + e_2}{c_m m_m + c_2 m_2 \beta_2}, \quad (7)$$

from (6), the intermediate water temperature becomes

$$T_m(t) = e^{-pt}\left[T(0) + \int_0^t e^{p\tau}\left\{b_1 T_i(\tau) + b_2\right\} d\tau\right]. \quad (8)$$

The second part of the derivation is about a temperature change in the inner protector and the inside temperature change, $c_i m_i \ll c_1 m_1$:

$$S + a_1\left\{T_m(t) - T_i(t)\right\} - q_c = c_i m_i \dot{T}_i + c_1 m_1 \frac{d}{dx}\left(\frac{\int_0^{L_1} T_{1,\mathrm{avg}}(x,t)\,dV}{V_1}\right) \sim c_1 m_1\left(\alpha_1 \dot{T}_m + \beta_1 \dot{T}_i\right), \quad (9)$$

where

$$\alpha_1 = \frac{L_1^2 - (2/3)\left(l_{11}+l_{12}+l_{13}\right)L_1 + (1/2)\left(l_{11}l_{12}+l_{12}l_{13}+l_{13}l_{11}\right)}{4L_1^2 - 2\left(l_{11}+l_{12}+l_{13}\right)L_1 + \left(l_{11}l_{12}+l_{12}l_{13}+l_{13}l_{11}\right)},$$

$$\beta_1 = \frac{3L_1^2 - (4/3)\left(l_{11}+l_{12}+l_{13}\right)L_1 + (1/2)\left(l_{11}l_{12}+l_{12}l_{13}+l_{13}l_{11}\right)}{4L_1^2 - 2\left(l_{11}+l_{12}+l_{13}\right)L_1 + \left(l_{11}l_{12}+l_{12}l_{13}+l_{13}l_{11}\right)}. \quad (10)$$

Substituting (5) and (8) into (9) results in

$$A\ddot{T}_i + B\dot{T}_i + CT_i = p\left(S + e_3\right) + b_2\left(a_1 + e_2\right). \quad (11)$$

This is a second-order nonhomogeneous differential equation, where

$$A = c_i m_i + c_1 m_1 \beta_1 \sim c_1 m_1 \beta_1,$$
$$B = pA + \alpha_1 b_1 c_1 m_1 + a_1 + e_1 \sim \frac{a_1 + a_2 + e_2}{c_m m_m + c_2 m_2 \beta_2} * c_1 m_1 \beta_1 + \frac{\alpha_1\left(a_1 + e_1\right)c_1 m_1}{c_m m_m + c_2 m_2 \beta_2} + a_1 + e_1,$$
$$C = a_2 b_1. \quad (12)$$

Because $B^2 - 4AC$ is always positive, its general solution is

$$T_i(t) = d_1 e^{r_1 t} + d_2 e^{r_2 t} + d_3. \quad (13)$$

d_1 and d_2 are arbitrary constants and r_1 and r_2 are $(-B \mp \sqrt{B^2 - 4AC})/2A$; they are always negative. d_3 equals $(1/(a_1 + e_1))\{(a_1 + e_2)T_o + e_3\} + (a_1 + a_2 + e_2)/(a_2(a_1 + e_1))S$. The first term can be eliminated as $r_1 \ll r_2$ and d_2 equals $T(0) - d_3$ because $T_i(t) = T(0)$. Equation (13) becomes

$$T_i(t) = \left\{T(0) - d_3\right\}e^{r_2 t} + d_3 = \left[T(0) - \left(\frac{1}{a_1 + e_1}\left\{\left(a_1 + e_2\right)T_o + e_3\right\} + \frac{a_1 + a_2 + e_2}{a_2\left(a_1 + e_1\right)}S\right)\right] \times e^{((-B + \sqrt{B^2 - 4AC})/2A)t} + \frac{1}{a_1 + e_1}\left\{\left(a_1 + e_2\right)T_o + e_3\right\} + \frac{a_1 + a_2 + e_2}{a_2\left(a_1 + e_1\right)}S. \quad (14)$$

3. Results and Discussion

The temperature inside the inner protector, that is, $T_i(t)$, continues to increase and converges at d_3. Thus, its maximum temperature, that is, $T_i(72\,\mathrm{hr})$, must be smaller than the limiting temperature T_{lim} of 80°C, as discussed above:

$$T_i(72\,\mathrm{hr}) \le T_{\mathrm{lim}}. \quad (15)$$

The variables affecting this criterion are the outer protector size/thickness/thermal conductivity, the inner protector thickness/thermal conductivity/heat capacity, and the number of cooler/current supplies. There are too many variables to derive the appropriate protector condition. Thus, some variables such as material properties were fixed in this analysis for the sake of computational simplification. Further analyses will be performed with different assumptions as deemed necessary in the future study.

There arises an issue whether the protection system needs to include a cooler. Regardless of whether to include a cooler or not, it will be good to use small a_2 and large size of outer protector. If the inner protector is strongly insulated, the system will need a cooler to remove heat from the inside of

the inner protector to the water. In this case, the smaller a_1, the larger the number of TECs, and the higher the current, the better. Equation (16) is a simplified form of (14) applying $c_m m_m + c_2 m_2 \beta_2 \gg c_1 m_1$. Consider

$$\begin{aligned} T_i(t) &\sim \left[T(0) - \left(\frac{1}{a_1 + e_1} \left\{ (a_1 + e_2) T_o + e_3 \right\} + \frac{a_1 + a_2 + e_2}{a_2 (a_1 + e_1)} S \right) \right] \\ &\times e^{((-(a_1+e_1)+\sqrt{(a_1+e_1)^2 - 2a_1 a_2 (c_1 m_1/(c_m m_m + c_2 m_2/2)))}/c_1 m_1)t} \\ &+ \frac{1}{a_1 + e_1} \left\{ (a_1 + e_2) T_o + e_3 \right\} + \frac{a_1 + a_2 + e_2}{a_2 (a_1 + e_1)} S. \end{aligned} \tag{16}$$

In the case where no cooler is used, heat should be well transferred between the inner air and the water because the heat from the transmitter itself is accumulated inside the air. The outer protector needs a strong insulation in both cases to protect heat invasion from the environment. Hence, $a_1 \gg a_2$, $c_m m_m + c_2 m_2 \beta_2 \gg c_1 m_1$, and $e_1 = e_2 = e_3 = 0$. It is reasonable to assume that β_1 and β_2 are 0.5 each. Equation (14) becomes

$$\begin{aligned} T_i(t) &\sim \left[T(0) - \left\{ T_o + \frac{S}{a_2} \right\} \right] \\ &\times e^{((-a_1+\sqrt{(a_1)^2 - 2a_1 a_2 (c_1 m_1/(c_m m_m + c_2 m_2/2)))}/c_1 m_1)t} \\ &+ T_o + \frac{S}{a_2}. \end{aligned} \tag{17}$$

The inner protector wall material and thickness are much less influential factors than other variables as long as inner protector wall material has high thermal conductivity. A material that has 1 J/g/K specific heat, 320 g/m^3 density, 5 W/m/K thermal conductivity, and 1 cm thickness is applied to the inner protector wall. Outer protector material is one of the best insulations whose specific heat, density, and thermal conductivity are 0.8 J/g/K, 250 kg/m^3, and 0.25 W/m/K, respectively [12, 13].

Figure 3 is a top view of 3-dimensional plot of $T_i(t)$ when t is 72 hours in (17). The y-axis in this figure is the length difference between the outer protector and the inner protector. The x-axis represents the thickness of the outer protector wall. The area above the line indicates that $T_i(t)$ is below 80°C and the area below the line indicates that the temperature is higher than 80°C. The protector has the minimum size at the minimum point (0.066, 0.278) of the line. Then, the outer protector size becomes 0.578 × 0.578 × 0.678 m^3 with 6.6 cm thickness. The lower and right part calculations of Figure 3 are meaningless because the outer wall and the inner wall are overlapped.

Figure 4 is the temperature distribution at 72 hours after the accident simulated by solidworks flow simulation. Figure 5 shows the inner air temperature along time, comparing equation-based and simulation-based calculations.

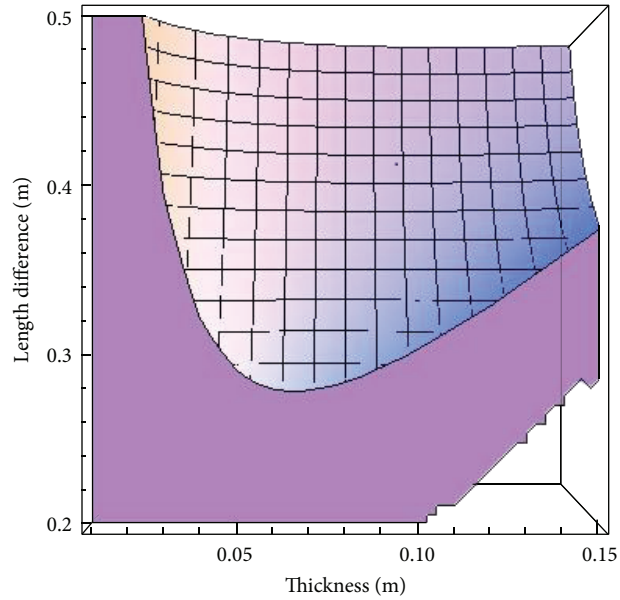

Figure 3: $T_i(t)$ along wall thickness and length difference between the inner and outer protectors.

The equation-based result yields a conservative result. The temperature reaches 70.99°C at 72 hours in the case of the simulation. The temperature profile difference between the equation-based and simulation-based calculations mainly comes from assumptions (1) and (3) described above. The temperature based on heat transfer equations increases more rapidly than the one based on the simulation during the initial phase, because the equation does not consider transient heat transfer and the heat capacity of the wall is underestimated. In assumption (1), it was presumed that there is no convective heat transfer and so the heat transfer between the solid surface and the fluid was assumed to be perfect. However, there is a heat transfer lag in real world and the simulation took into account this phenomenon. Figure 5 overall indicates that the increasing rate of the inner air temperature as predicted by the heat transfer equations quite well corresponds to the one as evaluated by the simulation, although there is a slight difference.

4. Conclusion

Reliable information through instrumentation systems is essential in mitigating severe accidents such as the one that occurred at the Fukushima Daiichi nuclear power plant. Thermal-hydraulic analyses performed for several major accident scenarios at a PWR plant, including LOFW, LOCA, and SBO, indicate that compartment temperature reaches 600°C in the worst case, although it decreases to 180°C in about 10 minutes. The instrument transmitters cannot perform their intended functions under such high-temperature condition.

In addition to high temperature, the instrumentation systems may also be required to function in harsh condition involving high pressure, high humidity, high radiation, and

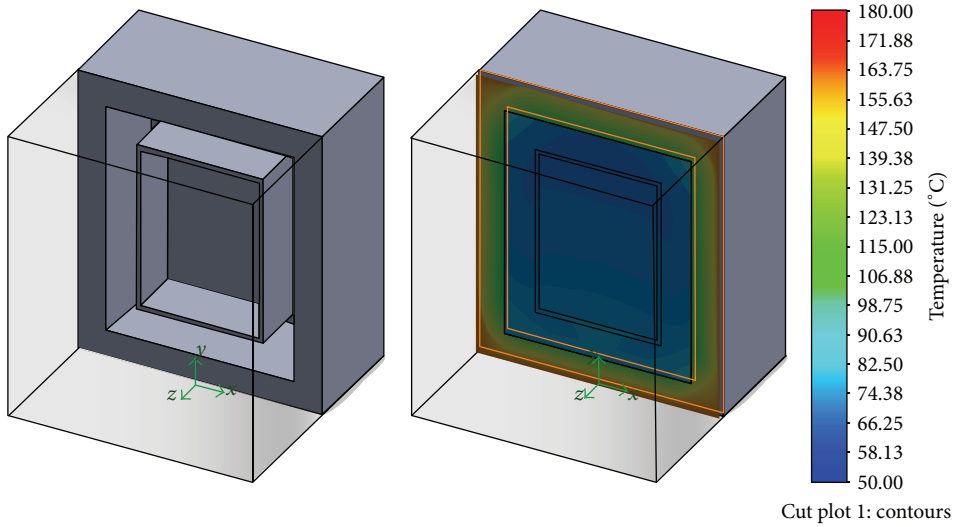

Figure 4: The result of simulation and temperature distribution at $t = 72$ hours.

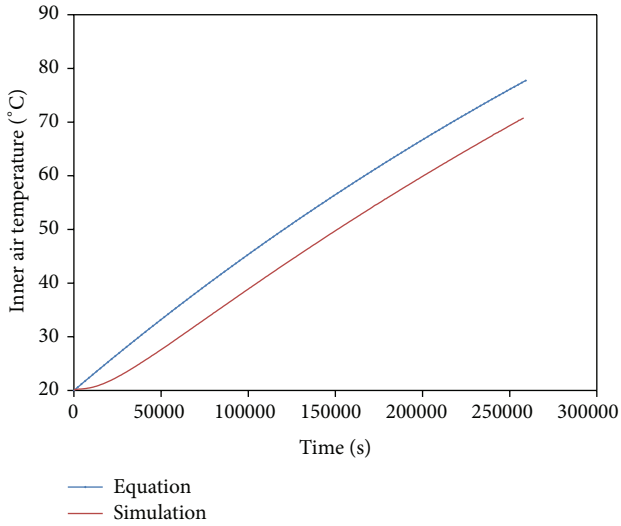

Figure 5: Temperature comparison of the results between equation-based and simulation-based calculations along time.

missiles generated during a severe accident. All those five elements pose a potential threat to the reliability of parameter detection at nuclear power plants. In this study, an analysis was carried out to design an instrument transmitter protecting device that can withstand harsh environment, especially high-temperature condition. Of the various threats to the instrumentation system, high temperature apparently poses the most serious threat, since thin shielding can get rid of pressure, humidity, radiation (alpha and beta), and missile effects.

In this study, a novel concept for designing an instrument transmitter protecting device was developed and investigated by analyzing the heat transfer mechanisms. The protection system may be developed either with or without a cooler, and the design without a cooler turns out to be more effective. The thermal properties and geometry of the protector material also influence the result. Thermal conductivity controls heat conduction itself; on the other hand, heat capacity of the material controls heat spreading by saving heat in the material. The inside heat generation has impact on long-term temperature and heat accumulation. So less heat generating equipment had better be considered. Our study also points out that transient heat transfer and convective heat transfer should be considered to avoid excessively conservatism in the analysis and as a result, obtain a more accurate solution.

Lastly, note that although transmitters can be easily protected from alpha and beta radiations due to the water included in the transmitter protecting device, gamma radiation effects ought to be investigated. The gamma ray dose rate in a reactor was estimated to be larger than 150 Gy/h [14]. Verification experiment is necessary to investigate protector performance in the gamma radiation environment. The next things to do are finding optimized protector structure and material property by developing a more thorough heat transfer model and verifying it through simulation and experiment.

Nomenclature

A_1: Inner protector area (m^2)
A_2: Outer protector area (m^2)
c_1: Specific heat of inner protector (J/kg·K)
c_2: Specific heat of outer protector (J/kg·K)
c_m: Specific heat of intermediate water (J/kg·K)
G: Geometry factor
I: Current (amps)
k_1: Inner protector thermal conductivity (W/m·K)
k_2: Outer protector thermal conductivity (W/m·K)
k_c: Thermal conductivity of TEC (W/m·K)

l: Length difference between inner and outer protector edges (m)
l_{11}, l_{12}, l_{13}: Inner protector length, width, and height (m)
l_{21}, l_{22}, l_{23}: Outer protector length, width, and height (m)
L_1: Inner protector thickness (m)
L_2: Outer protector thickness (m)
m_1: Mass of inner protector (kg)
m_2: Mass of outer protector (kg)
m_m: Mass of intermediate water (kg)
N: Number of TECs
T_c: Cold side temperature (°C)
T_h: Hot side temperature (°C)
T_i: Inside air temperature (°C)
T_{lim}: Limit temperature (°C)
T_m: Intermediate water temperature (°C)
T_o: Ambient temperature (°C)
$T(0)$: Initial temperature (°C)
S: Heat source (W).

Greek Letters

α: Seebeck coefficient (V/K)
ρ: Resistivity (Ω·m).

Conflict of Interests

The authors declare that there is no conflict of interests regarding the publication of this paper.

Acknowledgments

This work was supported by the International Cooperation of the Korea Institute of Energy Technology Evaluation and Planning (KETEP) under Grant funded by the Korea government Ministry of Trade, Industry and Energy (no. 20121610100030).

References

[1] OECD/NEA, *The Fukushima Daiichi Nuclear Power Plant Accident: OECD/NEA Nuclear Safety Response and Lessons Learnt*, Nuclear Energy Agency, Organization for Economic Co-operation and Development, 2013.

[2] C. Miller, A. Cubbage, D. Dorman, J. Grobe, G. Holahan, and N. Sanfilippo, *Recommendations for Enhancing Reactor Safety in the 21st Century: The Near-Term Task Force Review of Insights from the Fukushima Dai-Ichi Accident*, Nuclear Regulatory Commission, 2011.

[3] Nuclear Emergency Response Headquarters, *Report of Japanese Government to the IAEA Ministerial Conference on Nuclear Safety—The Accident at TEPCO's Fukushima Nuclear Power Stations*, Nuclear Emergency Response Headquarters, Government of Japan, 2011.

[4] The National Diet of Japan, Fukushima Nuclear Accident Independent Investigation Commission, *The Official Report of the Fukushima Nuclear Accident Independent Investigation Commission*, The Fukushima Nuclear Accident Independent Investigation Commission, Japan, 2012.

[5] KEPCO and KHNP, *APR1400 Design Control Document Tier 2 Chapter 19: Probabilistic Risk Assessment and Severe Accident Evaluation*, Korea Electric Power Corporation and Korea Hydro & Nuclear Power Company, 2013.

[6] Emerson Process Management Rosemount Nuclear Instruments Inc., "Rosemount 1152 alphaline datasheet—nuclear pressure transmitter," Reference Manual, Emerson Process Management Rosemount Nuclear Instruments Inc., Chanhassen, Minn, USA, 2007.

[7] US NRC, *Final Safety Evaluation Report Related to Certification of the AP1000 Standard Design*, Division of Regulatory Improvement Programs, Office of Nuclear Reactor Regulation, U.S. Nuclear Regulatory Commission, Washington, DC, USA, 2004.

[8] IAEA, "Design measures for prevention and mitigation of severe accidents at advanced water cooled reactors," in *Proceedings of the Technical Committee Meeting*, Vienna, Austria, October 1996.

[9] TEC Microsystems GmbH, *Thermoelectric Cooler Basics*, TEC Microsystems GmbH, Berlin, Germany, 2013.

[10] F. J. Disalvo, "Thermoelectric cooling and power generation," *Science*, vol. 285, no. 5428, pp. 703–706, 1999.

[11] Laird Technologies, *Thermoelectric Handbook*, Laird Technologies, St. Louis, Mo, USA, 2010.

[12] Microtherm, "Microtherm standard panel," Datasheet, 2012.

[13] Z. Luo, "A simple method to estimate the physical characteristics of a thermoelectric cooler from vendor datasheets," *Electronics Cooling*, vol. 14, no. 3, pp. 22–27, 2008.

[14] J. W. Cho and K. M. Jeong, "A performance evaluation of a notebook PC under a high dose-rate gamma ray irradiation test," *Science and Technology of Nuclear Installations*, vol. 2014, Article ID 362354, 8 pages, 2014.

Hindawi Publishing Corporation
Science and Technology of Nuclear Installations
Volume 2014, Article ID 123240, 12 pages
http://dx.doi.org/10.1155/2014/123240

Review Article

Insights on Accident Information and System Operations during Fukushima Events

Man Cheol Kim

School of Energy Systems Engineering, Chung-Ang University, 84 Heukseok-ro, Dongjak-gu, Seoul 156-756, Republic of Korea

Correspondence should be addressed to Man Cheol Kim; charleskim@cau.ac.kr

Received 15 May 2014; Accepted 25 May 2014; Published 5 June 2014

Academic Editor: Inn Seock Kim

As part of the development of an integrated perspective on lessons learned from the Fukushima Daiichi nuclear accident, this paper highlights lessons learned and implications relating to the accident information and system operational aspects during the events. Our analysis clearly indicates that the plant was neither designed nor prepared to withstand such an unexpected event, which included a complete loss of electrical power sources for a long period. The author focused on the accident information and system operational aspects of the Fukushima event, including lack of information, provision of wrong information, operator performance in life-threatening environments, and improvisation given lack of procedures and training. Suggestions for further improvement of the nuclear plant safety are then made with respect to preparation for beyond design basis events, provision of reliable essential information to operators, development of guidelines/procedures, training of operators, and development of operator support systems with consideration of severe accidents caused by unexpected events. It is hoped that the lessons learned from the accident will significantly contribute to the enhancement of nuclear plant safety.

1. Introduction

On March 11, 2011, an earthquake measuring 9.0 on the Richter magnitude scale (M 9.0) occurred off the Pacific coast of Tohoku; this earthquake, together with the subsequent tsunami, caused damage to the Fukushima Daiichi nuclear power plants (NPPs), resulting in severe core damage and considerable release of radioactive materials to the environment. Many organizations investigated the events at the Fukushima site, producing the following reports:

(i) the National Diet of Japan Fukushima Nuclear Accident Independent Investigation Commission (NAIIC report) [1];

(ii) the Investigation Committee on the Accident at Fukushima Nuclear Power Stations of Tokyo Electric Power Company by the Japanese Government (government report) [2, 3];

(iii) the Independent Investigation Commission on the Fukushima Nuclear Accident by the Rebuild Japan Initiative Foundation (RJIF report) [4];

(iv) the Tokyo Electric Power Company and its Fukushima Nuclear Accident Analysis Report (TEPCO report) [5];

(v) the Near-Term Task Force of the United States Nuclear Regulatory Commission (NTTF report) [6];

(vi) the American Nuclear Society Special Committee on Fukushima (ANS report) [7];

(vii) the ASME Presidential Task Force on Response to Japan Nuclear Power Plant Events (ASME report) [8];

(viii) the United Kingdom Office of Nuclear Regulation (UK ONR report) [9];

(ix) the Nuclear Energy Agency of the Organization for Economic Cooperation and Development (OECD/NEA report) [10].

These reports outline lessons learned in relation to the various aspects of the nuclear disaster. Installation or improvement of hardware (such as antitsunami walls, filtered vents, and passive autocatalytic recombiners (PARs), amongst others) is an often cited aspect. The disruption in command

and control has also been discussed frequently in such reviews.

Much research has been conducted to distill lessons learned from the accident. D'Auria et al. [11] reviewed the accident within a technological framework of nuclear reactor safety and provided relevant findings, observations, and recommendations. Hirano et al. [12] reviewed the behavior of reactors at Units 1, 2, and 3, identifying major safety issues such as design basis tsunami, accident management measures, and regulatory treatment of beyond design basis events (BDBEs), among others. Tanaka [13] reviewed the accident and highlighted lessons learned, such as the need for a unique and reliable regulatory body, the backfit rule, and higher engineering competence in light water reactors (LWRs). Urabe et al. [14] discussed lessons learned from the viewpoint of radiation protection from the Fukushima accident, such as the importance of urgent protective actions like evacuation and limiting the intake of foods harvested from contaminated areas.

In order to protect the NPPs and the public safety from danger, various activities are needed including accident prevention, accident response, and emergency preparedness. From a viewpoint of accident response, correct implementation of operation and recovery activities by the shift operators and the recovery team is essential. It is thus important to review and analyze, in a systematic and structured way, the lessons that were learned from the actual response of shift operators and management staff at the Fukushima Daiichi NPPs. Even though several studies have been performed on the human factor aspects of the accident [15] and resilience engineering perspective on the accident [16–18], it seems that there has been few study on the lessons learned from the information and operational aspect of the accident in relation to accident response.

As part of the development of an integrated perspective on lesson learned from the station blackout (SBO) conditions resulting from the M 9.0 earthquake and the subsequent tsunami, this paper highlights the responses of shift operators and emergency management staffs together with implications for accident information and system operational aspects. Section 2 outlines key characteristics relating to the accident. Section 3 discusses accident information and system operational aspects of the accident response. Section 4 outlines lessons learned and their implications, with special attention on instrumentation and control (I&C) systems and human operators in NPPs. Finally, Section 5 presents the conclusions of this paper.

2. Key Characteristics of Fukushima Accident

The Fukushima accident can be characterized as an occurrence of the unexpected events that the plant and the operators were not prepared to cope with, which eventually resulted in considerable core damage and radiation releases to the environment. The unexpected event involved the simultaneous loss of alternate current (AC) and direct current (DC) power in Units 1, 2, and 4 and a prolonged loss of AC power in Units 3 and 5. The unexpected event was not considered in the plant design and operation. There was no guideline or procedure applicable to such an event. Operators were not trained to manage and respond to such an event. Improvisation and trials and errors were only available strategies at the moment. Operators, who did not have enough knowledge of severe accident phenomena, had to find necessary response actions in a very short time and implement them in life-threatening environments.

2.1. Event Outside of the Design Basis. With the term design basis, a NPP is required to withstand a set of postulated accidents without imposing risk to the public health and environment. Additional regulatory requirements, such as the anticipated transient without scram (ATWS) rule (10 CFR 50.62 [19]) and the SBO rule (10 CFR 50.63 [19]) in the United States, were issued to complement regulations based on design basis events. According to the SBO rule, NPPs must be able to withstand an SBO for a specified duration of time and must also be able to recover from it. Station batteries and other necessary support systems are used for this purpose.

The establishment of requirements on design basis events and additional requirements is not intended to ignore those events that lie outside the boundary but rather to focus on those events that lie inside the boundary in order to maximize the safety of NPPs with limited time, resources, and effort. Inevitably, those events considered to lie outside the boundary receive less attention, partly because such boundaries defined only design basis conditions and not beyond design basis events.

In Fukushima Daiichi NPPs, the design basis for flooding by tsunamis was originally 3.1 m at the time of the construction permit, with this later reevaluated to 5.7 m based on the methodology proposed in 2002 [20]. Based on a recognition that tsunami heights may exceed the design basis, Sakai et al. [21] performed probabilistic tsunami hazard analysis in 2006, estimating the frequency of tsunamis higher than 15 meters in 50 years to be approximately four occurrences in every 100,000 years.

It has been argued that the design basis tsunami did not properly reflect historical tsunami experiences in Japan. Uchida and Matsuzawa [22] emphasized the importance of the relationship with a large tsunamigenic earthquake having a recurrence interval of 400–1300 years, as estimated on the basis of geological data. Shibata [23] provided a review of the two gigantic tsunamis, the 869 Jogan tsunami and the 1611 Keicho tsunami, which affected the Sendai plain prior to the 2011 Great East Japan earthquake/tsunami. Shishikura [24] reconstructed the tsunami inundation area of the 869 Jogan earthquake and concluded that the magnitude and source of the tsunami were very similar to those of the 2011 Great East Japan earthquake.

The tsunami of maximum height 15 meters (higher than the design basis) that followed the earthquake caused not only the loss of all AC power (which can be considered to lie inside the regulatory boundary, based on the SBO rule) but also the loss of DC power (which lies outside the boundary). The plant was neither designed nor prepared to withstand such an event. For example, the loss of DC power caused the isolation

interlock of the isolation condenser (IC) in Unit 1, in turn leading to the closure of all valves associated with the IC. If the loss of both AC and DC powers had been considered in the design of the plant, the interlock could have been designed to open all valves, so that core cooling could be maintained.

Narabayashi [25] is of the opinion that had the IC been appropriately operated, the accident would have been terminated quickly; the IC, the valves of which closed as a result of the IC isolation signal (caused by the loss of DC power), can, therefore, be considered a "fail-dangerous system," as opposed to the incorporation of a "fail-safe" mechanism that is typically the case at NPPs. However, one should also bear in mind that should any break occur in the piping of the IC, it would make sense to close the valves so that radioactive steam from the reactor pressure vessel (RPV) would not be released to the reactor building (R/B) or to the environment. Thus, while one type of design seems appropriate for one set of circumstances, such a design may not be as well suited to beyond design basis events. In order to determine optimal system design, systems interaction effects [7] should be carefully analyzed, with consideration and analysis of tradeoffs between advantages and disadvantages under various postulated scenarios. The designer of the Fukushima IC chose from a variety of options (open, close, or stop as is) that are available upon the detection of abnormalities associated with the IC and opted for valve closure to maximize safety, given that the loss of both AC and DC powers was not a consideration during the design phase.

2.2. Prolonged Loss of AC Power. Given that the plant was not designed or prepared for prolonged loss of AC power, the likelihood of the plant being unable to withstand such an event was significant. The Fukushima Daiichi NPPs could have withstood the event by restoring AC power (either through off-site power or through emergency diesel generators (EDGs)) over a very short period, probably less than two hours, since the reactor core of Unit 1 started to be uncovered around this time without IC operation. It should be noted that Fukushima Daiichi Units 5 and 6 and Fukushima Daini NPPs could withstand the event with one air-cooled EDG installed in Unit 6 and the available off-site power, respectively.

In an SBO situation, it is expected that turbine-driven pumps, such as RCIC pumps in Units 2, 3, and 4, and turbine-driven auxiliary feedwater pumps in pressurized water reactors (PWRs) and station batteries will be used to manage the situation for a specified time. Station batteries are expected to provide power to essential components for about four or eight hours, depending on the licensing design of the associated NPP. As noted by Al Shehhi et al. [26], successful mitigation of an SBO eventually requires restoration of AC power. The SBO rule also focuses in the main on restoration of AC power, either through off-site power or through on-site EDGs.

Even though the site superintendent quickly ordered the restoration of off-site power to restore AC power, TEPCO [5] indicated that early restoration of off-site power was extremely difficult. With the complete loss of both AC and DC powers, combined with the failure to quickly restore AC power, difficulties related to the maintenance of core cooling and containment integrity were present from the start.

Table 1 shows the timing of loss and restoration of AC power, as well as the timing of core damage. It took approximately twenty-three days to restore AC power after it was completely lost. It is assumed that RPV injection occurred at the same time that AC is recovered.

As mentioned in the ANS report [7], the dominant core damage scenario identified by probabilistic safety assessments (PSAs) of boiling water reactors (BWRs) results from an SBO combined with eventual failure of the reactor core isolation cooling (RCIC) and high-pressure coolant injection (HPCI) systems. It was very fortunate that the RCIC system in Unit 2 could operate for approximately 70 hours and that the RCIC and HPCI systems in Unit 3 could operate for approximately 35 hours. According to ANS report [7], one should not expect the RCIC system to run beyond 8 hours in an SBO situation. However, in this instance, AC power had not been restored after this interval, nor could an alternative injection to the reactor (after depressurization of the RPV) be established, inevitably resulting in core damage in Units 2 and 3. According to Tanabe [27] and Kataoka [28], core damage started to occur after 2, 5, and 2.5 hours after the loss of emergency core cooling capabilities in the case of Units 1, 2, and 3, respectively.

2.3. Shortage of Available Time. In a simulation of a hypothetical complete SBO at the Browns Ferry Nuclear Plant [29], core uncovery and core damage commenced after 33 and 70 minutes, respectively; this simulation represented a situation in which RCIC and HPCI systems were unavailable owing to closed valves or failed batteries.

According to the ANS report [7], when the emergency core cooling system (ECCS) cannot function properly, the reactor core starts to be uncovered in one to two hours, depending on the reactor design; core damage starts to occur approximately 30 minutes after the core is uncovered. This is in accordance with the Unit 1 MAAP analysis described in the TEPCO report [5], which indicates that top of active fuel (TAF) and bottom of active fuel (BAF) were reached at around 18:10 and 19:40, respectively, approximately 2.5 hours and 4 hours after the occurrence of the SBO. This analysis result is supported by observations of increasing radiation at around 22:00 in the reactor and turbine buildings of Unit 1.

As mentioned above, shift operators in Unit 1 only had one to two hours available to prevent core damage once the IC was not in service. Owing to the short time available for operators to respond to the accident situation when the ECCS cannot perform its intended function, fast recognition of and response to the situation are very important. Such fast response can be accomplished through preprepared and clearly described procedures and through regular training in accordance with these procedures. Without these elements, a rapid response cannot be expected.

2.4. Lack of Procedures and Training for Severe Accidents. As mentioned in the ASME report [8], current accident management in many NPPs is based on the availability of

Table 1: Restoration of AC power.

	Loss of AC power	Core damage	Lighting in main control room	RPV injection (restoration of AC power)
Unit 1	15:37 on March 11	17:42 on March 11	11:30 on March 24	12:12 on April 3
Unit 2		18:48 on March 14	16:46 on March 26	12:12 on April 3
Unit 3		05:18 on March 13		12:18 on April 3

plant status indications and available safety systems. In NPPs lacking both, as was the case during the accident at the Fukushima Daiichi NPPs, mitigation of accidents becomes very difficult. Such conditions were not within the boundary of design basis, and, therefore, NPPs were not sufficiently prepared for such conditions.

In the Fukushima Daiichi nuclear accident, the loss of all AC and DC power resulted not only in the inoperability of important equipment but also in the loss of essential instrumentation. Given that the plant conditions deviated from the basic assumptions underlying emergency operating procedures (EOPs) and accident management guidelines (AMGs) and given that no procedures or guidelines had been available for such conditions that actually occurred, it must have been extremely difficult for the operators to prevent core damage.

For procedures to be used effectively, operator training based on these procedures needs to be accomplished. According to the NAIIC report [1], training relating to the management of severe accidents performed in BWR operator training centers (BTCs) mainly comprised a personal computer- (PC-) based simulator exercise. Moreover, the simulator did not include the IC. Training with site simulators was conducted with instructors explaining how to operate equipment in front of the accident management control panel. Rather than saying that simulator training was insufficient, it would be fair to say that less attention was given to simulator training with severe accident operating procedures (SOPs) than was given to simulator training with EOPs. Needless to say, a severe accident scenario involving the total loss of AC and DC power was not considered in the simulator training.

2.5. Core Damage and Massive Radioactive Releases. The prolonged loss of AC power, combined with shortage of available time and lack of procedures and training, resulted in core damage in Units 1, 2, and 3. Thermal-hydraulic (TH) behavior and the progress of core damage were analyzed by TEPCO using MAAP, as described in the TEPCO report [5]. Sandia National Laboratory performed TH analysis using MELCOR, as described in report [30] and papers [31–33]. Accident progression analysis using MELCOR was also performed by Hoshi and Kawabe [34]. Ishikawa [35] applied THALES2 code to the analysis of accident progression.

Allison et al. [36] calculated possible core/vessel damage states of Units 1, 2, and 3 with RELAP/SCDAPSIM and concluded that not only fuel melting but also the failure of vessels in Unit 1 was likely significant. Parisi et al. [37] also conducted a simulation for Unit 1 with RELAP/SCDAPSIM, with results consistent with those of other simulation studies.

The quantity of radioactive releases due to the accident was estimated by Tomioka and Mørup [38] and Takemura et al. [39]. Le Petit et al. [40] analyzed fission product activities measured approximately 210 km away from the NPP and showed that the reactor cores were exposed to high temperatures for a prolonged period of time. Achim et al. [41] analyzed long-term dispersion of radionuclides and showed that at least 80% of the core inventory was released into the atmosphere.

3. Accident Information and System Operational Aspects

As discussed in Section 2, the plant was neither designed nor adequately prepared for the unexpected event that had actually occurred at the Fukushima NPPs. The total loss of AC power lasted much longer than ever imagined in the nuclear power community; too little time was available for the operators and the recovery team to properly respond to the rapidly evolving events; no guidelines were available at that time that could help them cope with such complex situations caused by the extreme natural disaster and the consequential loss of AC and DC power. Even though core damage could not have been prevented under such conditions, it is important to derive important lessons by looking into the actual situations during the events at Fukushima. Focus herein will be placed on the information and system operational aspects during the events.

3.1. Lack of Information. According to the ATHEANA human reliability analysis (HRA) method [42] that provides a rich and holistic understanding of the context concerning the human factors, four distinct activities are typically performed by the operators in coping with an operational event at NPPs: (1) monitoring/detection, (2) situation assessment, (3) decision making, and (4) implementation. One can easily comprehend that information is essential in each of these activities, and lack of information will have adverse effects on the human performance associated with these activities. Kim and Seong [43] and Lee and Seong [44] provided situation assessment models for shift operators that can be used to estimate such adverse effects based on Bayesian inference.

Given limited resources and staff with limited time available for accident response at Fukushima NPPs, it was important for correct decisions to be made at the earliest possible time during the accident in order to adequately cope

with the evolving events, with time and resources prioritized to respond to the most urgent situations first.

To prevent core damage, it was essential to provide sufficient coolant to each of the reactors and to transfer the decay heat from the reactor to the ultimate heat sink. Information about the RPV water level was crucial for accident management to ensure maintenance of an adequate amount of RPV coolant inventory. As the RPV pressure also had to be properly controlled in order to maintain the integrity of the RPV, the provision of suitable measures to depressurize the reactor in a controlled manner was also needed.

Had the RPV water level indicator in Unit 1 been available and monitored continuously, the decreasing trend in the RPV water level could have alerted shift operators to the fact that the IC was not operating. Drywell (D/W) pressure could also have provided information on the inventory inside the RPV, because an increase in D/W pressure indicates that the reactor has lost an amount of reactor coolant. Shift operators also needed to consider the possibility of a break or leakage in the RPV, which would have resulted in a decrease in the RPV water level and in RPV pressure and an increase in radiation levels in the reactor building (R/B), main control room (MCR), and eventually in the nearby environment.

In Units 3 and 5, DC power was not affected by the tsunami, and, therefore, essential information was available in the MCR. The author believes that the availability of information had significant contribution to the recovery of Unit 5. In Unit 5, because the plant parameters could be monitored in the MCR with the DC power supply, priorities could be given to the restoration of AC power by cross-connecting to the AC power in Unit 6, which was supplied by an air-cooled EDG.

With this in mind, it seems logical that the emergency response team first tried to restore essential instrumentation in the MCR of Units 1 and 2. The RPV water level indicator was restored first through connection with ten batteries in series; this was followed by the D/W pressure indicator, which was restored through connection with a temporary mobile generator located inside the MCR at the time. It is also noteworthy that the shift operators in Unit 5 first tried to restore the AC-powered instrumentations, which can be understood as an attempt to collect more information on the plant status to make optimum decisions at the moment.

The generation of steam from the IC in BWRs indicates that the heat generated inside the RPV is being removed. The amount of steam generation from the IC is proportional to the amount of heat removed inside the RPV. When there is no break or leakage, removal of heat inside the RPV means that inventory and pressure inside the RPV are being maintained. In the case of Unit 1, it was later discovered that heat removal was being performed through subsystem A of the IC, even though this was not known during the initial phase of accident progression. On April 1, 2011, the IC valves were found to be open in the case of the 3A and 2A valves (subsystem A) and closed in the case of the 3B and 2B valves (subsystem B). The shell side water level was found to be 63% and 83% for subsystems A and B, respectively.

In severe accident conditions, it was found to be difficult to obtain information from field indicators by dispatching operators owing to safety concerns. Unit 1 shift operators could not confirm the operational status of the IC, because the dispatched operator returned without information owing to the high radiation level in the R/B. Shift supervisors also hesitated to dispatch operators because of frequent aftershocks, tsunami warnings, and high radiation levels in the R/B. According to Kawano [45], there were 195 aftershocks with magnitude greater than M 5.0 on March 11 alone. The magnitude of three of these was greater than M 7.0.

With significantly insufficient information, decisions thus had to be made under conditions of much uncertainty. The decisions made by different parties involved in the accident were inconsistent, and an issue of command and control was raised owing to these differing decisions. Had there been sufficient information, it is highly likely that decisions made by the different parties would have been similar, possibly resulting in less confusion or conflict among them. It is believed that the lack of information played a significant role in the issue of an unclear command and control line during the progression of the accident.

3.2. Wrong Information. Historically, wrong information has often misled operators from correctly understanding the situation and making decisions accordingly. In the case of the Three Mile Island (TMI) accident [46], the indicator for the pilot operated relief valve (PORV) misled operators into wrongly believing that the PORV was closed. This occurred because the indicator light for the PORV was off, meaning that the electric power to the solenoid was cut off; shift operators interpreted this information to indicate the closure of the PORV. In reality, the PORV was stuck and remained in the open position. Because the shift operators did not realize that this was the case, reactor coolant was escaping from the reactor coolant system (RCS). This misunderstanding on the part of shift operators (or, in other words, the provision of wrong information by the PORV indicator) eventually resulted in damage to the reactor core.

Another example of the provision of wrong information in the TMI NPP was related to the pressurizer level. As the RCS continuously lost coolant through the stuck-open PORV, the pressurizer level shown at the indicator in the MCR gradually increased. This led shift operators to shut down the emergency core cooling pumps, eventually halting emergency injection to the reactor. From that point onwards, human errors have been classified into errors of omission and errors of commission, and significant research has been conducted on the latter especially due to its significant role during the progression of the TMI accident scenario.

In the case of Fukushima Daiichi Unit 1, there were at least two instances of providing wrong information to the shift operators: the notification of steam generation from the IC by the emergency response center (ERC) and the display of the wrong RPV water level. When the shift operators asked the ERC whether the IC was functioning, the ERC confirmed that steam had been generated from the IC at 16:44 on March 11, even though the amount of steam was insignificant. As in the

case of the TMI accident, the RPV water level indicator at the Fukushima Daiichi Unit 1 led operators to mistakenly believe that the reactor had sufficient water to cool the core down. An explanation on the probable cause of the wrong reactor water level indication is provided in the TEPCO investigation report [5].

It is generally speculated that wrong information misled shift operators and the emergency recovery team into focusing on the recovery of Unit 2 instead of Unit 1. The TEPCO report [5] argued that operators focused on the recovery of Unit 1; however, the NAIIC report [1] pointed out that Unit 2 was at first regarded as being most critical, even if Unit 1 was actually in a more critical condition, because the operational status of RCIC in Unit 2 was not known at the moment. This may mean that shift operators and the recovery team paid more attention to the recovery of Unit 2, until the RCIC operational status was confirmed from the field.

3.3. Operator Performance under Life-Threatening Situations. There have been some discussions on the contribution of human errors to the progress of the accident. For example, the government interim report [2] indicated the following problems regarding operator response to the accident:

(i) misjudgment of the operational situation of the IC in Unit 1 (see Table 2);

(ii) poor handling of alternative water injection in Unit 3 (see Table 3).

It is known that the RJIF report [4] also specifically indicated human errors during accident management, such as failures relating to the IC operation in Unit 1 and the shutdown of the HPCI in Unit 3. Among the chronicle records of shift operators' operations in Units 1 and 3 shown in Tables 2 and 3, those marked in bold are what are frequently considered as human errors during the response to the accident, with some backgrounds on why shift operators performed such misoperations.

In addition to the background of such operations, it is also worth reviewing the environment where the shift operators were placed and how HRA methods typically estimate human error probability (HEP) under such an environment. When the SBO occurred, after the NPPs had been hit by the earthquake and tsunami, the shift operators and recovery team found themselves in complete darkness, experienced frequent tremors caused by aftershocks, and may well have feared that their lives were in danger. Under such a life-threatening situation, with frequent aftershocks, tsunami warnings, hydrogen explosions, and high radiation levels, the shift operators, recovery team, and management staff had to manage the unprecedented accident to keep the progression of the accident under control.

In Technique for Human Error Rate Prediction (THERP) [47] and Accident Sequence Evaluation Program (ASEP) [48], developed a long time ago but still widely used in the HRA community, the HEP under life-threatening situations is roughly estimated to be 0.25 with error factor 5 for skilled shift operators. This means that human operators are likely to make mistakes or errors once every four important tasks. In Standardized Plant Analysis Risk-Human Reliability Analysis (SPAR-H) method [49], a multiplier of 5 to the HEP at hand was assigned as a performance shaping factor for the situation when shift operators were under extreme stress situations (less than life-threatening). Even though the situation at the time of the Fukushima accident was worse than the one assumed in THERP [47], ASEP [48], and SPAR-H [49] (namely, a large loss of coolant accident), the shift operators and emergency response team successfully established plans and performed planned tasks with only a few reported minor human errors.

The overall response of the shift operators and emergency response team is considered to be adequate, despite the harsh conditions and staff fears of losing their own lives in such a life-threatening situation.

3.4. Improvisation under Lack of Procedures and Training. The SBO, combined with the loss of DC power, resulted not only in the loss of instrumentation but also in the loss of control of valves, which was due to the loss of motive force. For example, owing to the loss of DC power, the IC valves could not be opened until 18:18 on March 11, when DC power was temporarily available. Shift operators encountered difficulties, particularly in opening the solenoid valves to control the air-operated containment vent valves.

Despite little time being available for shift operators to respond to the accident in order to prevent core damage, no procedures or guidelines were available and no information was provided to the operators. It is important to note that the EOPs and AMGs could not be applied owing to deviations from the basic assumptions necessary to apply them. Frequent aftershocks, tsunami warnings, and high radiation levels inside the R/B prohibited operators from recovery or information collection activities.

Under such circumstance, considerable improvisation was required to devise creative ways to manage the accident. Essential instrumentation was restored using car batteries. Car batteries and temporary air compressors were used in order to attempt to open the valves, until the opening of the valve was successfully accomplished.

The author agrees with the UK ONR's evaluation of shift operators' response [9], which notes that operators were successful in implementing early responses to the accident. It would be desirable though significant efforts are made in the future to avoid or at least reduce the instances where the shift operators have to undergo improvisation during time-critical situations such as the early stage of an accident.

4. Lessons Learned and Implications

One of the important lessons learned is that unexpected events may occur at NPPs, and operators need to be prepared for such unexpected events. For this reason, severe accidents involving core damage need to be considered in the nuclear plant design with proper training provided to the shift operators and the members of technical support centers (TSCs). Essential information should be provided to them in reliable manner without interruption to support their

Table 2: Records related to the operation of the IC and venting in Unit 1.

Date	Time	Event
March 11	2:46 pm	Earthquake, loss of offsite power, reactor trip, and IC autostart Fast cooldown (>55°C/hr) and operator closed MO-3A, 3B Control (open/close) of MO-3A (3 times before tsunami)
	3:42 pm	Tsunami and SBO (**operator unable to remember valve position**)
	6:18 pm	Temporary restoration of DC power MO-2A, 3A closed ⟶ open (confirmed with indication)
	6:25 pm	**MO-3A closed** (unable to observe steam, fear of water depletion) **No report to emergency response center**
	8:07 pm	RPV pressure (in the field) = 6.9 MPa
	9:30 pm	Temporary restoration of DC power MO-3A open (steam generation confirmed)
	11:50 pm	Battery connection to D/W pressure gauge (600 kPa)
March 12	2:30 am	D/W pressure = 840 kPa (P_{design} = 528.3 kPa)
	3:45 am	Repeated confirmation of vent operation
	5:46 am	Started to pump fresh water through fire pumps to the RPV
	8:27 am	Confirmed that evacuation is not complete
	8:37 am	Informed Prefectural Government of venting at 9:00 am
	9:03 am	Confirmed that evacuation is complete

Table 3: Records related to manual trip of HPCI in Unit 3.

Date	Time	Event
March 11	4:04 pm	RCIC manual start (operator confirmed low reactor water level)
March 12	11:36 am	RCIC trip. Unable to restart
	12:35 pm	HPCI autostart Operators pay attention to reactor level, HPCI flow
	8:36 pm	Depletion of battery. Loss of reactor level indicator
March 13	2:42 am	HPCI outlet pressure close to reactor pressure (0.8-0.9 MPa) Plan to depressurize reactor using SRV (to 0.61 MPa) **HPCI manual trip**
	2:45 am	Failure in SRV remote open (possibility that battery power low)
	5:00 am	Reactor pressure = 7.38 MPa
	7:00 am	Car batteries connected to SRV
	8:41 am	Venting line-up (except rupture disk) complete

various activities associated with accident management. This section outlines lessons learned and their implications from the accident, with special attention to instrumentation and control (I&C) systems and human operators to enhance the nuclear plant safety through proper design and accident management for such unexpected events.

4.1. Preparation for Beyond Design Basis Events. One of the important lessons learned from the accident would be the need for fundamental changes in safety approaches and thinking [50]. Yang [51] pointed out that the deterministic approach alone was found to be insufficient in deriving the design basis for tsunamis and that a probabilistic approach should, therefore, be used in a complementary manner to address large uncertainties associated with natural hazards. Deterministic safety assessment (DSA) and PSA were developed and conducted by different groups of people, as in the case of seismic PSA and tsunami PSA having been developed independently [52]. The complementary use and/or harmonization of deterministic and probabilistic approaches, such as in the approach proposed by Kang et al. [53], seems to be the right direction for future risk assessments based on the lessons learned from the accident.

In this sense, the risk-informed defense-in-depth framework, which was originally proposed by Fleming and Silady [54], has been receiving increasing attention as the USNRC's NTTF report [6] highlighted the concept as the new framework for the post-Fukushima era. After reviewing the Fukushima accident with the defense-in-depth (DID) and risk viewpoints, Yang [51] explained how risk insights can contribute to strengthening DID or developing a new risk-informed DID framework. Suzuki [55] interpreted the Japanese government's recommendation of swift utilization of PSA and improvements of safety measures as Japanese

safety regulations' departure from being a "zero-risk" culture, providing a lesson to all 31 countries with nuclear power.

In Europe, the attempt to consider more accident scenarios to enhance nuclear safety by taking both deterministic and probabilistic approaches into account resulted in the introduction of design extension conditions (DECs). DECs were originally proposed by European Utility Requirement (EUR) and appeared in International Atomic Energy Agency (IAEA) Draft Safety Standard DS 414 in, 2010, with this later formally published as IAEA SSR-2/1 [56]. The purpose of DECs was to further improve the safety of NPPs by addressing additional accident scenarios that involve accidents more severe than design basis accidents or involving multiple failures. DECs need to be derived on the basis of expert judgment, deterministic assessment, and probabilistic assessment. The inclusion of DECs in the regulatory boundary would impose strict requirements on the design and operation of NPPs, with consideration of accidents with complex sequences and severe accidents involving core damage. Examples of DECs considered in EURs are ATWS and SBO, which are also considered in the regulatory framework in the United States based on the risk insights from PSA studies. Containment bypass accident such as steam generator tube rupture (SGTR) accidents combined with main steam line break (MSLB) is another example of DEC.

In considering additional accident scenarios, the dependency between different events needs to be carefully examined. Pate-Cornell [57] noted that the M 9.0 earthquake and the 14-meter high tsunami during the Fukushima accident provide an example of the dependent conjunction that should have been properly addressed by reviewing historical records. Ebisawa et al. [52] pointed out that the dependency between seismic ground motion effects and/or tsunami effects has not been properly considered because seismic and tsunami PSAs were developed independently for reasons of efficiency.

Despite the high safety standards in the nuclear industry, severe accidents involving core damage could not be completely prevented. According to Kaiser [58], the three severe accidents (TMI, Chernobyl, and Fukushima) in commercial nuclear facilities occurred with a period of approximately 4,000 to 5,000 reactor years (RY). From the historical experience of such severe accidents, growing attention is being given to accident management. The report by the OECD/NEA task group on accident management [59] proposed the development of the integrative accident management (IAM) approach to provide the right balance and prioritization of accident prevention and accident management. Plant design needs to consider the accident management under severe accidents, such as essential information, operator support systems, and associated operator training.

4.2. Reliable Essential Information under Severe Accidents. From the accident information and system operation viewpoint, the need for essential information to make proper decisions would be one of the most important lessons learned from the accident. It was found that the information necessary to clearly understand the progression of severe accidents was not provided sufficiently for shift operators. Shift operators were uncertain as to whether core damage was occurring, how much of the core was damaged, how much hydrogen was generated by the zirconium-steam reaction, and so on, until they experienced the hydrogen explosions.

It is speculated that if the shift operators at Fukushima Daiichi Unit 1 had recognized the status of the IC and successfully performed necessary actions to recover its functions, core cooling at Unit 1 could have been maintained for some time. Even though the IC at Unit 1 could operate for about 10 hours (and its operation time could have been extended by making up the IC tanks with diesel-driven fire protection (DDFP) pumps, fire engines, and other such power sources), it is yet uncertain whether core damage could have been prevented by operating the ICs for an extended period. However, situations might have been quite different if it had been the case, since a lot of other options might have been developed and implemented, potentially avoiding core damage.

To provide essential information to shift operators in a reliable way, possible additional instrumentations for severe accidents may include the following:

(i) temperature measurements in various locations inside an RPV, including the lower head [7];

(ii) hydrogen concentration and radiation level measurements [7];

(iii) water level and temperature measurements for spent fuel pools [6, 7, 10].

Also, measures to provide protection for the essential information need to be considered for implementation at NPPs, such as the following:

(i) improved protection for station batteries [7, 10];

(ii) alternative connectable electrical power supplies for essential instrumentation [7, 10];

(iii) enhancement of essential instrumentation to survive under extreme environments [10];

(iv) DC power load shedding for essential instrumentation [10];

(v) better understanding of limitations of essential instrumentation [10].

In PWRs, steam generators (SGs) are analogous to the ICs in BWRs, and therefore the accident progression in Unit 1 provides important lessons on how to enhance the safety of PWRs. Based on the TH analysis with RELAP5/MOD3.3, Prošek and Cizelj [60] showed that core uncovery can be significantly delayed by using turbine-driven pump systems and manually depressurizing the RCS. The successful operation of the auxiliary feedwater system (AFWS), the successful dump of steam to the atmosphere (the ultimate heat sink), and, therefore, the successful depressurization of RCS should be carefully monitored. It should be also noted that pressurizer and accumulator level during depressurization can assist inventory control and prevent nitrogen injection from the accumulators. The FLEX methodology [61] provides much information on instrumentation and control requirements such as the essential parameters for key safety functions in PWRs and BWRs.

4.3. Operator Support Systems for Severe Accidents. The analysis of the response of Fukushima Daiichi Unit 1 shift operators gives the impression that they did not consider the status of the plant as being critical, though it actually was. Had they recognized that core damage might potentially occur just two hours after the occurrence of an SBO (given that the IC was not in service), their response might have been different. For instance, they might have assigned higher priority to the confirmation of the operational status of the IC.

Upon investigation of why ICs were not operating, it was found that the isolation interlock closed all valves associated with ICs when abnormalities (including the loss of DC power) were detected. The government interim report [2] criticized the shift operators on duty and the staff members of the emergency response centers as having insufficient understanding of the functioning of the IC, especially of its fail-safe feature. However, the author believes that it would be very difficult to memorize all interlock relations in the plant during periods of extreme stress, especially when such interlock operations are neither frequently encountered during normal operation nor covered in the operator training under simulated emergency conditions. It must be borne in mind that the loss of all AC and DC power constituted an extraordinary accident situation, to which neither EOPs nor AMGs could be applied.

Under such rare situations, operator support systems may provide important technical assistance to shift operators. A faster-than-real-time simulator [7] is an example that may help shift operators make important decisions, such as dispatching operators to the field (where radiation levels are high) for information collection and restoration of critical equipment, venting of radioactive steam to the environment, and evacuation of people living nearby. For this reason, the development of operator support systems for severe accidents needs to be encouraged.

5. Conclusions

Under the conditions of loss of both AC and DC powers that occurred after the earthquake and tsunami at Fukushima Daiichi NPPs, there may have been a slight chance of the plants recovering from the progression towards core damage. However, based on the recognition that the plants were not designed nor prepared to withstand such an event and that shift operators and management staff were likewise unprepared for this eventuality, the occurrence of core damage does not seem to have been avoidable. Nevertheless, it would be still important to review the accident by highlighting the accident information and system operation aspects from the wide range of information already known and to derive lessons learned from the performance of shift operators in such a hopeless situation.

In view of the fact that an effective response to an accident, with timely and proper operator actions, is pivotal to enhancing the safety of NPPs, the discussion in this paper pays special attention to the accident information and system operational aspects of the Fukushima accident. The accident information aspect was found to include lack of information and the provision of wrong information to shift operators. The system operational aspect was found to include operator performance under life-threatening situations and improvisation given lack of procedures and training. From the accident information and system operational aspects of the lessons learned, implications for improving the nuclear plant safety were derived, with examples including preparation for BDBEs, provision of reliable essential information to operators, development of guidelines/procedures, training of operators, and development of operator support systems, with consideration of severe accidents caused by unexpected events.

It is also worth looking into the potential contribution of research and development (R&D) for the improvement of operator response capability under severe accident conditions. It is unfortunate that the R&D results relating to severe accidents, which have accumulated over a long time period, could not provide immediate assistance to the shift operators in the MCR and the emergency response members in the TSC or elsewhere during the accident. The author believes that the development of operator support systems for severe accidents, such as an accident diagnosis tool, will serve as a connection point between the needs of the nuclear industry to enhance response capabilities for severe accidents and the accumulated knowledge on the R&D side.

To improve the nuclear plant safety based on the lessons learned from the chaotic accident at the Fukushima Daiichi NPPs, it is necessary to consider a broader spectrum of events and conditions, and train the shift operators and the emergency response staff against such events and conditions. More efforts are also needed to (1) identify potential hazards that may threaten the NPP safety; (2) devise and implement effective prevention and mitigation measures against such hazards; and (3) explore and implement recovery strategies and emergency preparedness measures following core damage or release of radioactive materials to the environment. The considerable activities, currently being carried out throughout the US nuclear industry to implement the FLEX methodology, are apparently in a right direction in this regard.

The nuclear industry learned very expensive lessons as a result of the Fukushima Daiichi nuclear accident. It is hoped that the lessons learned from the accident will significantly contribute to the improvement of nuclear plant safety in the most cost-effective manner.

Conflict of Interests

The author declares that there is no conflict of interests regarding the publishing of this paper.

Acknowledgments

This research was supported by Chung-Ang University Research Grants received in 2013. It was also supported by a Grant from the Nuclear Safety Research Program of the Korea Radiation Safety Foundation with funding by the Korean government's Nuclear Safety and Security Commission (Grant no. 1305008-0113-SB110).

References

[1] "The national diet of japan fukushima nuclear accident independent investigation commission," The Official Report of the Fukushima Nuclear Accident Independent Investigation Commission, The National Diet of Japan, 2012.

[2] "Investigation committee on the accident at Fukushima nuclear power stations of Tokyo electric power company (established by the cabinet)," Interim Report, 2011.

[3] "Investigation committee on the accident at Fukushima nuclear power stations of Tokyo electric power company (established by the cabinet)," Final Report, 2012.

[4] "Independent investigation commission on the Fukushima Daiichi nuclear accident," Investigation and Verification Report of Independent Investigation Commission on the Fukushima Daiichi Nuclear Accident, Discover Twenty-One, Rebuild Japan Initiative Foundation, 2012.

[5] Fukushima Nuclear Accidents Investigation Committee, Fukushima Nuclear Accidents Investigation Report, Tokyo Electric Power Company, 2012.

[6] C. Miller, A. Cubbage, D. Dorman, J. Grobe, G. Holahan, and N. Sanfilippo, *Recommendations for Enhancing Reactor Safety in the 21st Century: The Near-Term Task Force Review of Insights from the Fukushima Dai-Ichi Accident*, United States Nuclear Regulatory Commission, Washington, DC, USA, 2011.

[7] Special Committee on Fukushima, *Fukushima Daiichi: ANS Committee Report*, American Nuclear Society, La Grange Park, Ill, USA, 2012.

[8] *The ASME Presidential Task Force on Response to Japan Nuclear Power Plant Events, Forging a New Nuclear Safety Construct*, The American Society of Mechanical Engineers, New York, NY, USA, 2012.

[9] HM Chief Inspector of Nuclear Installations, *Chief Nuclear Inspector's Report on Lessons Fukushima*, Office for Nuclear Regulation, Bootle, UK, 2011.

[10] Nuclear Energy Agency, "The Fukushima Daiichi nuclear power plant accident: OECD/NEA nuclear safety response and lessons learnt," Tech. Rep. NEA no. 7161, Organisation for Economic Cooperation and Development/Nuclear Energy Agency (OECD/NEA), 2013.

[11] F. D'Auria, G. Galassi, P. Pla, and M. Adorni, "The Fukushima event: the outline and the technological background," *Science and Technology of Nuclear Installations*, vol. 2012, Article ID 507921, 25 pages, 2012.

[12] M. Hirano, T. Yonomoto, M. Ishigaki et al., "Insights from review and analysis of the Fukushima Dai-ichi accident," *Journal of Nuclear Science and Technology*, vol. 49, no. 1, pp. 1–17, 2012.

[13] S.-I. Tanaka, "Accident at the Fukushima Dai-ichi nuclear power stations of TEPCO—outline & lessons learned," *Proceedings of the Japan Academy B*, vol. 88, no. 9, pp. 471–484, 2012.

[14] I. Urabe, T. Hattori, T. Iimoto, and S. Yokoyama, "Radiation protection lessons learned from the TEPCO Fukushima No. 1 NPS accident," *Journal of Nuclear Science and Technology*, vol. 51, no. 2, pp. 136–149, 2014.

[15] H. Sakuda and M. Takeuchi, "Safety-critical human factors issues derived from analysis of the TEPCO Fukushima Daiichi accident investigation reports," *Nuclear Safety and Simulation*, vol. 4, no. 2, pp. 135–146, 2013.

[16] E. Hollnagel and Y. Fujita, "The Fukushima disaster-systemic failures as the lack of resilience," *Nuclear Engineering and Technology*, vol. 45, no. 1, pp. 13–20, 2013.

[17] Y. Ohsuga, T. Yoshida, and H. Sakuda, "Critical review on what factors affected the evolution of the Fukushima accident," *Nuclear Safety and Simulation*, vol. 4, no. 1, pp. 10–21, 2013.

[18] J. Park, T. P. Seager, P. S. C. Rao, M. Convertino, and I. Linkov, "Integrating risk and resilience approaches to catastrophe management in engineering systems," *Risk Analysis*, vol. 33, no. 3, pp. 356–367, 2013.

[19] *10 CFR Part 50: Domestic Licensing of Production and Utilization Facilities*, United States Nuclear Regulatory Commission, Washington, DC, USA, 1956.

[20] International Atomic Energy Agency, *IAEA International Fact Finding Expert Mission of the Fukushima Dai-Ichi NPP Accident Following the Great East Japan Earthquake and Tsunami*, International Atomic Energy Agency, Vienna, Austria, 2011.

[21] T. Sakai, T. Takeda, H. Soraoka, K. Yanagisawa, and T. Annaka, "Development of a probabilistic tsunami hazard analysis in Japan," in *Proceedings of the 14th International Conference on Nuclear Engineering (ICONE-14)*, Miami, Fla, USA, July 2006.

[22] N. Uchida and T. Matsuzawa, "Coupling coefficient, hierarchical structure, and earthquake cycle for the source area of the 2011 off the Pacific coast of Tohoku earthquake inferred from small repeating earthquake data," *Earth, Planets and Space*, vol. 63, no. 7, pp. 675–679, 2011.

[23] A. Shibata, "Importance of the inherited memories of great tsunami disasters in natural disaster reduction," in *Proceedings of the International Symposium on Engineering Lessons Learned from the 2011 Great East Japan Earthquake*, Tokyo, Japan, March 2012.

[24] M. Shishikura, Y. Sawai, and Y. Namegaya, "Reconstruction of the 869 Jogan Earthquake, the predecessor of the 2011 Tohoku earthquake, by geological evidence combined with tsunami simulation," in *Proceeding of the International Symposium on Backward Problems in Geotechnical Engineering and Monitoring of Geo-Construction*, pp. 25–28, Osaka, Japan, 2011.

[25] T. Narabayashi, "Lessons learned from the Fukushima Daiichi nuclear power plant accident," in *Proceedings of the 7th International Symposium On Turbulence, Heat and Mass Transfer*, Palermo, Italy, September 2012.

[26] A. S. Al Shehhi, S. H. Chang, S. H. Kim, and H. G. Kang, "Analysis of economics and safety to cope with station blackout in PWR," *Annals of Nuclear Energy*, vol. 59, pp. 63–71, 2013.

[27] F. Tanabe, "Analyses of core melt and re-melt in the Fukushima Daiichi nuclear reactors," *Journal of Nuclear Science and Technology*, vol. 49, no. 1, pp. 18–36, 2012.

[28] I. Kataoka, "Review of thermal-hydraulic researches in severe accidents in light water reactors," *Journal of Nuclear Science and Technology*, vol. 50, no. 1, pp. 1–14, 2013.

[29] D. D. Yue and W. A. Condon, "Severe-accident-sequence assessment of hypothetical complete-station blackout at the browns ferry nuclear plant," in *Proceedings of the International ANS/ENS Topical Meeting on Probabilistic Risk Assessment*, New York, NY, USA, September 1981.

[30] R. Gauntt, D. Kalinich, J. Cardoni et al., "Fukushima Daiichi accident study (status as of April 2012)," Tech. Rep. SAND2012-6173, Sandia National Laboratories, Albuquerque, NM, USA, 2012.

[31] R. Gauntt, D. Kalinich, J. Cardoni, and J. Phillips, "MELCOR simulations of the severe accident at the Fukushima 1F1 reactor," in *Proceedings of the International Meeting on Severe Accident Assessment and Management: Lessons Learned from Fukushima Dai-ichi*, pp. 212–221, San Diego, Calif, USA, November 2012.

[32] J. Phillips, J. Cardoni, R. Gauntt, and D. Kalinich, "MELCOR simulations of the severe accident at the Fukushima 1F2 reactor," in *Proceedings of the International Meeting on Severe Accident Assessment and Management : Lessons Learned from Fukushima Dai-ichi*, pp. 334–342, San Diego, Calif, USA, November 2012.

[33] J. Cardoni, R. Gauntt, D. Kalinich, and J. Phillips, "MELCOR simulations of the severe accident at the Fukushima 1F3 Reactor," in *Proceedings of the International Meeting on Severe Accident Assessment and Management 2012: Lessons Learned from Fukushima Dai-ichi*, pp. 346–359, San Diego, Calif, USA, November 2012.

[34] H. Hoshi and R. Kawabe, "Accident sequence analysis of unit 1 to 3 using MELCOR code," in *Proceedings of the Technical Workshop on TEPCO's Fukushima Dai-ichi NPS Accident*, Tokyo, Japan, July 2012.

[35] J. Ishikawa, "Analysis for accident progression with THALES2 code," in *Proceedings of the Technical Workshop on TEPCO's Fukushima Dai-ichi NPS Accident*, Tokyo, Japan, July 2012.

[36] C. M. Allison, J. K. Hohorst, B. S. Allison et al., "Preliminary assessment of the possible BWR core/vessel damage states for Fukushima Daiichi station blackout scenarios using RELAP/SCDAPSIM," *Science and Technology of Nuclear Installations*, vol. 2012, Article ID 646327, 25 pages, 2012.

[37] C. Parisi, A. Del Nevo, E. Negrenti, and M. Sepielli, "Simulation & analysis of the severe accident of the unit 1 of Fukushima Daiichi NPP," in *Energia, Ambiente e Innovazione*, pp. 56–61, 2012.

[38] R. Tomioka and M. Mørup, "A Bayesian analysis of the radioactive releases of Fukushima," in *Proceedings of the 15th International Conference on Artificial Intelligence and Statistics (AISTATS '12)*, la Palma Canary Islands, Spain, April 2012.

[39] T. Takemura, H. Nakamura, M. Takigawa et al., "A numerical simulation of global transport of atmospheric particles emitted from the Fukushima Daiichi nuclear power plant," *Scientific Online Letters on Atmosphere*, vol. 7, pp. 101–104, 2011.

[40] G. le Petit, G. Douysset, G. Ducros et al., "Analysis of radionuclide releases from the fukushima dai-ichi nuclear power plant accident part I," *Pure and Applied Geophysics*, vol. 171, pp. 629–644, 2014.

[41] P. Achim, M. Monfort, G. le Petit et al., "Analysis of radionuclide releases from the fukushima dai-ichi nuclear power plant accident part II," *Pure and Applied Geophysics*, vol. 171, pp. 645–667, 2014.

[42] S. E. Cooper, A. M. Ramey-Smith, J. Wreathall et al., "A Technique for Human Error Analysis (ATHEANA)—technical basis and methodology description," Tech. Rep. NUREG/CR-6350, United States Nuclear Regulatory Commission, Washington, DC, USA, 1996.

[43] M. C. Kim and P. H. Seong, "An analytic model for situation assessment of nuclear power plant operators based on Bayesian inference," *Reliability Engineering and System Safety*, vol. 91, no. 3, pp. 270–282, 2006.

[44] H.-C. Lee and P.-H. Seong, "A computational model for evaluating the effects of attention, memory, and mental models on situation assessment of nuclear power plant operators," *Reliability Engineering and System Safety*, vol. 94, no. 11, pp. 1796–1805, 2009.

[45] A. Kawano, "Facts and lessons of the Fukushima nuclear accident and safety improvement—the operator viewpoints," in *Proceedings of the DOE Nuclear Safety Workshop*, Bethesda, Maryland, September 2012.

[46] J. G. Kemeny, *The Need for Change: The Legacy of TMI*, The President's Commission on the Accident at TMI, Washington, DC, USA, 1979.

[47] A. D. Swain and H. E. Guttman, "Handbook of human reliability analysis with emphasis on nuclear power plant applications," Tech. Rep. NUREG/CR-1278, United States Nuclear Regulatory Commission, Washington, DC, USA, 1983.

[48] A. D. Swain, "Accident sequence evaluation program human reliability analysis procedure," Tech. Rep. NUREG/CR-4772, United States Nuclear Regulatory Commission, Washington, DC, USA, 1987.

[49] D. Gertman, H. Blackman, J. Marble, J. Byers, and C. Smith, "The SPAR-H human reliability analysis method," Tech. Rep. NUREG/CR-6883, United States Nuclear Regulatory Commission, Washington, DC, USA, 2005.

[50] G. Vayssier, "Present day EOPs and SAMG—where do we go from here?" *Nuclear Engineering and Technology*, vol. 44, no. 5, pp. 225–236, 2012.

[51] J.-E. Yang, "Fukushima dai-ichi accident: lessons learned and future actions from the risk perspectives," *Nuclear Engineering and Technology*, vol. 46, no. 1, pp. 27–38, 2014.

[52] K. Ebisawa, M. Fujita, Y. Iwabuchi, and H. Sugino, "Current issues on PRA regarding seismic and tsunami events at Muliti units and sites based on lessons learned from Tohoku earthquake/tsunami," *Nuclear Engineering and Technology*, vol. 44, no. 5, pp. 437–452, 2012.

[53] D. G. Kang, S.-H. Ahn, and S. H. Chang, "A combined deterministic and probabilistic procedure for safety assessment of beyond design basis accidents in nuclear power plant: application to ECCS performance assessment for design basis LOCA redefinition," *Nuclear Engineering and Design*, vol. 260, pp. 165–174, 2013.

[54] K. N. Fleming and F. A. Silady, "A risk informed defense-in-depth framework for existing and advanced reactors," *Reliability Engineering and System Safety*, vol. 78, no. 3, pp. 205–225, 2002.

[55] T. Suzuki, "Deconstructing the zero-risk mindset: the lessons and future responsibilities for a post-Fukushima nuclear Japan," *Bulletin of the Atomic Scientists*, vol. 67, no. 5, pp. 9–18, 2011.

[56] IAEA, "Safety of nuclear power plants: design, IAEA specific safety requirements," Tech. Rep. SSR-2/1, International Atomic Energy Agency, Vienna, Austria, 2012.

[57] E. Paté-Cornell, "On "black swans" and "perfect storms": risk analysis and management when statistics are not enough," *Risk Analysis*, vol. 32, no. 11, pp. 1823–1833, 2012.

[58] J. C. Kaiser, "Empirical risk analysis of severe reactor accidents in nuclear power plants after fukushima," *Science and Technology of Nuclear Installations*, vol. 2012, Article ID 384987, 6 pages, 2012.

[59] Nuclear Energy Agency, "Accident management insights after the Fukushima Daiichi NPP accident," Tech. Rep. NEA/CNRA/R(2014)2, Organisation for Economic Cooperation and Development/Nuclear Energy Agency (OECD/NEA), 2014.

[60] A. Prošek and L. Cizelj, "Long-term station blackout accident analyses of a PWR with RELAP5/MOD3.3," *Science and Technology of Nuclear Installations*, vol. 2013, Article ID 851987, 15 pages, 2013.

[61] Nuclear Energy Institute, "Diverse and flexible coping strategies (FLEX) implementation guide," Tech. Rep. NEI 12-06, Rev.0, Nuclear Energy Institute, Washington, DC, USA, 2012.

Hindawi Publishing Corporation
Science and Technology of Nuclear Installations
Volume 2014, Article ID 874134, 5 pages
http://dx.doi.org/10.1155/2014/874134

Research Article

Estimation of Intervention Distances for Urgent Protective Actions Using Comparative Approach of MACCS and InterRAS

Mazzammal Hussain,[1] Salah Ud-Din Khan,[2] Waqar A. Adil Syed,[1] and Shahab Ud-Din Khan[3]

[1] *Department of Physics, Faculty of Basic and Applied Sciences, International Islamic University, H-10, Islamabad 44000, Pakistan*
[2] *Deanship of Scientific Research, College of Engineering, King Saud University, P.O. Box 800, Riyadh 11421, Saudi Arabia*
[3] *Tokamak Design Division, Institute of Plasma Physics, Chinese Academy of Sciences, 350 Shushanhu Road, Hefei, Anhui 230031, China*

Correspondence should be addressed to Salah Ud-Din Khan; drskhan@ksu.edu.sa

Received 19 January 2014; Revised 1 April 2014; Accepted 3 May 2014; Published 28 May 2014

Academic Editor: Inn Seock Kim

Distances for taking evacuation as a protective measure during early phase of a nuclear accident have been approximated using MELCOR Accident Consequence Code System (MACCS). As a reference data, the source term of Pakistan Research Reactor 1 (PARR-1) and meteorological data of Islamabad, Pakistan, have been considered. Based on comparison with published data and international radiological assessment (InterRAS) code results, it is concluded that MACCS is a rational tool for estimation of urgent protective actions during early phase of nuclear accident by taking into account the variations in meteorological and release concentrations parameters.

1. Introduction

A range of probable accidents are associated with nuclear power plants starting with minor incident to immense disaster. Different researchers had used MACCS code to analyze the nuclear power plants accident consequences. Jongtae Jeong and Wondea Jung studied estimation of early health effects for different combinations of release parameters and meteorological data using MACCS code for Younggwang 3 and 4 nuclear power plants in Korea concluding that, with the same amount of radioactive material released to the atmosphere, a large difference in early health effects from case to case was observed [1]. Haste and coworkers attempted to demonstrate a MELCOR-MACCS capability to simulate the accident scenarios for the whole plant, including the containment response and off-site consequences arising from fission product release from the containment. The results provided a good basis for the NPP analysis foreseen [2]. Ke-Shih performed reevaluation of emergency planning zones (EPZs) for nuclear power plants (NPPs) using MACCS2 code and concluded that the radius identified previously is a reasonable conservative value of EPZs for each of the three operating NPPs in Taiwan [3]. Jeong and Ha studied influence of source term release parameters on health effects for Younggwang 3 and 4 nuclear power plants in Korea using MACCS code and concluded that the research work will be very useful for developing strategies for reducing off-site consequences of accident management if they are combined with influence of weather conditions [4]. Thaning and Baklanov considered a simulated accident at a nuclear power plant that could cause a large release of radioactivity into the atmosphere. The consequence analysis was performed using a 3-dimensional mesoscale model and MACCS code [5].

2. Research Methodology

2.1. Computational Technique: MACCS Code. Sandia National Laboratories developed MELCOR Accident Consequence Code System (MACCS) for the consequence assessment of

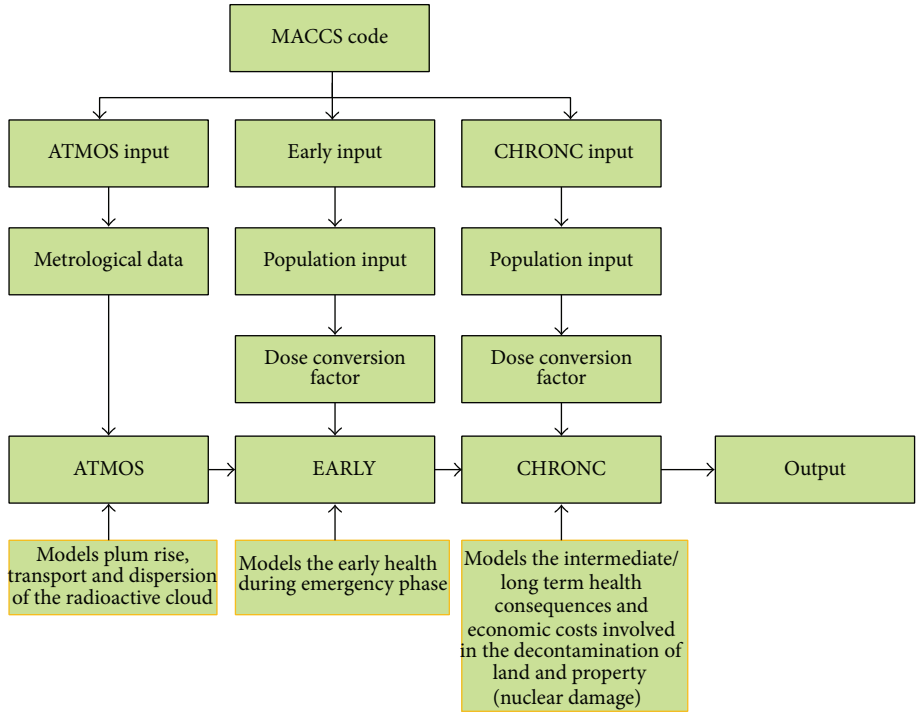

Figure 1: Flow diagram of MACCS code.

severe accidents at nuclear power plants. MACCS is organized into three modules, the ATMOS module which performs the atmospheric transport and deposition portion of the calculation, the EARLY module which estimates the consequences of the accident immediately after the accident usually within the first week, and the CHRONC module which estimates the long term consequences of the accident. The flow diagram of MACCS code [6–8] is shown in Figure 1.

In MACCS code, Gaussian plume model has been used for the study of atmospheric dispersion of radioactive material and vertical and crosswind distributions. The plume dimensions are defined in vertical and crosswind direction by the standard deviations (σ_y, σ_z) of the normal distribution of material concentration in crosswind and vertical directions. The general form of the Gaussian plume equation is

$$\chi(x,y,z) = \frac{Q}{2\pi\overline{u}\sigma_y\sigma_z} \times \exp\left[-\frac{1}{2}\left(\frac{y}{\sigma_y}\right)^2\right] \exp\left[-\frac{1}{2}\left(\frac{z-h}{\sigma_z}\right)^2\right], \quad (1)$$

where $\chi(x,y,z)$ is the time integrated air concentration (Bq-s/m^3) at the downwind location (x,y,z), Q is the source strength (Bq), $\overline{u}$ is the mean downwind speed, σ_y and σ_z are the standard deviations (m) of the normal concentration distribution along crosswind and vertical direction, and h is the release height (m).

Equation (1) is not applicable when plume expands vertically and is bounded by mixing layer or by the ground. To solve this problem, ground and mixing layers are considered as totally reflecting boundaries. This is achieved by adding a mirror image source below the ground and above the inversion layer. By considering this effect in (1), the centerline air concentration $\chi(x = 0,\ y = 0,\ z = H)$ and ground concentrations $\chi(x = 0,\ y = 0,\ z = 0)$, after time of release to the time at which the concentrations become uniform along vertical direction, are given by

$$\begin{aligned}\chi(x, y = 0, z) &= \frac{Q}{2\pi\sigma_y\sigma_z\overline{u}}\left[\exp\left[-\frac{1}{2}\left(\frac{z-H}{\sigma_z}\right)^2\right]\right. \\ &\quad + \exp\left[-\frac{1}{2}\left(\frac{z+H}{\sigma_z}\right)^2\right] \\ &\quad + \sum_{n=1}^{5}\left\{\exp\left[-\frac{1}{2}\left(\frac{z-H-2nL}{\sigma_z}\right)^2\right]\right. \\ &\quad + \exp\left[-\frac{1}{2}\left(\frac{z+H-2nL}{\sigma_z}\right)^2\right] \\ &\quad + \exp\left[-\frac{1}{2}\left(\frac{z-H+2nL}{\sigma_z}\right)^2\right] \\ &\quad \left.\left. + \exp\left[-\frac{1}{2}\left(\frac{z+H+2nL}{\sigma_z}\right)^2\right]\right\}\right], \end{aligned} \quad (2)$$

where $H = (h + \Delta h)$ is the height of the plume centerline (m), the initial release height of the plume before plume rise (m),

Δh = the amount of plume rise (m), and L = the height (m) of the inversion layer (mixing height).

In MACCS, only first five terms are considered and the rest of the terms are neglected. When a uniform vertical distribution is attained, the following equation is used to calculate centerline air concentration:

$$\chi(x, y = 0, z) = \frac{Q}{\sqrt{2\pi}\bar{u}\sigma_y L}. \quad (3)$$

For the estimation of radiation doses during early phase of nuclear emergency, the following pathways are taken into consideration:

(i) external and internal exposure from cloud shine,

(ii) exposures from ground shine,

(iii) internal exposure from resuspension inhalation and skin doses from deposited material onto the skin,

(iv) acute and lifetime doses from early exposures.

2.2. Meteorological Conditions. For the execution of MACCS code, the hourly-based data for the year 2010 of Islamabad collected from the ground station (with an approximate height of 10 meters) has been used. As the near surface wind speed increases with altitude, the same data if used for the stake height (61 m) will overestimate the plume rise. This could produce significant underestimation of the radiation doses. To incorporate the effect of wind speed (m/s) with altitude, the following theoretical formula was used to estimate the wind speed at higher altitudes:

$$u = u_o\left(\frac{z}{z_o}\right)^p, \quad (4)$$

where u = wind speed at height z (m/s), u_o = wind speed at surface (m/s), and p = parameter (dimensionless) that varies with stability class and surface roughness.

The wind rose for the reported year is presented in Figure 2. The percentage value of wind direction remained 3.7% in north, 8.7% in northeast, 8.4% in east, 13.8% in southeast, 10.8% in south, 38.3% in southwest, 6.4% in west, and 10% in northwest, respectively. Data presented in Figure 2 represents that dominant wind direction was southwest (38.3%) during year 2010. The dominant atmospheric stability class as presented in Figure 3 was stability class-F.

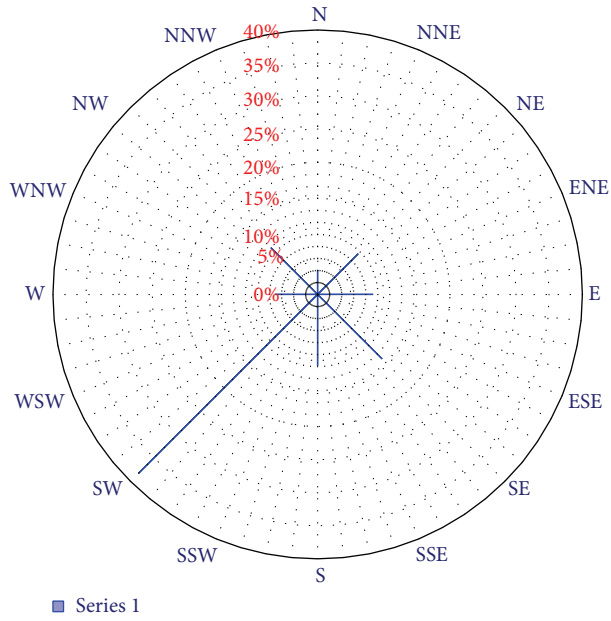

Figure 2: Wind rose for sixteen directions.

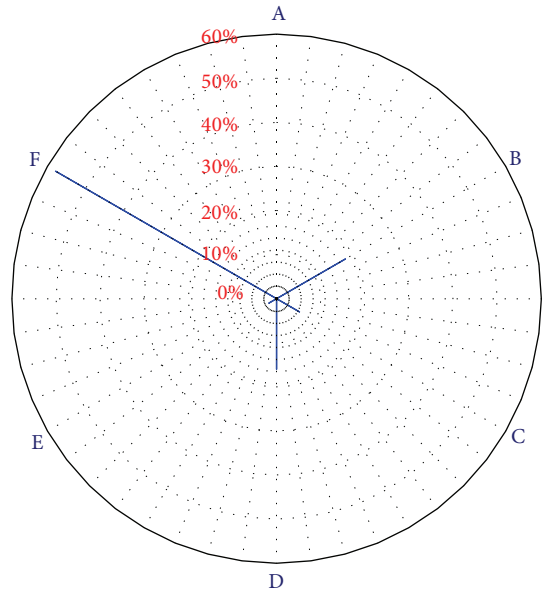

Figure 3: Dominant stability class.

3. Initial Conditions and Assumptions

3.1. Source Term and Release Fraction. The source term for the fission product in the reactor core was taken from the international published data [6] for a postulated accidental airborne release from Pakistan Research Reactor 1 (PARR-1), Islamabad, on upgraded power of 10 MW. The fractions of releases were based on USNRC document NUREG-1150. The release fractions of 1, 0.4, 0.3, 0.05, and 0.02 for noble gases, halogens, alkali metals, the tellurium group, and the Ba-Sr group, respectively, have been considered.

3.2. Meteorological Options. MACCS code provides different options for the selection of the meteorological data. The following four meteorological options (MO) have been used to estimate the radiation doses:

(i) MO-1: user specified day and hour,

(ii) MO-2: weather bin sampling,

(iii) MO-3: constant weather boundary data,

(iv) MO-4: special case (maximum wind speed).

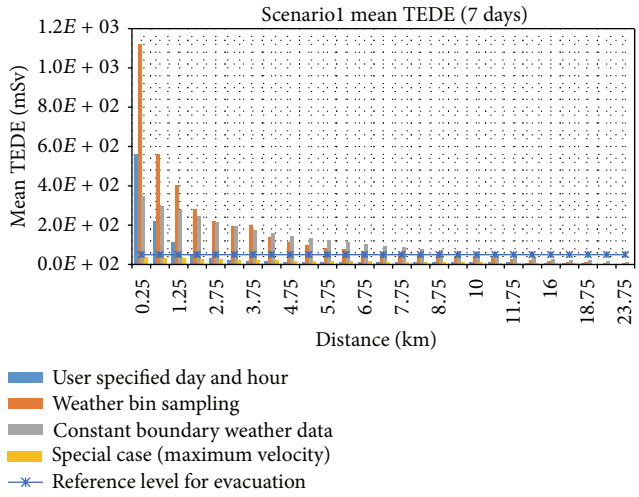

Figure 4: Scenario 1 mean TEDE (7 days).

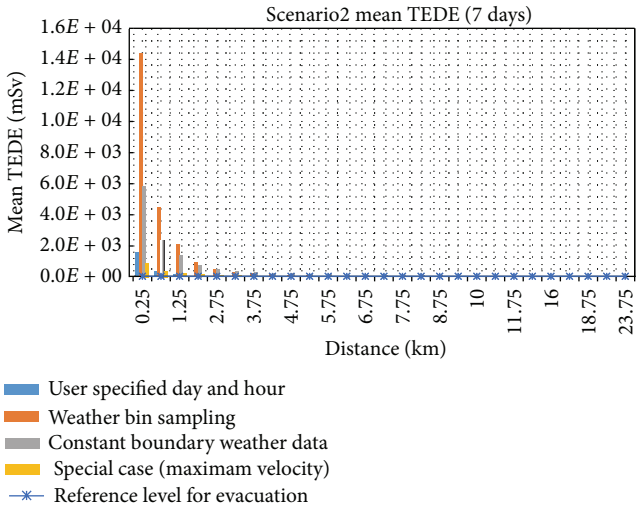

Figure 5: Scenario 2 mean TEDE (7 days).

3.3. Release Scenarios

Scenario 1. In this scenario, the releases and meteorological data have been considered at height of 61 meters (stake releases). The total effective dose equivalent (TEDE) for whole body modeled using four different meteorological options is presented in Figure 4.

Scenario 2. In this scenario, the releases and meteorological data have been considered at ground level (10 m). The TEDE for whole body modeled by using four different meteorological options is presented in Figure 5.

3.4. Comparison of Doses for Constant Weather Condition. The comparison of radiation doses of the scenarios has been made with the literature data (using the meteorological conditions of the site [6]) for 61-meter height using constant weather conditions. The comparison is presented in Figure 6.

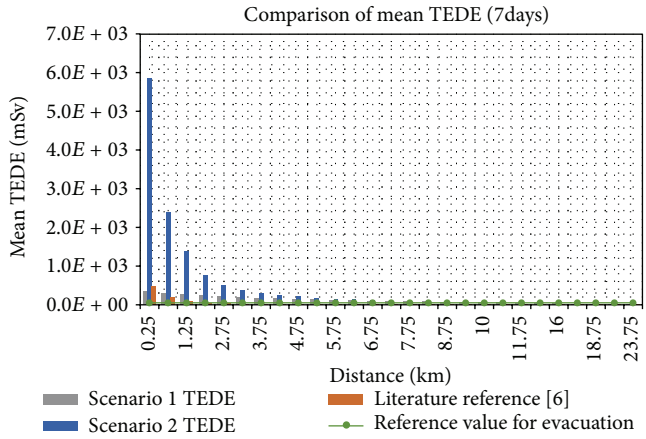

Figure 6: Comparison of mean TEDE (7 days) for constant weather.

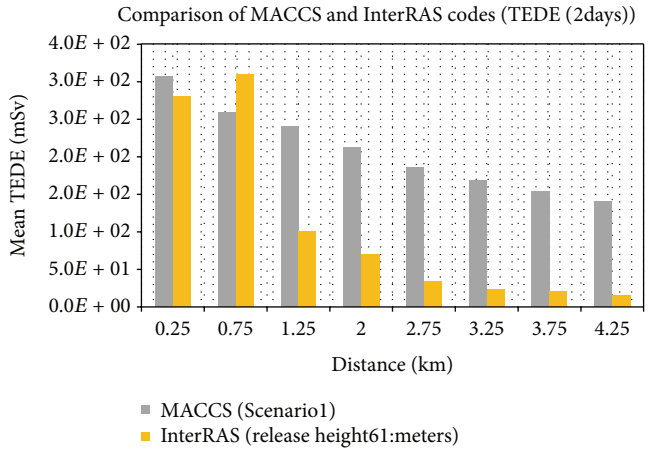

Figure 7: Comparison of MACCS and InterRAS codes.

4. Comparison of MACCS and InterRAS Codes

Comparison of MACCS code with InterRAS code [9, 10] for releases at the height of 61 meters using constant weather conditions has been made. The InterRAS code estimate radiation doses maximum up to 48 hours. The doses estimated using InterRAS code are comparable to doses estimated using MACCS code. The comparison of MACCS and InterRAS code results is presented in Figure 7.

4.1. Mean TEDE Trends (One Week). Mean TEDE for different release heights and meteorological conditions has been analyzed and presented in Figures 4–6. Through analysis, it was found that radiation doses reduce exponentially over the distance.

It was found that the protective action "evacuation" was required at different distances in different accident situations. The radiation doses fall below the intervention level for

Table 1: Evacuation intervention distance for different MET options.

Scenarios	Intervention (evacuation) distances (Km)			
	MO-1	MO-2	MO-3	MO-4
Scenario 1	2.00	7.75	10.00	0.25
Scenario 2	2.75	6.75	10.75	4.75
Literature [6]	—	—	2.75	—

evacuation (50 mSv) at 10 kilometers for Scenario 1, 10.75 kilometers for Scenario 2, and 2.75 kilometers for constant weather condition using site specific data.

4.2. Mean Distance for Intervention Levels. The intervention level for evacuation (50 mSv) was achieved at different distances for different emergency scenarios and for different meteorological options. Mean distances (Km) for taking intervention (evacuation) for different meteorological options (MO) are presented in Table 1.

A comparison of MACCS and InterRAS code output results (mean effective dose equivalent to whole body for two days) for constant weather conditions has been presented in Figure 7. From the trend analysis, it is found that the maximum of 5.10×10^3 mSv has been observed at mean distance of 0.25 km. At the nearby distances, the doses estimated using InterRAS code are comparable to doses estimated using MACCS code.

5. Summary and Conclusion

The most frequent wind direction southwest, that is, 38.3%, and the prevailing stability class F, that is, 58.16%, were recorded during year 2010. Intervention distance for evacuation remained in the range 2.0 to 2.75 kilometers for user specified MET data; 6.75 to 7.75 kilometers for weather bin sampling method; 2.75 to 10.75 kilometers for constant weather data; and 0.25 to 4.75 kilometers for maximum wind speed. With site specific meteorological conditions, intervention distance range is very low, that is, 2.0 to 2.75 kilometers, which is very close to the already published value, that is, 1 to 2 kilometers, using "InterRAS" code.

The seven-day TEDE has been modeled and compared with the reference levels [11] for evacuation, that is, 50 mSv for not more than seven days. It is found that the protective action "evacuation" was required at different distances in different accident scenarios.

MACCS code during early phase of nuclear emergency reasonably estimates the radiation doses by taking into account the variation in meteorological data, release duration, and concentrations. MACCS code could be an efficient tool to be used during early phase of nuclear emergencies if integrated with pre- and postprocessor for handling and presentation of data.

Conflict of Interests

The authors declare that there is no conflict of interests regarding the publication of this paper.

Acknowledgment

The authors would like to extend their sincere appreciation to the deanship of scientific research at King Saud University for its funding of this research through research group Project no. RGP VPP-255.

References

[1] J. Jeong and W. Jung, "The estimation of early health effects for different combinations of release parameters and meteorological data," *Journal of Korean Nuclear Society*, vol. 33, no. 6, pp. 557–565, 2001.

[2] T. Haste, J. Birchley, E. Cazzoli, and J. Vitazkova, "MELCOR/MACCS simulation of the TMI-2 severe accident and initial recovery phases, off-site fission product release and consequences," *Nuclear Engineering and Design*, vol. 236, no. 10, pp. 1099–1112, 2006.

[3] J. Wu, Y. Yang, I. Chen, H. Chen, and K. Chuang, "Reevaluation of the emergency planning zone for nuclear power plants in Taiwan using MACCS2 code," *Applied Radiation and Isotopes*, vol. 64, no. 4, pp. 448–454, 2006.

[4] J. Jeong and J. Ha, "The influence of source term release parameters on health effects," *Journal of The Korean Nuclear Society*, vol. 31, no. 3, pp. 294–302, 1999.

[5] L. Thaning and A. Baklanov, "Simulation of the atmospheric transport and deposition on a local/meso- and regional scale after hypothetical accidents at the Kola nuclear power plant," *Science of the Total Environment*, vol. 202, no. 1–3, pp. 199–210, 1997.

[6] "MELCOR Accident Consequence Code System (MACCS)," User's Guide, NUREG/CR–4691-Vol. 1.

[7] "MELCOR Accident Consequence Code System (MACCS)," Model Description, NUREG/CR–4691-Vol. 2.

[8] "MELCOR Accident Consequence Code System (MACCS)," Programmer's Reference Manual, NUREG/CR–4691-Vol. 3.

[9] C. Lin and L. Peng, "Study of interRAS application in early radiation consequences assessment of attacked nuclear power plant," in *Proceedings of the 11th China Symposium on Computer Application in Modern Science and Technology*, pp. 105–108, Beijing, China, 2003.

[10] M. Hussain, S. U. Khan, and W. A. Syed, "Estimation of emergency planning zones for nuclear research reactor using plume dispersion code," in *Proceedings of the 20th International Conference on Nuclear Engineering Collocated with the ASME, Power Conference (ICONE20-POWER '12)*, pp. 479–483, Anaheim, Calif, USA, July-August 2012.

[11] "Regulations on Management of a Nuclear or Radiological Emergency-PAK/914," 2008.

Hindawi Publishing Corporation
Science and Technology of Nuclear Installations
Volume 2014, Article ID 980418, 10 pages
http://dx.doi.org/10.1155/2014/980418

Research Article

Extended Station Blackout Coping Capabilities of APR1400

Sang-Won Lee, Tae Hyub Hong, Mi-Ro Seo, Young-Seung Lee, and Hyeong-Taek Kim

Korea Hydro and Nuclear Power, Central Research Institute, 70 Gil, Yuseong-Daero 1312, Yuseong-Gu, Daejeon 305-343, Republic of Korea

Correspondence should be addressed to Sang-Won Lee; sangwon@khnp.co.kr

Received 17 January 2014; Revised 16 April 2014; Accepted 29 April 2014; Published 25 May 2014

Academic Editor: Enrico Zio

The Fukushima Dai-ichi nuclear power plant accident shows that an extreme natural disaster can prevent the proper restoration of electric power for several days, so-called extended SBO. In Korea, the government and industry performed comprehensive special safety inspections on all domestic nuclear power plants against beyond design bases external events. One of the safety improvement action items related to the extended SBO is installation of external water injection provision and equipment to RCS and SG. In this paper, the extended SBO coping capability of APR1400 is examined using MAAP4 to assess the effectiveness of the external water injection strategy. Results show that an external injection into SG is applicable to mitigate an extended SBO scenario. However, an external injection into RCS is only effective when RCS depressurization capacity is sufficiently provided in case of high pressure scenarios. Based on the above results, the technical basis of external injection strategy will be reflected on development of revised severe accident management guideline.

1. Introduction

One of the representative accidents related to the electric power in nuclear power plants is a Station Blackout (SBO). SBO is initiated by a loss of all offsite power with a concurrent failure of both Emergency Diesel Generators (EDGs). With no Alternate Current (AC) power source, most of the active safety systems that perform safety functions are not available. To prevent SBO scenarios from becoming worse, nonsafety class Alternative AC (AAC) power is installed as a redundancy to provide electricity to the essential equipment that perform safety function [1, 2]. However, if the AAC is also unavailable, only active equipment that are powered by Direct Current (DC) from station batteries or passive systems could work. Normally, Turbine-Driven Auxiliary Feedwater Pumps (TD-AFWP), which extract steam from the main steam line, are only available means to supply cooling water to the steam generators (SG). Reactor Coolant System (RCS) natural circulation and heat transfer to the secondary via the steam generators are the primary means to cool the core because the Reactor Coolant Pumps (RCPs) are unavailable to provide a forced circulation. The capacity of a DC battery is about 4~8 hrs; thus, operator should restore the existing electric power before it exhausts. If electric power cannot be restored within this time due to a complicated situation, SBO with the complete depletion of batteries is a total loss of heat sink situation and proceeds to a severe accident condition. Probabilistic Safety Assessment (PSA) results show that SBO is one of the dominant sequences that lead to the core damage and containment failure in the APR1400 [3] as shown in Table 1.

The Fukushima Dai-ichi nuclear power plant accident shows that an extreme natural disaster can prevent the proper restoration of electric power for several days, so-called extended SBO [4]. After the Fukushima Dai-ichi accident, several kinds of analyses on SBO are performed. One of them is BWR long term SBO calculation using TRAC-BF [5]. Calculated results are compared with the observed data at the unit 2 reactor of the Fukushima Dai-ichi nuclear power plant and shown to be in good agreement. In PWR, a study shows the effectiveness of availability of long term secondary cooling to delay the time before core uncovers and significant heatup [6, 7]. Results show that the available time for restoration of AC power is extended for at least the batteries capacity extension time. Another study was performed about comparison of extended SBO scenarios against PWR, BWR, and PWHR using MAAP code without operator action [8]. Results show that core damage occurs within 10 hrs after

Table 1: Level 1 PSA initiating event.

Event	Percent (%)
SBO	60.8
Small break LOCA	16.8
Mediumb LOCA	3.3
SGTR	2.9
RV failure	2.7
Intersystem LOCA	2.6
General transient	10.9

the initial event. Most of the studies are focused on the plant behavior without operator action or improvement of accident management using existing permanent equipment, such as extension of battery capacity and operability of TD-AFW.

As for regulation activity, US NRC recommends strengthening SBO mitigation capability for design basis and beyond design basis external events. Detailed recommendations [9] include

(i) establishment of a minimum coping time of 8 hrs,

(ii) preparation of the equipment, procedure, and training necessary to implement an extended SBO coping time of 72 hrs for core and spent fuel pool (SFP) cooling,

(iii) establishment of preplan and prestage offsite resources to support uninterrupted core and SFP cooling.

In Korea, the government and industry performed comprehensive special safety inspections on all domestic nuclear power plants against beyond design bases external events after the Fukushima Dai-ichi nuclear power plant accident. The major concerns of these inspections were protection against extreme natural hazards, prevention and/or mitigation of severe accidents, emergency preparedness, and the design of structures and equipment against earthquakes and coastal flooding. As a result, a total of 50 recommendations were defined as safety improvement action items. They were classified into 5 categories and will be implemented by 2015.

Some of the action items related to mitigation measures against extended SBO sequences are

(i) upgrading the design basis of AAC diesel generators,

(ii) installation of a water-proof gate to EDG room,

(iii) securing the availability of portable power generator vehicles,

(iv) installation of external water injection provision and equipment to RCS and SG.

Among those items, effectiveness of external injection into RCS and SG needs to be examined. Therefore, in this paper, the overall extended SBO coping capability of APR1400 is analyzed to examine the effectiveness of the external water injection strategy and estimate proper operator action timing to reflect on the optimal revised severe accident management guideline. Section 2 presents SBO related procedures to prevent and/or mitigate the sequences as well as the mitigation facilities installed in APR1400. The modeling and analyses results using the MAAP severe accident analysis code are provided in Sections 3 and 4, and a summary of the SBO coping capabilities in APR1400 are discussed in Section 5.

2. SBO Related Operating Procedures and Mitigation Facilities

2.1. SBO Related Operating Procedures. The purpose of this section is to identify the main operator actions to be analyzed and to estimate the operator action timing during a SBO scenario. The APR1400 Emergency Operational Procedure (EOP) and Severe Accident Management Guideline (SAMG) were developed based on the PWR owner's group reference documents [10, 11] and these documents were modified [12, 13] to reflect the APR1400 plant specific design characteristics [14].

When a SBO occurs, the reactor is tripped by either Reactor Protection System (RPS) trip signal or gravity drop of control rod due to the loss of electric power. Then operators initiate an EOP. After performing standard posttrip action to verify the plant status, the operators confirm the diagnosis of the event and, if properly diagnosed, the SBO procedure is initiated. It is one of the event oriented procedures that recover the essential safety functions more effectively than symptom oriented procedure. If operators cannot diagnose the specific event, functional recovery guideline, especially the RCS heat removal procedure, is performed. The two procedures commonly provide the operator action for recovery of RCS heat removal safety function shown below.

The primary operator action is to recover the AAC power. If it is not successful, core cooling using safety injection tank (SIT) is applicable when RCS depressurization is achieved because APR1400 Safety Injection Pump (SIP) is an active system and needs electricity to activate. So, the operator should perform the RCS and core heat removal using the TD-AFWP and SG Atmospheric Dump Valve (ADV) to cool the RCS via heat transfer to the SG. The TD-AFW flow control valve is powered by a DC battery, and its design capacity is about 8 hrs. If existing electric power is not recovered until battery exhaustion time, there are no further means to cool the RCS. Then, eventually, a core boil-off occurs. When the core exit temperature reaches 922 K (1200 F), SAMG is initiated (Figures 6 and 10).

In SAMG, the operator performs once again the recovery action of the existing electric power or portable external power. This step is a continuously applicable step. Therefore, at the same time, the operator should monitor the 7 major safety functions sequentially and perform corresponding mitigation measures when certain safety functions are challenged. SBO related mitigation measures are mitigation-1 (depressurizes the RCS), mitigation-2 (injection into the SG), and mitigation-3 (injection into the RCS). The schematic flowchart of the procedures is summarized in Figure 1.

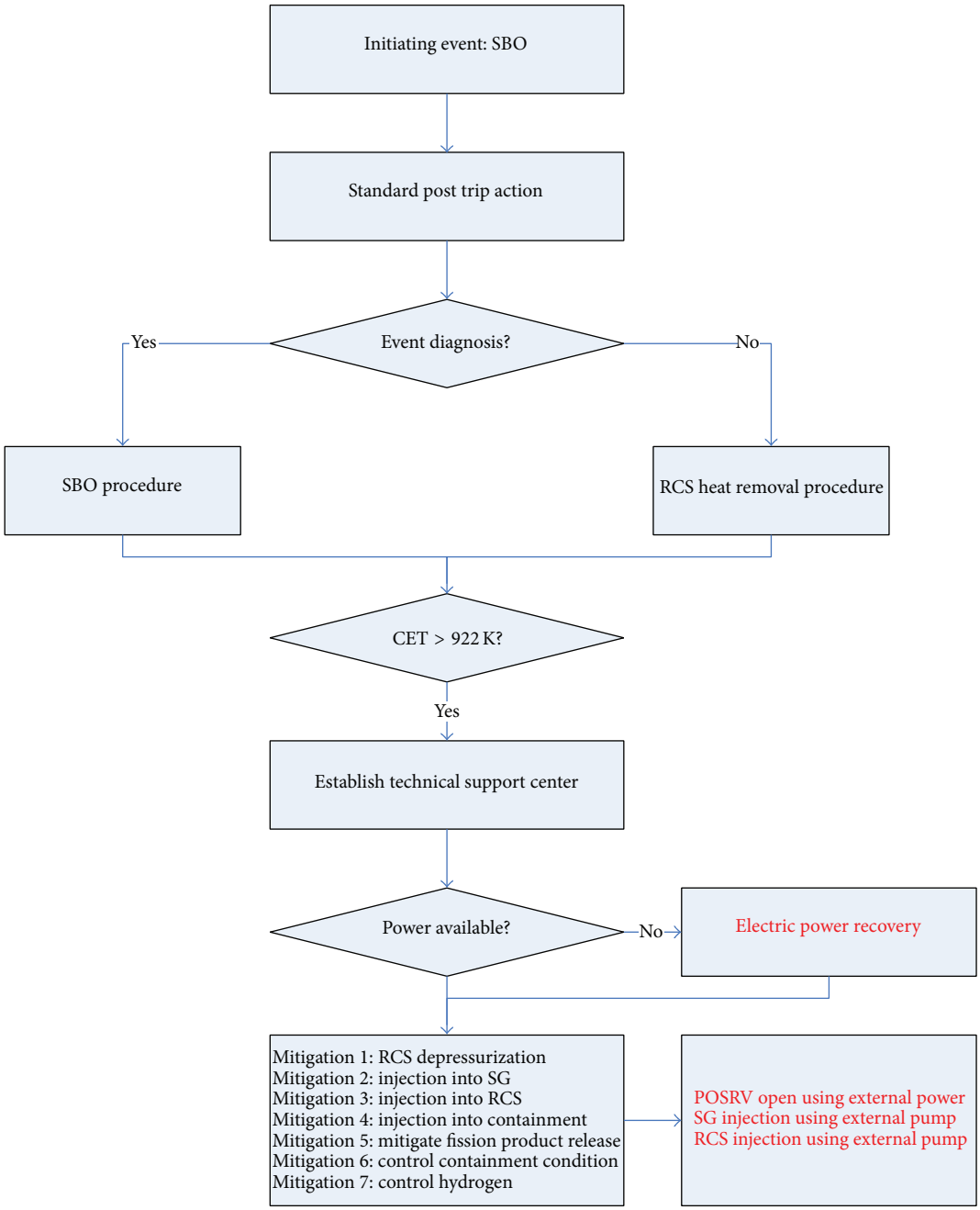

Figure 1: Flowchart of the SBO related procedure.

The right two columns are the revised procedure to reflect the external injection strategy.

2.2. Design Characteristics to Cope with Extended SBO. To cope with a SBO, the APR1400 is equipped with an AAC power supply with a capacity of at least 2~3 days. Also, an auxiliary charging pump is installed parallel to the existing charging pumps to provide seal injection water to the four RCPs to prevent the leakage of coolant through the RCP seals. DC power from the battery provides a reliable source of power for safety related control and monitoring equipment for at least 8 hrs.

In addition, post-Fukushima action items including the provision of an external injection system are recently reflected. The RCS external injection flow path is installed at the discharge of the existing Emergency Core Cooling (ECC) pump. SG injection flow paths are also installed along the discharge line of the AFW pump. A total of three commercial external pumps are on standby condition in each unit, one for RCS injection and two for each SG injection. Several water sources in site boundary that are available can be used, such as a raw water tank, two condensate water tanks, and two AFW tanks. Detailed SG external injection flow paths are shown in Figure 2.

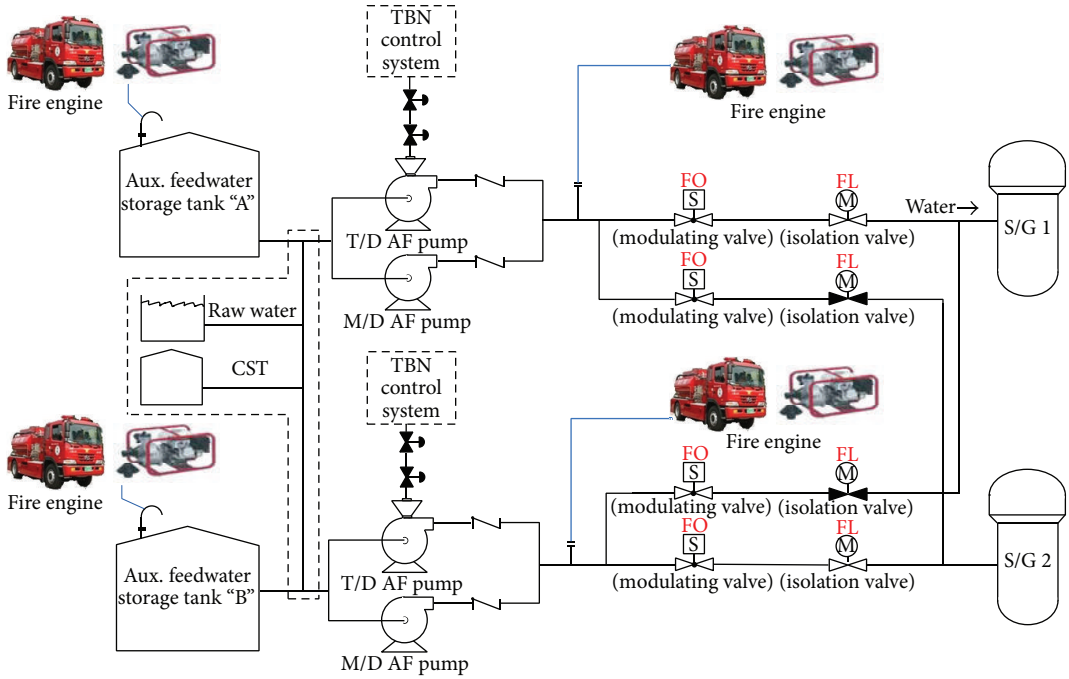

Figure 2: Schematics of SG external injection.

3. Numerical Model

Extended SBO analyses on APR1400 are performed using the MAAP severe accident computer code. The MAAP code can analyze severe accidents following large and small break Loss of Coolant Accidents (LOCAs), SBO, and various general transients. Developed for the Electric Power Research Institute (EPRI) by Fauske et al., MAAP4.0.7 is used here. The MAAP4 code can perform integral analyses of reactor system and containment behaviors including core heatup, degradation, relocation, reactor vessel failure, containment failure, and fission product behaviors [15]. MAAP4 has simplified thermohydraulic model and solved first order differential equations for conservation of mass and energy. However, it produces reasonable prediction capabilities comparable to MELCOR and SCDAP [16]. MAAP4 is widely used in Korea in severe accident analysis and level 2 PSA for APR1400 design [17, 18].

A noding diagram for APR1400 is shown in Figure 3. RCS are divided into 14 nodes based on generalized models of PWRs, in which the type and number of components and the geometry are predetermined. RCS system consists of two primary loops; each one consists of one SG, one hot leg, and two RCPs and cold legs. Also, four Pilot Operated Safety and Relief Valves (POSRVs) located on the top of the pressurizer are modeled. Each of the POSRVs has two valves in serial that perform spring loaded safety depressurization function and motor operated steam relief function. Secondary system consists of SG, main feedwater pumps, auxiliary feedwater pump, main steam line, main steam isolation valve (MSIV), 20 main steam safety valves (MSSV), and 4 ADV located upstream of the MSIV. The containment is divided into 14 nodes.

In-containment refueling water storage tank (IRWST), one of the advanced design features in APR1400, is modeled as one of the containment nodes as shown in Figure 3. The flow paths from IRWST to suction of safety injection and containment spray pump and return flow path of the discharged coolant from containment spray and/or break flow to the IRWST are modeled. Direct vessel injection flow path is connected to the reactor vessel upper downcomer to incorporate into APR1400 SIS design. However, in-vessel retention (IVR) strategy, one of the representative severe accident mitigation strategies in APR1400, is not considered in this analysis because ex-reactor vessel cooling is not applicable when reactor cavity is in dry condition in SBO sequences.

External primary injection flow path is located at discharge line of SIS piping. Injection flow rate is calculated based on the existing commercial portable pump performance curve and the flow path pressure drop calculation from the external pump to the RCS injection point. External secondary injection flow path is located at discharge line of AFW piping and injection flow rate is also implemented similarly as mentioned above.

The RCP seal leakage flow rate is considered as 1.325 liter/s, most probable flow rate, for each RCP in this calculation [19]. Initial and boundary condition for this calculation is summarized in Table 2.

4. Results and Discussion

4.1. Base Case. In this section, the effectiveness of the TD-AFWP operation is analyzed. When a SBO with concurrent failure of AAC occurs, a reactor and turbine trip

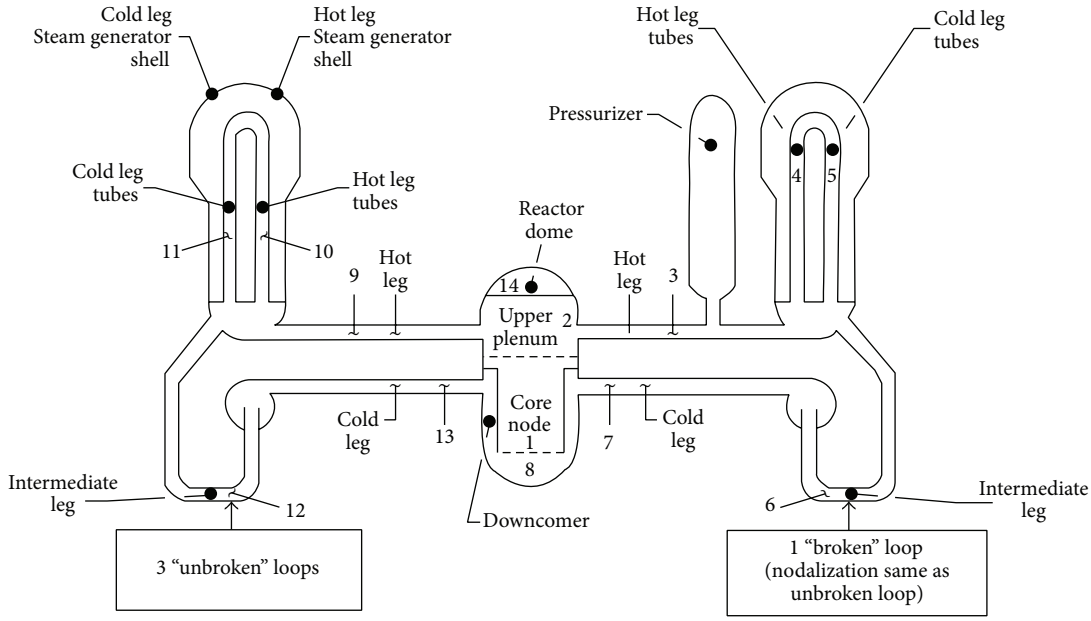

(a) RCS noding diagram

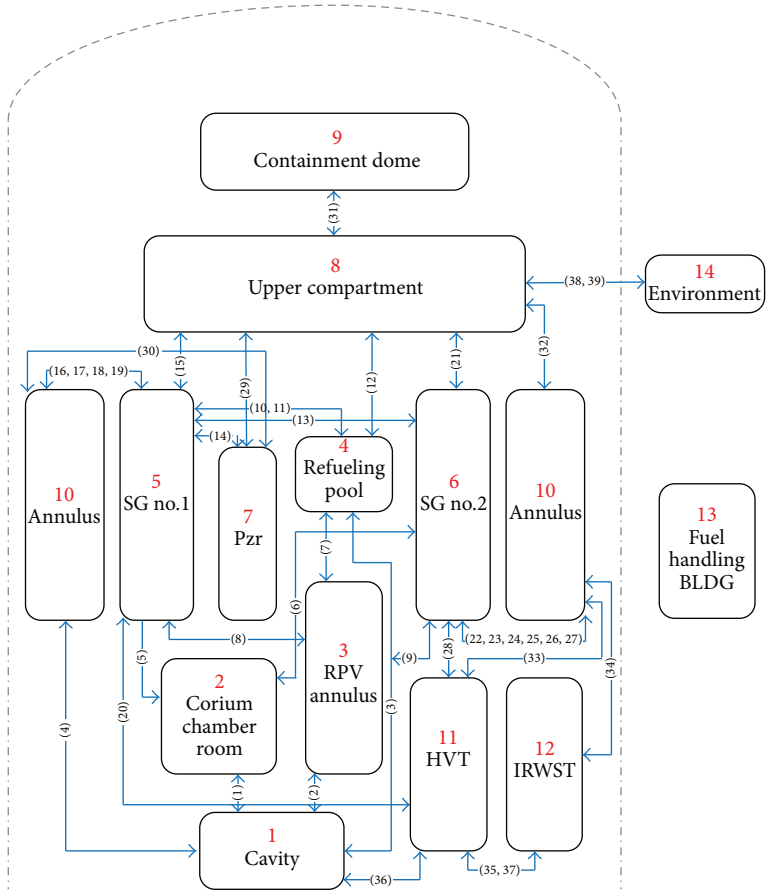

(b) Containment noding diagram

Figure 3: MAAP noding diagram.

Table 2: Initial and boundary conditions.

Parameter	Value
Reactor power (MWth)	3983
Primary/secondary pressure (MPa)	15.5/6.89
Hot leg/cold leg temperature (K)	597.0/563.7
RCP seal flow rate (liter/s)	1.325
RCS mass flow rate (kg/s)	20,991
Steam mass flow rate/SG (kg/s)	1130.2
SIT set pressure (MPa)	4.025
POSRV capacity (kg/s)	68.0 at 17.0 MPa
ADV capacity (kg/s)	138.6 at 6.9 MPa
External injection pump shutoff pressure (MPa)	1.5
Secondary injection flow rate (liter/s)	14.7 at 0.1 MPa
Primary injection flow rate (liter/s)	49.3 at 0.1 MPa

is initiated. All active systems including emergency core cooling system, shutdown cooling system, and motor driven auxiliary feedwater system become inoperable. Then, the SG pressure rapidly increases to the MSSV opening set-point and releases steam to the environment periodically to maintain secondary pressure boundary integrity. RCS single phase natural circulation is established through the SG heat removal. However, the SG water source is not provided; the SG level is continuously decreased. At this time, the operator initiates an EOP and tries to restore the proper actuation of the TD-AFWP based on SBO procedures. This operator action is assumed 30 min after the initiating event in this calculation.

If this action is not successful, the SG inventory is depleted at 1.3 hrs. Then, the RCS pressure reincreases and POSRVs start to open. The RCS inventory is continuously discharged into the containment and core starts to uncover at 1.9 hrs. At this time, hot leg counter current natural circulation is established. Superheated steam from the vessel flows into the SG hot side plenum through the upper part of the hot leg and excessive heatup of heat structure occurs. There is some mixing of the superheated steam in the SG hot side plenum, and some of the relatively low temperature steam returns to the core through lower part of the hot leg. So, there is circumferential temperature stratification in hot leg piping and it could lead to creep rupture. This phenomenon is reflected based on Larson Miller creep rupture failure model in MAAP4. This counter current natural circulation is maintained up to 3.2 hrs until core level is completely depleted. During this time, core degradation and melting occur in the RCS. Eventually, the RCS fails due to the failure of the incore instrument tube caused by molten corium relocation to the lower head at 3.7 hrs. Because high pressure is maintained before RCS fails, a large amount of superheated steam and hydrogen is discharged into containment after RCS fails. Also, interaction between molten core material and cavity water that is discharged from SIT leads to large amount of steam generation in the cavity. So, the containment pressure rapidly increased. Also, hydrogen and noncondensable gas are steadily generated by molten core concrete interaction in the base-mat.

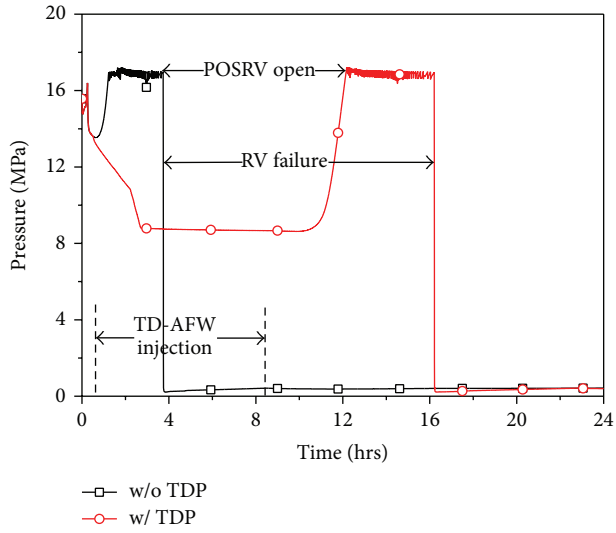

Figure 4: RCS pressure history.

On the other hand, if TD-AFWP actuation is successful, the SG water inventory is recovered before it is depleted and RCS heat removal is reestablished until the battery is exhausted at 8.5 hrs. During this period, the RCS pressure continuously decreases to 8.5 MPa, slightly above the SG pressure, due to heat transfer to the secondary system as shown in Figure 4. TD-AFW flow rate is ~15 kg/s until SG reaches its normal water level. And flow rate continuously decreases as the decay heat level decreases. This condition is maintained if the TD-AFW flow is provided. However, if the operator action to recover the existing electric power is not successful until the battery exhaustion time, the TD-AFW flow rate is terminated. Then, the core starts to boil off after SG inventory dries out as shown in Figure 5. Eventually, the RCS inventory is also depleted and CET reaches 922 K at 12.6 hrs. The operator initiates SAMG, but no mitigation measures are available if the restoration of existing electric power is not successful. Then, the RCS lower head fails at 15.0 hrs.

This calculation shows that TD-AFW could effectively cool down the RCS until the battery is exhausted and provide approximately 11 hrs of additional time to avoid core uncovering if TD-AFW initiation operator action is successful.

To verify the sensitivity on injection duration, 72 hrs of TD-AFW operational case is analyzed. Results show that the stable core cooling is maintained until the 72 hrs. These results show that the extension of battery capacity to 72 hrs can be an effective way to implement an extended SBO coping time of 72 hrs if TD-AFW operability is maintained. The major sequences of events are summarized in Table 3.

4.2. Effectiveness of External Secondary Injection Operator Action. In this section, the effectiveness of an external injection strategy into the SG is examined. The event scenario before the SAMG entry condition is identical to those of previous section. When the CET reaches 922 K, the operator should transfer the procedure from EOP to SAMG. In SAMG, after a technical support center is established, the primary

Table 3: Major sequences of events.

Event	SBO w/o TDP	SBO w/ TDP	Secondary injection	Primary injection
Rx trip	0.0 sec	0.0 sec	0.0 sec	0.0 sec
Main steam safety valve open	8.5 sec	8.5 sec	8.5 sec	8.5 sec
TDP actuation	—	1800 sec	1800 sec	1800 sec
TDP termination	—	8.5 hrs	8.5 hrs	8.5 hrs
SG dryout	1.2 hrs	10.9 hrs	10.9 hrs	10.9 hrs
POSRV open	1.3 hrs	11.6 hrs	11.6 hrs	11.6 hrs
Core uncovered	1.9 hrs	12.0 hrs	12.0 hrs	12.0 hrs
SAMG entry	2.2 hrs	12.6 hrs	12.6 hrs	12.6 hrs
External injection	—	—	13.1 hrs	13.1 hrs
SIT actuation	—	—	14.8 hrs	13.6 hrs
Relocation to lower head	3.7 hrs	15.0 hrs	—	—
Rx failure	3.7 hrs	15.0 hrs	—	—

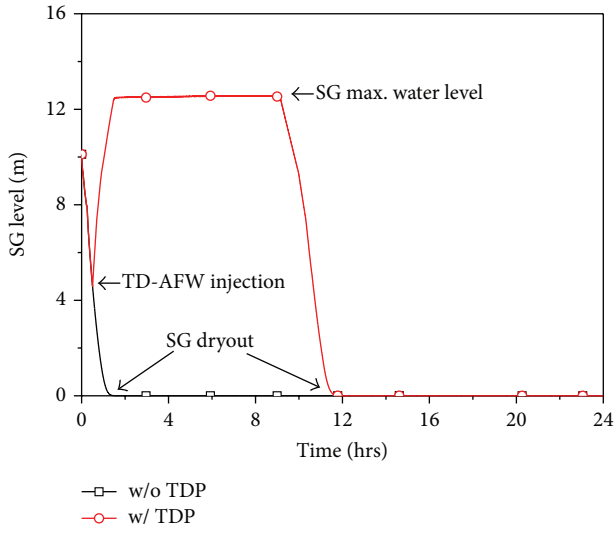

Figure 5: SG water level.

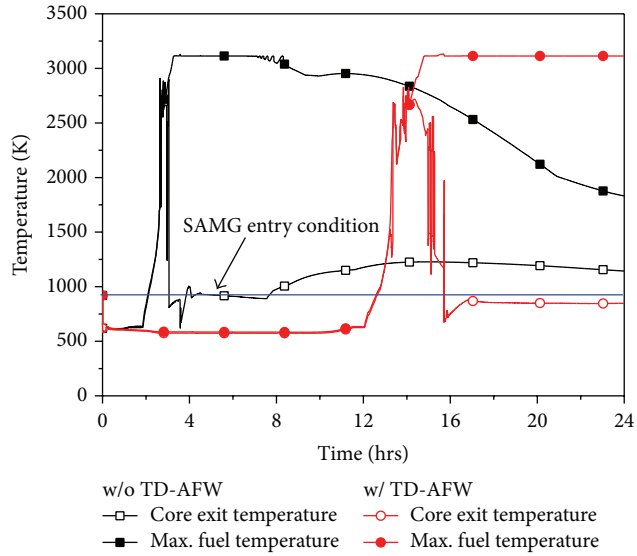

Figure 6: Core exit and fuel temperature.

operator action is to recover the existing electric power or prepare the external power generator in site boundary. If the external power generator is active, it provides electric power to essential instrumentation and control valves, including the main control room, the SG level and pressure indicators, containment pressure instrumentation, and the RCS and SG depressurization valves.

Then, SAMG mitigation-2 procedure for a secondary injection initiates. Detailed actions are depressurizing the SG pressure below the pump shutoff head by opening main steam line ADV in each SG. This action is performed manually if external electric power is not available. Then, water is injected into the SG using an external pump. This operator action time is assumed as 30 min. As shown in Figure 7, the SG pressure rapidly decreases when the ADV is fully opened. Then, the SG water level is recovered continuously as shown in Figure 8. At this time, a RCS natural circulation flow path is formed and the RCS is cooled down and pressure decreases. When RCS pressure reaches the Safety Injection Tank (SIT) actuation set-point of 4.0 MPa, the RCS water level is recovered rapidly. The external injection flow rate of each loop is 10 kg/s~15 kg/s initially and decreases to 5 kg/s when SG level is fully recovered by operator action to prevent SG overfilling. Then, the external injection and ADV flow rate are balanced and maintain a stable condition as shown in Figure 9. This flow rate is compatible to removal of decay heat generated in the core. The maximum core exit temperature decreases after 1500 K peak and the core integrity is maintained. The fraction of clad reacted in vessel is within 1% of total amount of clad as summarized in Table 4. Figure 11 shows the integrated water inventory required for 72 hrs of injection to the SG. Approximately, 2500 tons of cooling water is required. The total water inventories of two AFW tanks and CST tanks are 4,000 ton and 1,700 ton, respectively. So, the cooling water source is sufficient to provide up to 72 hrs.

These calculation results show that the external injection into the SG is an effective procedure to mitigate an extended SBO scenario when this is successfully performed within 30 min after SAMG initiation. Moreover, this strategy can be

Table 4: Major severe accident progression parameter.

	SBO w/o TDP	SBO w/ TDP	Secondary injection	Primary injection
H2 generation (kg)	649.2	596.6	18.4	11.4
Clad reacted in vessel (%)	50.1	46.1	1.42	0.88
Aerosol generated (kg)	1570.2	1175.3	0.0	0.0
UO2 mass in cavity (kg)	108468.0	104843.2	0.0	0.0

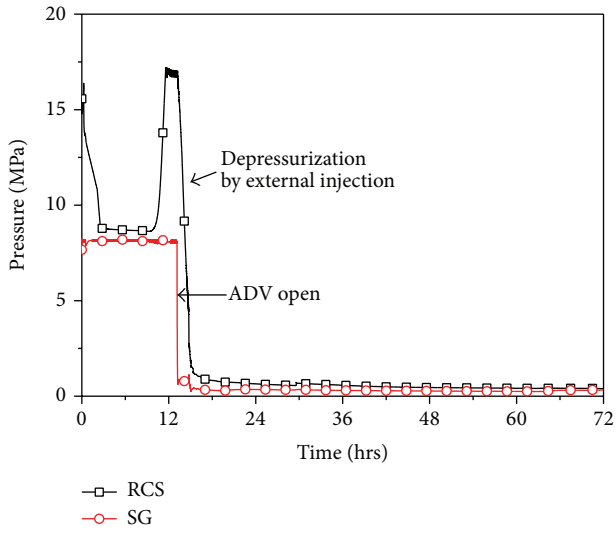

Figure 7: Secondary injection RCS and SG pressure.

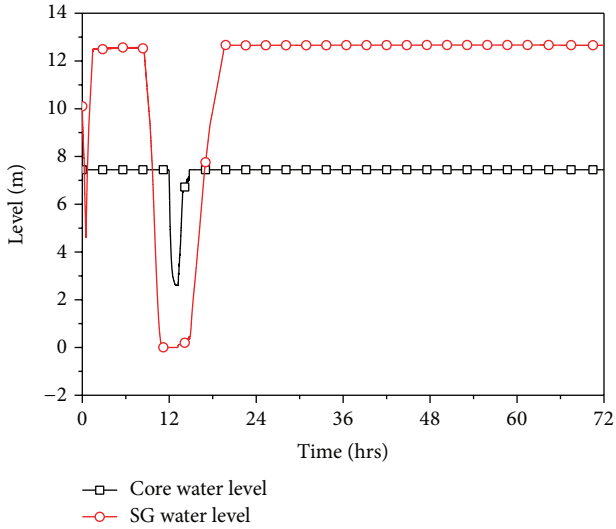

Figure 8: Secondary injection RCS and SG water level.

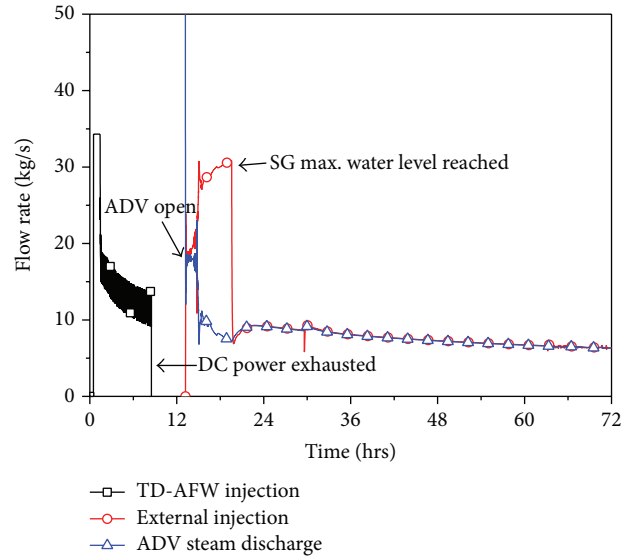

Figure 9: Secondary injection flow rate.

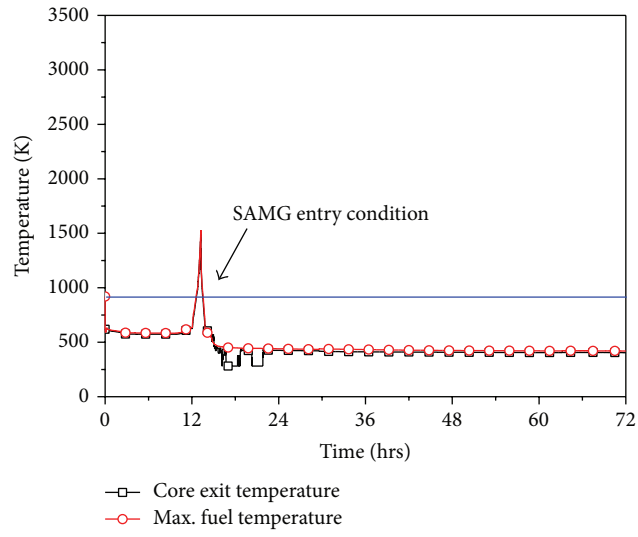

Figure 10: Secondary injection core exit and fuel temperature.

undertaken without a portable power generator because SG depressurization can be performed by an operator manually.

4.3. Effectiveness of External Primary Injection Operator Action. In this section, the effectiveness of an external injection strategy into the RCS is examined. The event scenario is identical to that in previous section except that the external injection location is the RCS. To inject water into the RCS, SAMG mitigation-1 (RCS depressurization) is prerequisite because external injection pump shutoff head is relatively low. To depressurize the RCS, the preparation of an external power generator is essentially required because the POSRV cannot be opened manually due to the unaccessibility to the inside

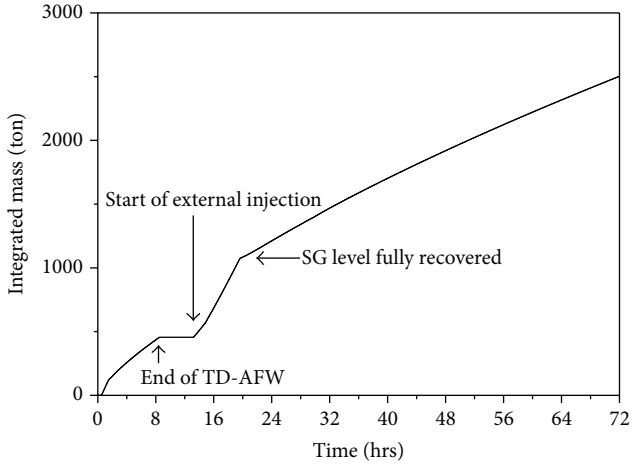

Figure 11: Integrated mass inventory of secondary injection.

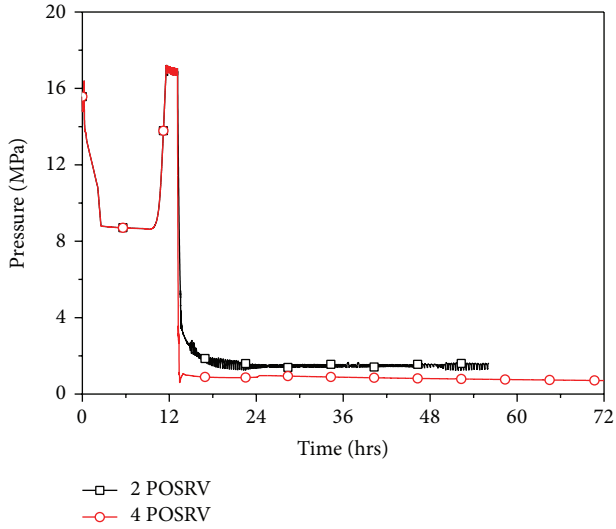

Figure 12: Primary injection RCS pressure.

of the containment. If a portable power generator is in place, the operator opens two out of four POSRVs 30 min after the SAMG entry condition because a portable power generator can provide only one of two electric trains. Then, SAMG mitigation-3 (Injection into RCS) initiates. The RCS pressure trend is shown in Figure 12. After the POSRVs are opened, the RCS pressure reaches the SIT injection set point and the SIT water starts to flow into the core. Then, a large amount of steam and hydrogen is generated in the core due to the direct contact cooling between SIT water and core materials. Due to limited depressurization capacity of POSRV, RCS pressure spikes continuously occur and do not sufficiently decrease to external injection pump shutoff head pressure. As a result, the RCS injection strategy is not successful in this case.

For a sensitivity on depressurization capacity, 4 POSRV opening cases are analyzed. As shown in Figure 13, 4 POSRV cases sufficiently depressurize the RCS. Primary injection is successful and RCS cool-down is completed.

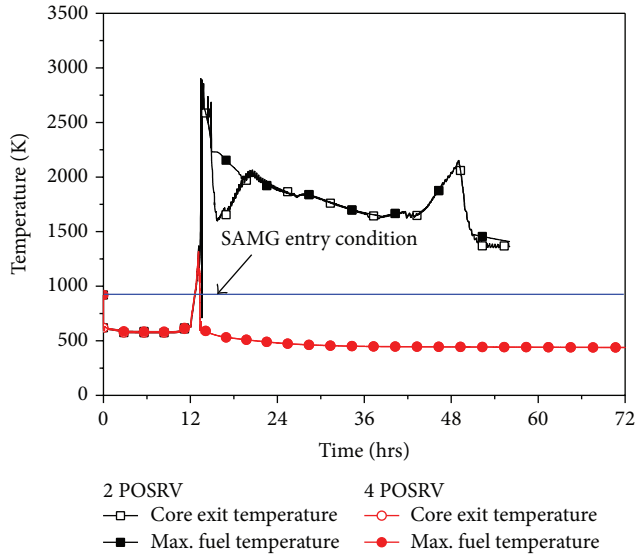

Figure 13: Primary injection core exit and fuel temperature.

The calculation results show that an external injection into the RCS is only effective when the RCS depressurization capacity is sufficiently provided in case of high pressure severe accident scenarios.

5. Conclusions

After the Fukushima Dai-ichi nuclear power plant accident, mitigation measures against extended SBO sequences were investigated in Korea. Therefore, the overall extended SBO coping capability of the APR1400 is examined to assess the effectiveness of an external water injection strategy.

The following are the conclusions:

(i) SBO without operator action leads to a core damage at 2.0 hrs and Rx failure at 3.7 hrs in APR1400;

(ii) a TD-AFW can effectively cool down the RCS and provide approximately 12 hrs of additional time for the operator to recover the existing electric power to prevent core damage;

(iii) extension of battery capacity can be an effective way to implement an extended SBO coping time of 72 hrs;

(iv) an external injection strategy into SG using commercial pump is an effective strategy to mitigate an extended SBO scenario when it is successfully prepared within 30 min after SAMG initiation;

(v) an external injection into RCS using commercial pump is only effective when RCS depressurization capacity is sufficiently provided in case of high pressure severe accident scenarios.

Based on the above results, the technical basis on external injection strategy will be implemented on development of optimal revised severe accident management procedure.

Abbreviations

AAC: Alternative AC
ADV: Atmospheric dump valve
AFW: Auxiliary feedwater
CET: Core exit temperature
CST: Condensate storage ank
ECC: Emergency core cooling
EDG: Emergency diesel generator
EOP: Emergency operational procedure
IRWST: In-containment refueling water storage tank
LOCA: Loss of coolant accident
MAAP: Modular accident analysis package
MSIV: Main steam isolation valve
POSRV: Pilot operated safety and relief valve
PSA: Probabilistic safety assessment
RCP: Reactor coolant pump
RPS: Reactor protection system
SAMG: Severe accident analysis guideline
SBO: Station blackout
SIS: Safety injection system
SIT: Safety injection tank
SFP: Spent fuel pool
TD-AF: Turbine driven auxiliary feedwater
RCS: Reactor Coolant System.

Conflict of Interests

The authors declare that there is no conflict of interests regarding the publication of this paper.

References

[1] U.S. NRC, "Station Blackout," Regulatory Guideline 1.155, 1988.

[2] U.S. NRC, "Station Blackout Rule," Regulations Title 10 Code of Federal Regulations, 1988.

[3] KHNP, "Probabilistic safety assessment and severe accident," APR1400 Standard Safety Analyses Report, 2002.

[4] TEPCO, *Overview of the Earthquake & Tsunami and Nuclear Accident : The Great East Japan Earthquake and Current Status of Nuclear Power Stations*, 2011.

[5] T. Watanabe, M. Ishigaki, and M. Hirano, "Analysis of BWR long-term station blackout accident using TRAC-BF1," *Annals of Nuclear Energy*, vol. 49, pp. 223–226, 2012.

[6] A. Prošek and L. Cizelj, "Long-term station blackout accident analyses of a PWR with RELAP5/MOD3.3," *Science and Technology of Nuclear Installations*, vol. 2013, Article ID 851987, 15 pages, 2013.

[7] A. Volkanovski and A. Prošek, "Extension of station blackout coping capability and implications on nuclear safety," *Nuclear Engineering and Design*, vol. 255, pp. 16–27, 2013.

[8] S.-Y. Park and K.-I. Ahn, "Comparative analysis of station blackout accident progression in typical PWR, BWR, and PHWR," *Nuclear Engineering and Technology*, vol. 44, no. 3, pp. 311–322, 2011.

[9] U.S. NRC, *Recommendations for Enhancing Reactor Safety in the 21st Century*, The Near-Term Task Force Review of Insight from the Fukushima Dai-ichi Accident, 2011.

[10] PWROG, *Emergency Procedure Guidelines Rev.5.2*, CEN-152, 2001.

[11] PWROG, *Severe Accident Management Guideline*, MUHP-2310, 1994.

[12] KHNP, *Emergency Operational Guidelines for APR1400, Rev.01*, 2002.

[13] KHNP, *APR1400 Severe Accident Management Guideline*, 2012.

[14] S. J. Cho, B. S. Kim, M. G. Kang, and H. G. Kim, "The development of passive design features for the Korean Next Generation Reactor," *Nuclear Engineering and Design*, vol. 201, no. 2, pp. 259–271, 2000.

[15] EPRI, *MAAP4-Modular Accident Analysis Program for LWR Power Plants*, 1994.

[16] K. Vierow, Y. Liao, J. Johnson, M. Kenton, and R. Gauntt, "Severe accident analysis of a PWR station blackout with the MELCOR, MAAP4 and SCDAP/RELAP5 codes," *Nuclear Engineering and Design*, vol. 234, no. 1–3, pp. 129–145, 2004.

[17] C. H. Park, D. Y. Lee, I. J. U. C. Lee, K. Y. Suh, and G. C. Park, "Comparative study of loss-of-coolant accident using MAAP4.03 and RELAP5/MOD3.2.2," in *Proceedings of the 10th International Conference on Nuclear Engineering (ICONE '02)*, pp. 22032.1–22032.8, April 2002.

[18] J. Hwan Jeong, M. G. Na, S. P. Kim, and J. Woon Park, "Analysis of severe accident scenarios in APR1400 using MAAP4 code," in *Proceedings of the International Conference on Atomic Physics (ICAPP '02)*, 2002.

[19] Westinghouse, *WOG2000 RCP Seal Leakage Model for Westinghouse PWRs*, 2002.

Hindawi Publishing Corporation
Science and Technology of Nuclear Installations
Volume 2014, Article ID 150985, 8 pages
http://dx.doi.org/10.1155/2014/150985

Research Article

A Critical Heat Generation for Safe Nuclear Fuels after a LOCA

Jae-Yong Kim,[1] Dong-Bock Kim,[2] Hee-Jeong Cho,[3] Soon-Bum Kwon,[4] and Young-Doo Kwon[4]

[1] *Korea Atomic Energy Research Institute, No. 111 Daedeokdaero 989 Road, Daejeon 305-353, Republic of Korea*
[2] *Department of Global Marketing, Modeun Elevator Co., Ltd., No. 241 Ilbansaneop-gil Geochang-gun, Kyungsangnam-do, Namsang-myeon 670-881, Republic of Korea*
[3] *Graduate School of Mechanical Engineering, Kyungpook National University, No. 80 Daehakro, Daegu 702-701, Republic of Korea*
[4] *School of Mechanical Engineering & IEDT, Kyungpook National University, No. 80 Daehakro, Daegu 702-701, Republic of Korea*

Correspondence should be addressed to Young-Doo Kwon; ydkwon@knu.ac.kr

Received 17 January 2014; Revised 28 March 2014; Accepted 24 April 2014; Published 18 May 2014

Academic Editor: Inn Seock Kim

This study applies a thermo-elasto-plastic-creep finite element procedure to the analysis of an accidental behavior of nuclear fuel as well as normal behavior. The result will be used as basic data for the robust design of nuclear power plant and fuels. We extended the range of mechanical strain from small or medium to large adopting the Hencky logarithmic strain measure in addition to the Green-Lagrange strain and Almansi strain measures, for the possible large strain situation in accidental environments. We found that there is a critical heat generation after LOCA without ECCS (event category 5), under which the cladding of fuel sustains the internal pressure and temperature for the time being for the rescue of the power plant. With the heat generation above the critical value caused by malfunctioning of the control rods, the stiffness of cladding becomes zero due to the softening by high temperature. The weak position of cladding along the length continuously bulges radially to burst and to discharge radioactive substances. This kind of cases should be avoid by any means.

1. Introduction

This study applies a thermo-elasto-plastic-creep finite element procedure to the analysis of an accidental behavior of nuclear fuels as well as normal behavior. The result will be used as a basic data for the robust design of nuclear power plant and fuels. We extended the range of mechanical strain from small or medium to large adopting the Hencky logarithmic strain measure in addition to the Green-Lagrange strain and Almansi strain measures for the possible large strain situation in accidental environments.

The accidental situation is one of the most severe cases where LOCA is involved simultaneously. In most LOCA simulation, the power is generated 100% at the initial state and assumed to be shut down suddenly through the reactor trip at the beginning of the accident. However, the case assumes an accident unusual to the normal LOCA without ECCS (event category 5) [1–3], and the power is not completely but partly shut down. Therefore, we may call it a kind of RIA compared with the nominal full shutdown. The coolant behaves also most severely to exhibit an instant loss of pressure and level as one might expect an explosive failure of reactor shell.

2. Finite Element Analysis of Nuclear Fuels

Finite element analysis procedures of nuclear fuels have been developed by many researchers [5–7] and mostly applied to basic designs of them. The nominal operation of the nuclear power plant is known to exhibit the highest pellet temperature between 1100~1400°C and the clad temperature 400~600°C [8]. In this study, we introduce the thermo-elasto-plastic-creep analysis procedure based on Green-Lagrange strain measure first. For the analysis of the fuels under accidental situation like LOCA, we extended the procedure to large strain capability adopting logarithmic strain measure and additive decomposition of plastic strain. Through the adoption of additive decomposition method, we could provide a continuation between small-medium strain analysis and large strain analysis including creep phenomena.

2.1. Thermo-Elasto-Plastic-Creep Analysis. Thermo-elasto-plastic-creep analysis procedure has been developed by many researchers [4, 6, 9–12]. Most of them adopted Green-Lagrange or Almansi strain measures adequate for small-medium strain. It is briefly introduced here. For the thermo-elasto-plastic-creep analysis of nuclear fuel, it is necessary to obtain time-dependent temperatures solving the following well- known transient equation of heat transfer:

$$\begin{aligned} k\left(T_{,xx}+T_{,yy}\right)+Q-c\rho\dot{T}=0,\\ q=f_B \quad \text{on } \Gamma_f,\\ q=h\left(T-T_\infty\right) \quad \text{on } \Gamma_h, \end{aligned} \tag{1}$$

where T = temperature, k = coefficient of the thermal conductivity, ρ = density, c = specific heat, q = heat flow rate, f_B = heat flux, and h = convective heat transfer coefficient.

The partial differential equation of heat transfer (1) is expressed in other forms of functional to be minimized as in (2) [13].

Consider

$$\begin{aligned} \prod = \int \left(\frac{1}{2}\left\{\mathbf{T}_\partial\right\}^T[\kappa]\left\{\mathbf{T}_\partial\right\}-QT+c\rho T\dot{T}\right)dV\\ +\int\left(f_BT+hT_\infty T-\frac{1}{2}hT^2\right)dS, \end{aligned} \tag{2}$$

where $[\kappa]$ = conductivity matrix and $\{\mathbf{T}_\partial\}$ = temperature gradient.

After we introduce finite elements with proper shape functions and minimize the functional, the following finite element equation is derived:

$$\begin{aligned} {}^{t+\Delta t}\mathbf{C}^{(i)}\,{}^{t+\Delta t}\dot{\mathbf{T}}^{(i)}+\left({}^{t+\Delta t}\mathbf{K}^K+{}^{t+\Delta t}\mathbf{K}^C\right)\Delta\mathbf{T}^{(i)}\\ ={}^{t+\Delta t}\mathbf{Q}+{}^{t+\Delta t}\mathbf{Q}^{C(i-1)}-{}^{t+\Delta t}\mathbf{Q}^{K(i-1)}, \end{aligned} \tag{3}$$

$${}^{t+\Delta t}\mathbf{T}^{(i)}={}^{t+\Delta t}\mathbf{T}^{(i-1)}+\Delta\mathbf{T}^{(i)}. \tag{4}$$

Superscript i indicates the quantity of iterative state i at time $t+\Delta t$; therefore, ${}^{t+\Delta t}\mathbf{C}$ is the heat capacity matrix at time $t+\Delta t$, ${}^{t+\Delta t}\dot{\mathbf{T}}$ is the rate of temperature at time $t+\Delta t$, ${}^{t+\Delta t}\mathbf{K}^K$ is the conductivity matrix at time $t+\Delta t$, and ${}^{t+\Delta t}\mathbf{K}^C$ is the convection matrix at time $t+\Delta t$. $\Delta\mathbf{T}$ is the incremental nodal point temperature, ${}^{t+\Delta t}\mathbf{Q}$ is the nodal point heat input vector, ${}^{t+\Delta t}\mathbf{Q}^C$ is the nodal point heat contribution due to convection, and ${}^{t+\Delta t}\mathbf{Q}^K$ is the equivalent nodal point heat contribution. Accordingly, to solve the unknown nodal point temperature, ${}^{t+\Delta t}\mathbf{T}$, the equilibrium iteration will be performed repeatedly until the difference in the right hand terms of (3) is smaller than the convergence tolerance.

After obtaining the temperature distributions of fuel, the incremental equilibrium equation for the quasi-static motion of the fuel can be solved to obtain the incremental displacements:

$${}^{t+\Delta t}\mathbf{K}^{(i-1)}\,\Delta\,{}^{t+\Delta t}\mathbf{U}={}^{t+\Delta t}\mathbf{P}-{}^{t+\Delta t}\mathbf{R}^{(i-1)}, \tag{5}$$

where ${}^{t+\Delta t}\mathbf{K}^{(i-1)}$: stiffness matrix, $\Delta\mathbf{U}^{(i)}$: incremental displacement, $\Delta\,{}^{t+\Delta t}\mathbf{U}^{(i)}$: ${}^{t+\Delta t}\mathbf{U}^{(i-1)}+\Delta\,{}^{t+\Delta t}\mathbf{U}^{(i)}$, ${}^{t+\Delta t}\mathbf{P}$: external load, ${}^{t+\Delta t}\mathbf{R}^{(i-1)}$: equivalent load, and all quantities ${}^{t+\Delta t}\mathbf{X}^{(0)}={}^{t}\mathbf{X}$.

The stiffness ${}^{t+\Delta t}\mathbf{K}^{(i-1)}$ has linear term and geometrically nonlinear term. The temperatures are included in the external load resulting in the thermal deformation, and the thermal stain derived from the thermal deformation is considered in the evaluation of mechanical strain to compute the mechanical stresses.

The deviatoric stress is computed from the deviatoric elastic strain disregarding plastic and creep strain as

$${}^{t+\Delta t}\mathbf{S}=\frac{{}^{t+\Delta t}E}{1+{}^{t+\Delta t}\nu}\left({}^{t+\Delta t}\mathbf{e}'-{}^{t+\Delta t}\mathbf{e}^P-{}^{t+\Delta t}\mathbf{e}^C\right). \tag{6}$$

The mean stress is computed from the mechanical mean strain as in (5).

Consider

$${}^{t+\Delta t}\sigma_m=\frac{{}^{t+\Delta t}E}{1-2\,{}^{t+\Delta t}\nu}\left({}^{t+\Delta t}e_m-{}^{t+\Delta t}e_{\text{th}}\right), \tag{7}$$

where ${}^{t+\Delta t}\mathbf{S}$ = deviatoric stress tensor, ${}^{t+\Delta t}\mathbf{e}'$ = deviatoric strain tensor, ${}^{t+\Delta t}\mathbf{e}^p$ = plastic strain tensor, ${}^{t+\Delta t}\mathbf{e}^c$ = creep strain tensor, ${}^{t+\Delta t}\sigma_m$ = mean stress, ${}^{t+\Delta t}e_m$ = mean strain, ${}^{t+\Delta t}e_{\text{th}}$ = thermal strain, ${}^{t+\Delta t}E$ = Young's modulus, and ${}^{t+\Delta t}\nu$ = Poisson's ratio.

If we split the plastic and creep stains at $t+dt$ into the terms at time t and incremental terms, (7) becomes

$${}^{t+\Delta t}\mathbf{S}=\frac{E}{1+\nu}\left({}^{t+\Delta t}\mathbf{e}''-\Delta\mathbf{e}^p-\Delta\mathbf{e}^c\right), \tag{8}$$

where

$${}^{t+\Delta t}\mathbf{e}''={}^{t+\Delta t}\mathbf{e}'-{}^{t}\mathbf{e}^p-{}^{t}\mathbf{e}^c. \tag{9}$$

Creep strain may be represented by various creep laws, such as power creep law or exponential creep law. To confirm plastic stress based on the given displacement, ${}^{t+\Delta t}u^{(i)}$, it must satisfy one of the yield criteria. Adopting the von Mises yield criterion,

$$f_y={}^{t+\Delta t}\overline{\sigma}^2-{}^{t+\Delta t}\sigma_y^2=0, \tag{10}$$

where

$$\begin{aligned} &{}^{t+\Delta t}\overline{\sigma}=\sqrt{1.5\,{}^{t+\Delta t}\mathbf{S}\cdot{}^{t+\Delta t}\mathbf{S}}\text{: von Mises equivalent stress,}\\ &{}^{t+\Delta t}\sigma_y=\text{yield stress.} \end{aligned} \tag{11}$$

We have to solve the equation to obtain the deviatoric stress tensor. By applying the following flow rules of plastic and creep deformations,

$$\Delta \mathbf{e}^{p} = \Delta\lambda\, {}^{t+\Delta t}\mathbf{S},$$

$$\Delta \mathbf{e}^{c} = \Delta t\, {}^{\tau}\gamma\, {}^{\tau}\mathbf{S},$$

$$\tau = (1-\alpha)\, t + \alpha\,(t+\Delta t)\text{: relaxed time}$$

$$\alpha = \text{relaxation parameter},$$

$$\Delta\lambda = \frac{1.5\Delta \overline{e}^{p}}{{}^{t+\Delta t}\overline{\sigma}}\text{:}$$

incremental parameter for equivalent

plastic strain and equivalent stress at $t + \Delta t$,

$$\gamma = \frac{1.5\Delta \overline{e}^{c}}{{}^{\tau}\overline{\sigma}}\text{:} \tag{12}$$

parameter for relating incremental equivalent

creep strain and equivalent creep at $t + \Delta t$.

We obtain

$${}^{t+\Delta t}\mathbf{S} = \frac{1}{{}^{t+\Delta t}a_{E} + \alpha\Delta t\, {}^{\tau}\gamma + \Delta\lambda}\left[{}^{t+\Delta t}\left(\mathbf{e}'' - (1-\alpha)\,\Delta t\, {}^{\tau}\gamma\, {}^{t}\mathbf{S}\right)\right], \tag{13}$$

where

$$a_{E} = \frac{(1+\nu)}{E}. \tag{14}$$

Taking product of both sides of the equation, we obtain the equation

$$f_{g} = a^{2}\, {}^{t+\Delta t}\overline{\sigma}^{2} + b\, {}^{\tau}\gamma - c^{2}\, {}^{\tau}\gamma^{2} - d^{2} = 0, \tag{15}$$

where

$$a = {}^{t+\Delta t}a_{E} + \alpha\Delta t\, {}^{\tau}\gamma + \Delta\lambda = \frac{1}{2G'},$$

$$b = 3\,(1-\alpha)\,\Delta t\, {}^{t+\Delta t}\mathbf{e}'' \cdot {}^{t}\mathbf{S},$$

$$c = (1-\alpha)\,\Delta t\, {}^{t}\overline{\sigma}, \tag{16}$$

$$d^{2} = 1.5\, {}^{t+\Delta t}\mathbf{e}'' \cdot {}^{t+\Delta t}\mathbf{e}''.$$

The function, left side of (15), is known as the effective stress function and has to satisfy the condition of zero. Because $\overline{\sigma}$ is function of plastic strain and $\Delta\lambda$ is also a function of plastic strain and yield stress, the equation has to be solved simultaneously for $\overline{\sigma}$ and $\Delta\lambda$ using a root finding algorithm. We tried both Newton method and bisection method. The latter method is very reliable without being affected by the derivative of function. For the assumed ${}^{t+\Delta t}\overline{\sigma} = {}^{t+\Delta t}\sigma_{y}$, we compute $\Delta\lambda$ first and check whether the equation is satisfied. If not, follow the usual root finding algorithm to find the ${}^{t+\Delta t}\overline{\sigma} = {}^{t+\Delta t}\sigma_{y}$ and $\Delta\lambda$ simultaneously that satisfy the chosen type of yield criterion.

Here, we propose a first stage constitutive modulus as

$$C'' = \frac{1}{{}^{t+\Delta t}a_{E} + \lambda + \Delta t\, {}^{\tau}\gamma} = 2G''; \tag{17}$$

see Figure 2.

The tangent constitutive matrix $\mathbf{C}^{\mathrm{EPC}}$ can be obtained using the perturbation method [4, 14]. Each column of the matrix $\mathbf{C}^{\mathrm{EPC}}$ is the column of perturbed stress tensor divided by the magnitude of perturbed element of corresponding strain. However, at the first stage of interaction, one can use quasi-elastic modulus of Figure 1(b) [4], where C'' is more close to the tangent modulus than C'. We could find fast convergence with C'' than with C' in several examples.

2.2. Large Strain (Hencky Logarithmic) Measure. For large strain analysis, we need some basic relations that are briefly introduced here [9, 10, 15–18]. Deformation gradient is represented by

$${}^{t}_{0}\mathbf{X} = \frac{\partial\, {}^{t}\mathbf{x}}{\partial\, {}^{0}\mathbf{x}} = {}^{t}\mathbf{J}^{T}\left({}^{0}\mathbf{J}^{-1}\right)^{T}, \tag{18}$$

where $\mathbf{J}$ is the transformation between the cantesian coordinate and natural coordinate systems. It can be decomposed as

$${}^{t}_{0}\mathbf{X} = {}^{t}_{0}\mathbf{R}\, {}^{t}_{0}\mathbf{U} \tag{19}$$

into rotation tensor ${}^{t}_{0}\mathbf{R}$ and right stretch tensor ${}^{t}_{0}\mathbf{U}$. Right Cauchy-Green gradients are expressed using the deformation gradient

$${}^{t}_{0}\mathbf{C} = {}^{t}_{0}\mathbf{X}^{T}\, {}^{t}_{0}\mathbf{X}. \tag{20}$$

Solving the following equivalent problem,

$${}^{t}_{0}\mathbf{C}\, {}^{t}_{0}\mathbf{P} = {}^{t}_{0}\mathbf{\Lambda}^{2}\, {}^{t}_{0}\mathbf{P}. \tag{21}$$

We obtain a diagonal matrix ${}^{t}_{0}\mathbf{\Lambda}$ of principal stretches and their direction matrix. The right stretch matrix is obtained as

$${}^{t}_{0}\mathbf{U} = {}^{t}_{0}\mathbf{P}\, {}^{t}_{0}\mathbf{\Lambda}\, {}^{t}_{0}\mathbf{P}^{T}. \tag{22}$$

Therefore, the rotation matrix is given by

$${}^{t}_{0}\mathbf{R} = {}^{t}_{0}\mathbf{X}\, {}^{t}_{0}\mathbf{U}^{-1}. \tag{23}$$

Then, the Henckey logarithmic strain tensor is given by

$${}^{t}_{0}\mathbf{E}_{H} = \frac{1}{2}\, {}^{t}_{0}\mathbf{P}\, {}^{t}_{0}\mathbf{H}\, {}^{t}_{0}\mathbf{P}^{T}, \tag{24}$$

where

$${}^{t}_{0}\mathbf{H} = \ln \mathbf{\Lambda}^{2}. \tag{25}$$

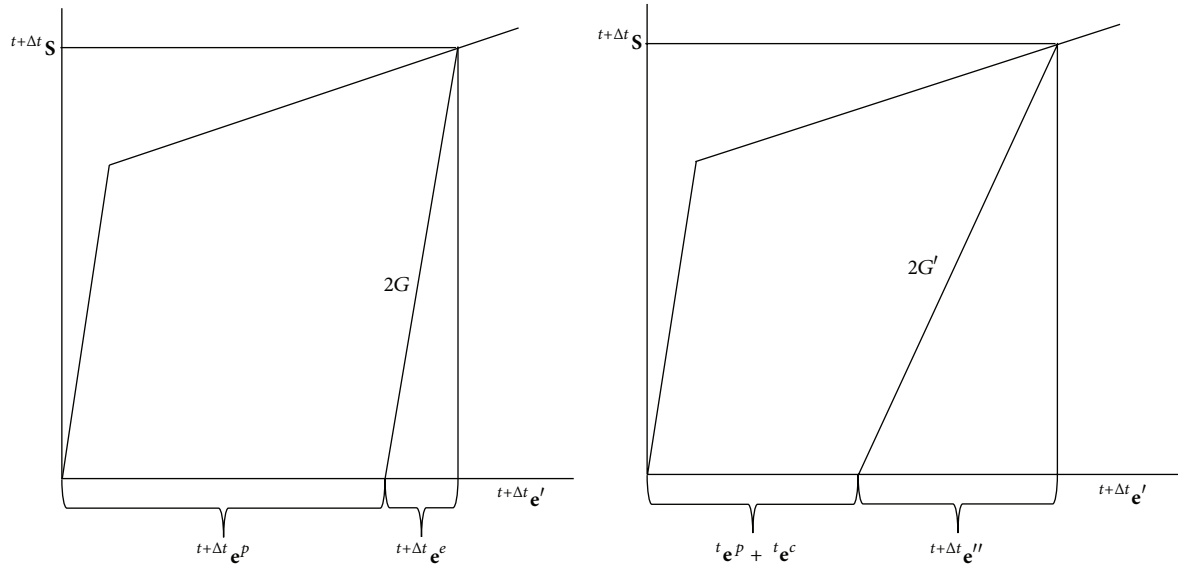

(a) Elastic (b) Quasi-elastic [4]

Figure 1: First stage constitutive modulus.

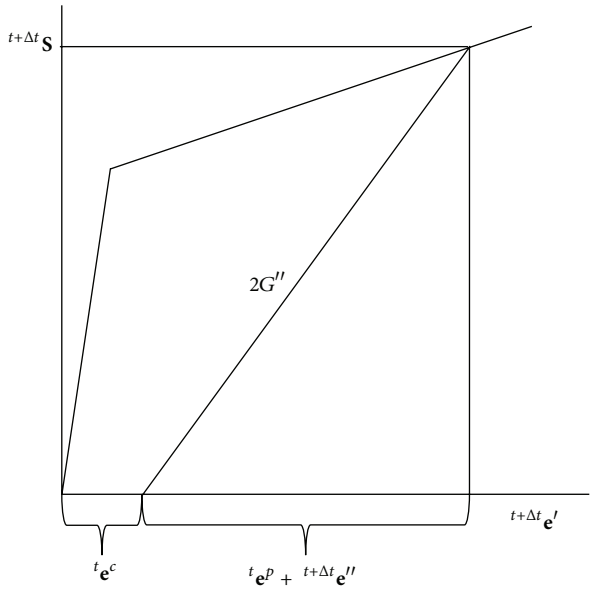

Figure 2: Proposed first stage quasi-elastic modulus.

We can also represent the Green-Lagrange strain tensor as

$$ {}^t_0\mathbf{E}_G = \frac{1}{2}\left({}^t_0\mathbf{C} - \mathbf{I}\right) \tag{26} $$

and the Almansi strain tensor as

$$ {}^t_0\mathbf{E}_A = \frac{1}{2}\left(\mathbf{I} - {}^0_t\mathbf{C}\right). \tag{27} $$

The Henckey logarithmic strain tensor can also be written as

$$ {}^t_0\mathbf{E}_H = \ln {}^t_0\mathbf{U} = \frac{1}{2}\ln {}^t_0\mathbf{C}. \tag{28} $$

We computed the above equations and compared them (three kinds of marks) with theoretical (29) in Figure 3:

$$ \begin{aligned} {}^t_0e_{11} &= \frac{1}{2}\left({}^t_0\lambda^2 - 1\right)\text{: Green-Lagrange strain,} \\ {}^te_{11} &= {}^t_0\lambda\text{: Small strain,} \\ {}^t_0E^{(H)}_{11} &= \ln {}^t_0\lambda\text{: Logarithmic strain,} \\ {}^t_te^A_{11} &= \frac{1}{2}\left(1 - {}^t_0\lambda^{-2}\right)\text{: Almansi strain.} \end{aligned} \tag{29} $$

Using the above procedure of thermo-elasto-plastic-creep with logarithmic strain measure with additive decomposition of plastic strain, our additive decomposition method follows the procedures in [9, 10, 15] except that we do not decompose plastic deformation gradient multiplicatively as

$$ \mathbf{X}^E_A = {}^{t+\Delta t}_0\mathbf{X}\left({}^t_0\mathbf{X}^p\right)^{-1} \tag{30} $$

at the trial elastic state first but considered it additively as in (6) and (8). Therefore, we do not loose continuation between the later large strain procedure and the former small strain procedure including creep deformation.

The case without creep deformation in the following example compares the two procedures of large strain problems, additive decomposition and multiplicative decomposition. The first one is uniaxial isochoric extension with the following condition [15]:

$E = 200$ MPa: Young's modulus;

$\nu = 0.3$: Poisson's ratio;

$\sigma_y = 0.75$ MPa: yield stress;

$H = 2$ MPa: hardening modulus.

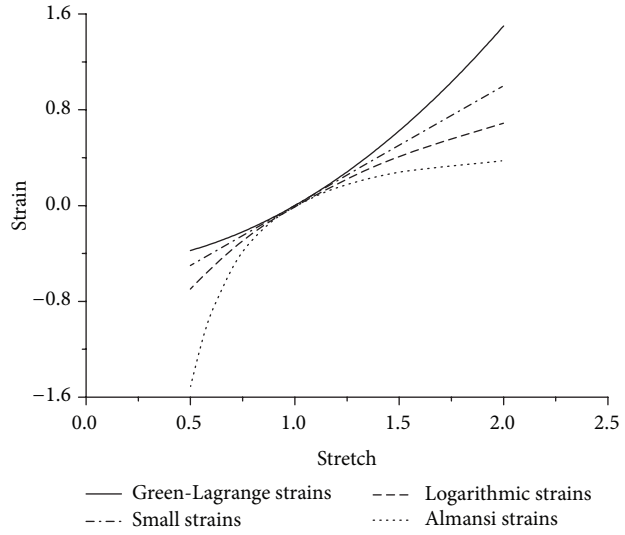

Figure 3: Strain-stretch relations for various strain measures.

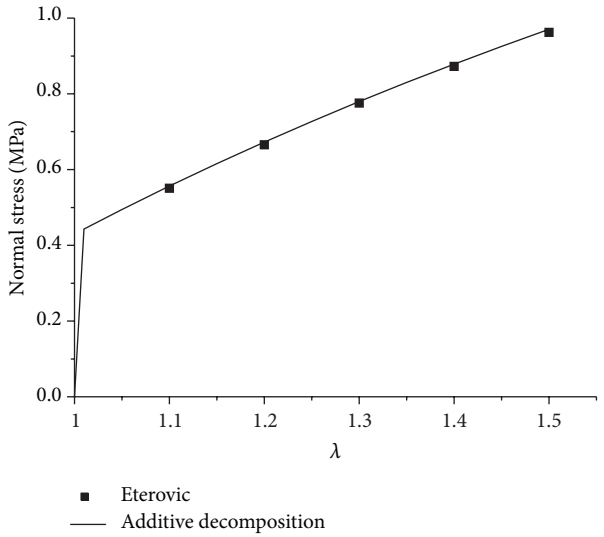

Figure 4: Normal stress σ_x along stretch λ.

The results are compared in Figure 4 showing a good agreement.

The second example is shear deformation; the result is compared with the result of the literature (solid square) obtained by the multiplicative decomposition in Figure 5.

We also compared the following example (Figure 6) under shear load in Figure 7, which tests not only the stress integration process but also the equilibrium iteration procedure too.

3. Behavior of Nuclear Fuels after Loss of Cooling Accidents

In the usual case of LOCA, the control rods are inserted into the fuel rods to shut down the reactor. The power is reduced successfully. However, such as the Fukushima accident, the

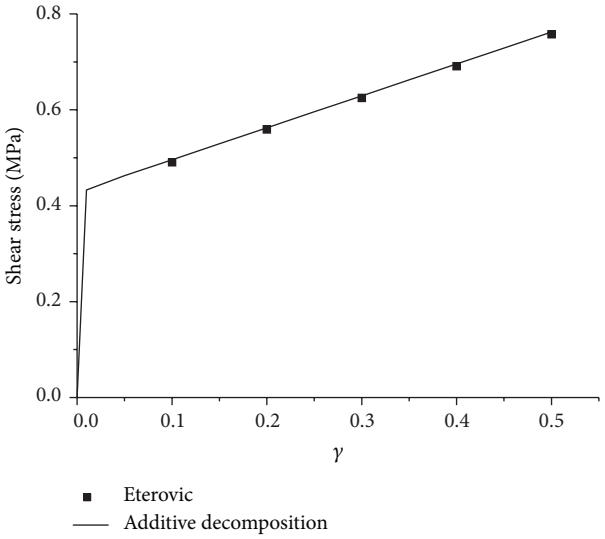

Figure 5: Shear stress τ_{12} along shear strain γ.

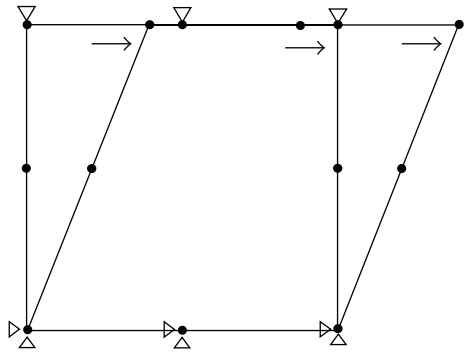

Figure 6: FEM model for shear load analyses of multiplicative and additive decomposition methods.

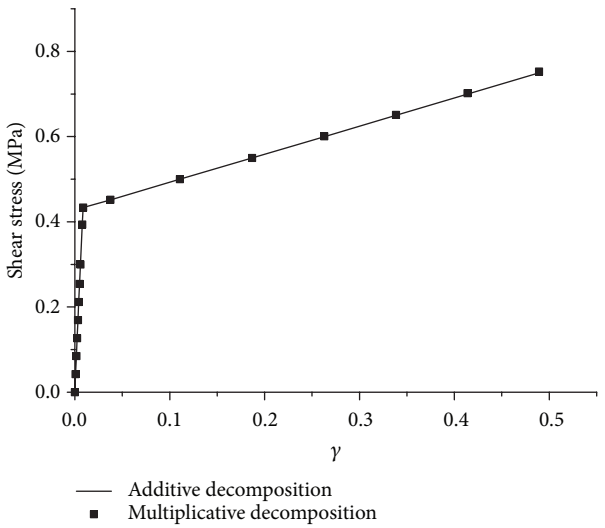

Figure 7: Shear stresses under shear loads for different decompositions of plastic strain.

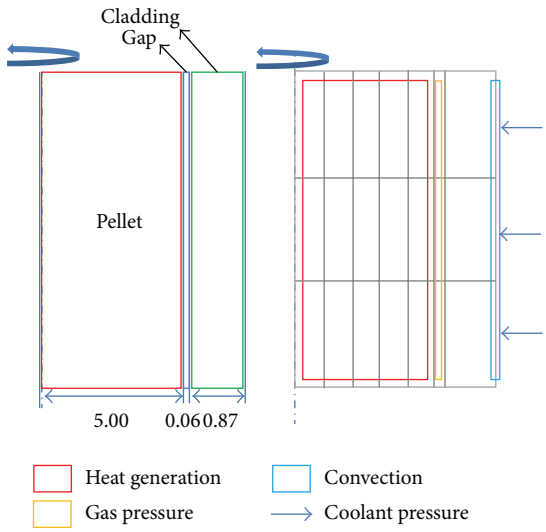

Figure 8: Solid nuclear fuel model and boundary conditions.

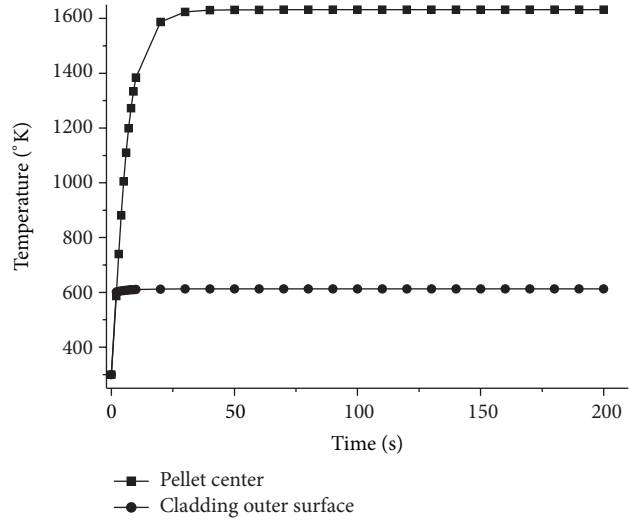

Figure 9: Temperatures changes at pellet center and cladding outer surface along the time.

Table 1: Applied condition.

Coolant pressure	15.5 MPa
Gap pressure	3.45 MPa
Gap conductivity	0.5 mJ/s·mm·°K
Heat generation	450 mJ/mm^3·s
Heat transfer coefficient	75 mJ/s·mm^2 · °K
T_∞	600°K

control rods could not be inserted to the rods because of the malfunction of inserting system located at the lower part of the reactor. Therefore, we assumed that the heat generation of the fuels is partly reduced and partly working. In the literature concerning LOCA scenario, we saw a 100% power generation adopted in the analysis.

Before we analyze the behavior of nuclear fuels after LOCA (loss of coolant accident), we analyzed normal operation first using the following condition. The material properties of fuel components are the same as in the literature [6]. Mesh generation of the fuel rod was conducted using the quadrilateral 8-node elements, and the boundary conditions were applied as in Figure 8.

The boundary conditions include the application of heat generation to the pellet and the application of coolant pressure and convection resulting from the coolant to cladding. By applying gas pressure to the gap between the pellet and cladding, the overall environment when actual nuclear fuel rods are activated is shown in Table 1.

Figure 9 shows the temperature changes at pellet center and outer surface of the cladding along time, and temperatures go into steady state before 100 sec.

Suppose that there is a LOCA (loss of coolant pressure and relative heat transfer coefficient changed from 7500 mJ/s·mm^2 · °K to 75 mJ/s·mm^2 · °K) at time 70 sec. Moreover, there is an additional situation of the malfunctioning of control rod.

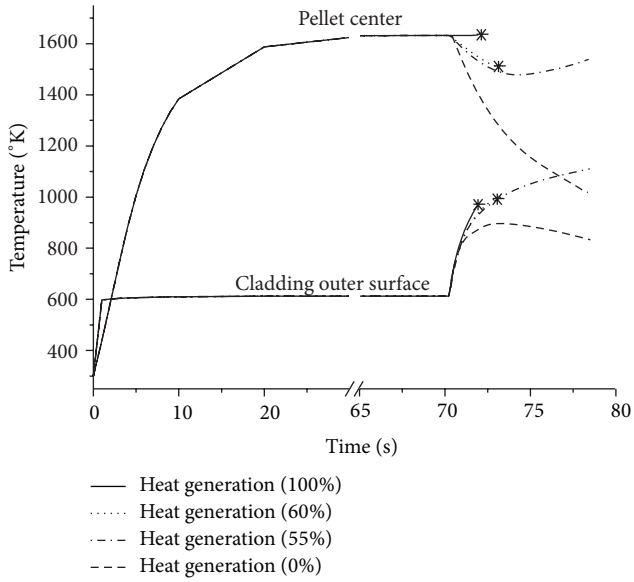

Figure 10: Temperatures changes at pellet center and cladding outer surface after LOCA at 70 sec.

We assumed that one of four conditions of heat generation (complete shutdown = 0%, 55%, and 60% and full heat generation = 100%) is maintained after the LOCA. Figure 10 shows temperature changes at the two positions. As one may expect, shutdown makes the rapid drops of temperature at both positions of fuel. For the intermediate heat generations, the temperatures of pellet drop first and then increase afterwards. The temperature of clad increases fast and slowly increases later on. Finally, sharp increase of temperature is detected at the clad for full heat generation. The asterisk marks denote that the analyses have been stopped due to the instability of clad stiffness caused by the softening by temperature increase, surpassing the hardening by strain. The load applied to the clad due to the rod internal pressure is

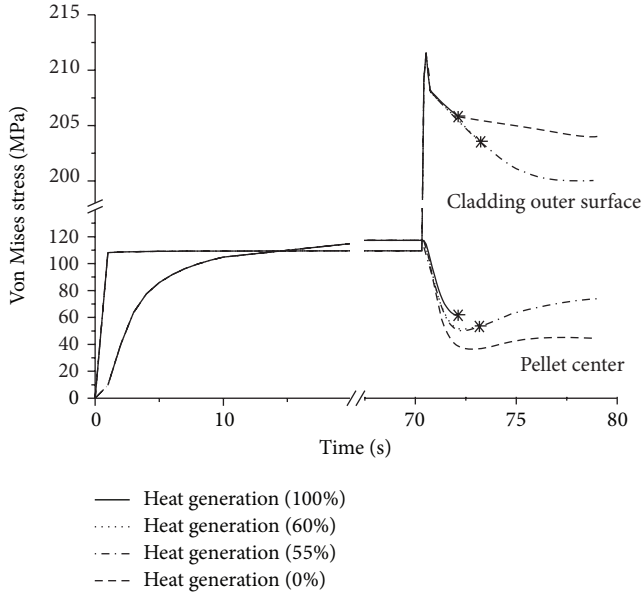

Figure 11: Von Mises stresses changes at pellet center and cladding outer surface after LOCA at 70 sec.

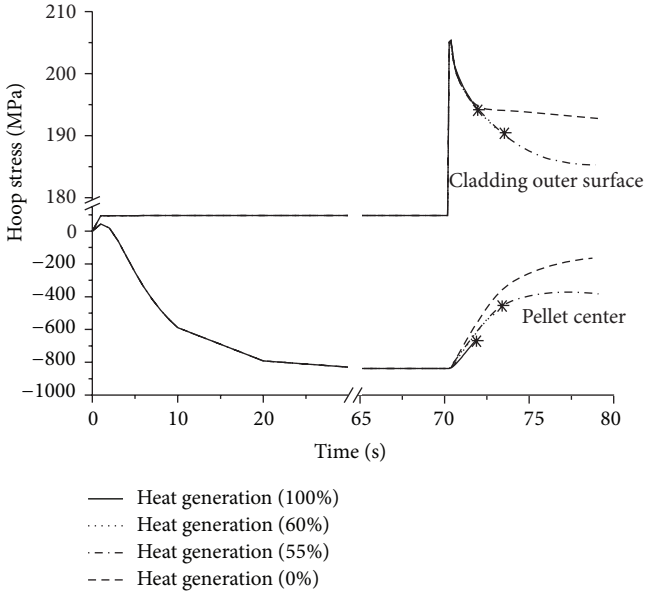

Figure 12: Hoop stresses changes at pellet center and cladding outer surface after LOCA at 70 sec.

supported by the strength of clad. However, if the temperature of the clad is too high, Young's modulus and strength of the clad are reduced, and it cannot sustain the applied load. Once it cannot resist the load and starts to deform, the situation is out of control and the clad becomes thinner and thinner causing larger and larger stresses resulting in fuel failure. This phenomenon is a kind of instability like a buckling.

The variations of von Mises stress of clad are shown in Figure 11. The heat generations above 55% induced instability at the clad to cause continuous expansion to burst at the weakest point along the length.

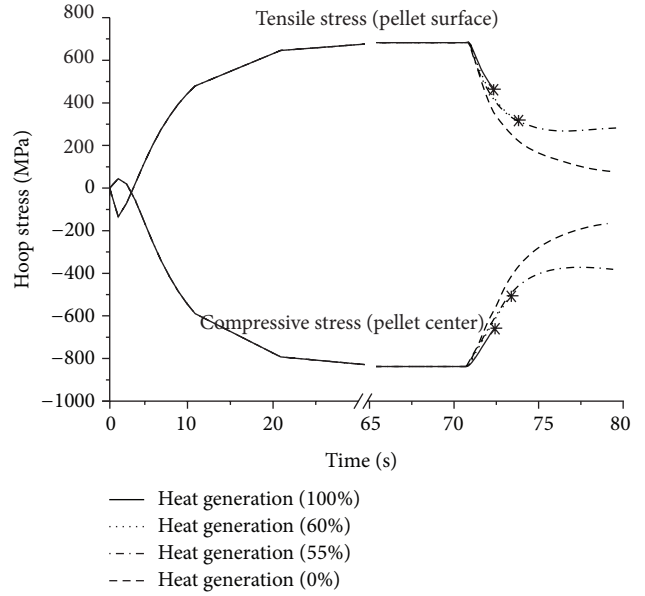

Figure 13: Compressive and tensile stresses changes at pellet center and outer surface after LOCA at 70 sec.

In the early stage, there is a gap between the pellet and clad. After a long time of operation, the coolant pressure compresses the clad to cause a creep phenomenon and the gap is gone. Then the contact stress between pellet and clad raises the compressive stress at the inner part of the pellet. If this stress is above the ultimate strength of the pellet material, pellet may be fractured to pieces and may give some harm to the clad.

Hoop stresses at the center of pellet and clad surface are shown in Figure 12. We may have temporal time interval for the rescue of the plant in accident for the condition of heat generation under 55% of full generation. Over 60%, a catastrophic situation occurs when the clad of zero stiffness expands continuously to bust and discharge radioactive substances, a situation we have to avoid by any means.

Figure 13 exhibits the tendencies of thermal stresses in the pellet. Except the very early stage, outer portion of the pellet experiences tensile hoop stress, and the inner portion of it experiences compressive stresses. Every case including full heat generation shows lowering of thermal stresses in the pellet, which is thought to originate from smaller temperature difference between the extreme positions and insulation effect at the outer surface of the clad due to the loss of coolant. What is ironic is that the LOCA results in the reduction of temperature gradient in the pellet and causes more even distribution of temperature within the pellet to make it safer.

4. Conclusions

We extended the finite element procedure of code TEPC (thermo-elasto-plastic-creep) from small and medium strain to Hencky logarithmic strain measure for the large strain analysis to handle the case that may happen in accidental situation. The TLPC (thermo-large strain-plastic-creep) which is the extended version of the TEPC has been applied to the

analysis of nuclear fuels under LOCA without ECCS (event category 5) as well as normal operation.

A LOCA is concerned with the system pressure decrease, the rod internal pressure, the hoop stress on the cladding, the temperature of the cladding, strain, and so forth. We added an accidental condition of malfunctioning of the control rod system resulting in incomplete shutdown of the fuel power. And we checked a critical remaining heat generation that causes clad failure. The results are summarized as follows.

(i) The fuels under consideration have reached quasi-steady state condition after 70 sec. The maximum core temperature was 1631°K, and the outer cladding temperature was 612.6°K when there was no contact between the pellet and cladding.

(ii) We adopted a LOCA without ECCS (event category, 5), and the external pressure of the fuel rod has zero gauge pressure. After the LOCA (lower heat transfer coefficient of 75 $mJ/s \cdot mm^2 \cdot {}^\circ K$) at time 70 sec with the heat generation of the pellet under the critical value, there was no instability at the cladding for the time being, which means one may have temporal time interval for the rescue of the system by recovery of the cooling system or shutdown of the system letting the heat generation be zero.

(iii) After the LOCA at time 70 sec, there was an unstable condition that the stiffness of the cladding becomes zero which is followed by a local uncontrollable expansion of clad to burst, with above critical heat generation of the pellet.

For the analysis of this kind of unstable situation, we need certain special analyzing methods. One method is a postbuckling method usually applied to static problems, and it is expected to be improper for this kind of transient problem. The other one is a dynamic analysis, which usually is not necessary for this kind of quasi-static problem; however, it is expected to be the most effective technique which can handle the problem of zero stiffness.

Conflict of Interests

The authors declare that there is no conflict of interests regarding the publication of this paper.

Acknowledgments

This research was supported by the Basic Science Research Program through the National Research Foundation of Korea (NRF) funded by the Ministry of Education (NRF-2012R1A1A2008903). The authors are partially supported by BK21 plus project of the National Research Foundation of Korea.

References

[1] J. N. Lillington, *Light Water Reactor Safety: The Development of Advanced Models and Codes for Light Water Reactor Safety Analysis*, Elsevier Science, Amsterdam, The Netherlands, 1995.

[2] Nuclear Energy Agency OECD, "Nuclear fuel behavior in loss-of-coolant accident (LOCA) conditions," State-of-the-Art-Report, 2009.

[3] IAEA, *Analysis of Severe Accidents in Pressurized Heavy Water Reactors*, IAEA-TECEOC-1594, 2008.

[4] M. Kojic and K. J. Bathe, "The "Effective-stress-function" algorithm for thermo-elasto-plasticity and creep," *International Journal for Numerical Methods in Engineering*, vol. 24, no. 8, pp. 1509–1532, 1987.

[5] M. Suzuki and H. Saitou, *Light Water Reactor Fuel Analysis Code FEMAXL-IV(VER.2); Detailed Structure and User's Manual*, Department of Reactor Safety Research Nuclear Safety Research Center, Tokai Research Establishment, Japan Atomic Energy Research Institute Tokai-mura, Ibaraki-Ken, Japan, 1997.

[6] Y. D. Kwon, S. B. Kwon, H. J. Song, M. S. Kim, and J. S. Kim, *Evaluation of Nuclear Fuel Behaviors Using Finite Element*, KAERI, 2010.

[7] Y. D. Kwon, Y. S. Yang, J. S. Kim, and S. B. Kwon, "A study on the flow characteristics in an annular type fuel pellet of PWR," *Journal of Mechanical Science and Technology*, vol. 27, no. 1, pp. 257–261, 2013.

[8] C. B. Lee, Y. S. Yang, D. H. Kim, S. K. Kim, and J. G. Bang, "A new mechanistic and engineering fission gas release model for a uranium dioxide fuel," *Journal of Nuclear Science and Technology*, vol. 45, no. 1, pp. 60–71, 2008.

[9] K. J. Bathe, *Finite Element Procedures*, vol. 2, no. 3, Prentice Hall, Englewood Cliffs, NJ, USA, 1996.

[10] M. Kojic and K. J. Bathe, *Inelastic Analysis of Solids and Structures*, Computational Fluid and solid Mechanics, 2004.

[11] W. E. Haisler and D. R. Sanders, "Elastic-plastic-creep-large strain analysis at elevated temperature by the finite element method," *Computers & Structures*, vol. 10, no. 1-2, pp. 375–381, 1979.

[12] M. D. Snyder and K. J. Bathe, "A solution procedure for thermo-elastic-plastic and creep problems," *Nuclear Engineering and Design*, vol. 64, no. 1, pp. 49–80, 1981.

[13] R. D. Cook, D. S. Malkus, M. E. Plesha, and R. J. Witt, *Concepts and Applications of Finite Element Anylysis*, John Wiley & Sons, New York, NY, USA, 2002.

[14] C. Miehe, "Numerical computation of algorithmic (consistent) tangent moduli in large-strain computational inelasticity," *Computer Methods in Applied Mechanics and Engineering*, vol. 134, no. 3, pp. 223–240, 1996.

[15] A. L. Eterovic and K. Bathe, "A hyperelastic-based large strain elasto-plastic constitutive formulation with combined isotropic-kinematic hardening using the logarithmic stress and strain measures," *International Journal for Numerical Methods in Engineering*, vol. 30, no. 6, pp. 1099–1114, 1990.

[16] J. C. Simo, "A framework for finite strain elastoplasticity based on maximum plastic dissipation and the multiplicative decomposition: part I. Continuum formulation," *Computer Methods in Applied Mechanics and Engineering*, vol. 66, no. 2, pp. 199–219, 1988.

[17] F. J. Montáns and K. J. Bathe, "On the stress integration in large strain elastoplasticity," *Computational Fluid and Solid Mechanics*, vol. 2003, pp. 494–497, 2003.

[18] M. Á. Caminero, F. J. Montáns, and K. Bathe, "Modeling large strain anisotropic elasto-plasticity with logarithmic strain and stress measures," *Computers & Structures*, vol. 89, no. 11-12, pp. 826–843, 2011.

Hindawi Publishing Corporation
Science and Technology of Nuclear Installations
Volume 2014, Article ID 206258, 12 pages
http://dx.doi.org/10.1155/2014/206258

Research Article

Study on Nuclear Accident Precursors Using AHP and BBN

Sujin Park,[1] Huichang Yang,[2] Gyunyoung Heo,[1] Muhammad Zubair,[3] and Rahman Khalil Ur[1]

[1] *Department of Nuclear Engineering, Kyung Hee University, Yongin Si, Gyeonggi Do 446-701, Republic of Korea*
[2] *Industrial Services TUV Rheinland Korea Ltd. 197-28 Guro-dong, Guro-gu, Seoul 152-719, Republic of Korea*
[3] *Department of Basic Sciences, University of Engineering and Technology, Taxila, Pakistan*

Correspondence should be addressed to Gyunyoung Heo; gheo@khu.ac.kr

Received 5 February 2014; Accepted 19 April 2014; Published 14 May 2014

Academic Editor: Joon-Eon Yang

Most of the nuclear accident reports used to indicate the implicit precursors which are not easily quantified as underlying factors. The current Probabilistic Safety Assessment (PSA) is capable of quantifying the importance of accident causes in limited scope. It was, therefore, difficult to achieve quantifiable decision-making for resource allocation. In this study, the methodology which facilitates quantifying these precursors and a case study were presented. First, four implicit precursors have been obtained by evaluating the causality and hierarchy structure of various accident factors. Eventually, it turned out that they represent the lack of knowledge. After four precursors are selected, subprecursors were investigated and their cause-consequence relationship was implemented by Bayesian Belief Network (BBN). To prioritize the precursors, the prior probability is initially estimated by expert judgment and updated upon observations. The pair-wise importance between precursors is calculated by Analytic Hierarchy Process (AHP) and the results are converted into node probability tables of the BBN model. Using this method, the sensitivity and the posterior probability of each precursor can be analyzed so that it enables making prioritization for the factors. We tried to prioritize the lessons learned from Fukushima accident to demonstrate the feasibility of the proposed methodology.

1. Introduction

A number of causes can initiate accidents in nuclear power plants (NPPs). These causes can be divided broadly into two categories: explicit and implicit factors. Explicit factors are relatively easy to be quantitatively assessed and statistically evaluated, such as equipment malfunction and unavailability due to test or maintenance. On the other hand, implicit factors are difficult to be quantified, such as independence of regulatory agencies, safety culture, and professional ethic.

One representative method of quantifying the priority of accident causes is Probabilistic Safety Assessment (PSA) in nuclear area. PSA can deal with the statistically quantifiable factors such as the failure of equipment and a part of human errors, while PSA is not typically relevant to the factors that are difficult to be quantified but sometimes more fundamental precursors. In order to stably maintain and efficiently improve nuclear safety, the quantitative ranking of these factors and reasonable decision-making based on this ranking are required. Also, through this, the efficient distribution of limited resources or budget can be expected.

The Fukushima accident opens new horizons of knowledge for human to think and analyze such aspects of incidents that do not usually occur in normal life. A critical examination of the accident reveals that the accumulation of various technical and nontechnical lapses only compounded the nuclear disaster. After the accident, a number of research papers [1–4] and reports [5–8] appeared discussing the different aspects of the accident. According to International Atomic Energy Agency (IAEA), some important lessons learned include the following [9]:

(i) the availability of an external event Probabilistic Safety Assessment (PSA) model would be an effective tool in performing the assessment;

(ii) there are insufficient defence-in-depth provisions for tsunami hazards;

(iii) an updating of regulatory requirements and guidelines should be performed;

(iv) the complicated structures of organizations can result in delays in urgent decision-making.

After Fukushima accident, the importance of implicit or qualitative factors is emphasized, while the specific methodology to evaluate them still seems lacking.

In this paper, by combining two effective mathematical modeling tools, Analytic Hierarchy Process (AHP) and Bayesian Belief Network (BBN), four factors underlying nuclear accidents were derived considering the hierarchical structure and causality of variously candidates. In the process of determining these accident factors, the opinion of experts, having different age, region, and expertise, has been considered. As a result, we decided four factors that have high contribution during the whole plant life-cycle and are not overlapped in terms of their functions. These four factors recognized are essentially associated with the lack of human knowledge and they are obviously not easy to be quantified, but they should be. These factors will be called as precursors. The precursors and their subprecursors have been investigated in terms of their relative significance to a goal, the possibility of accident inducing design extended conditions since we aim at discussing the lesson learned from Fukushima accident. Similarly, with determining the precursors, the methodology of prioritizing the accident precursors is based on BBN and AHP, but in distinctive ways. In previous studies, the methodologies utilizing BBN and AHP have been formulated for supporting decision-making processes. Limiting to nuclear field, the applications for the risk analysis [10–13], decision-making support [14, 15], and the evaluation of systems' importance [16–18] were reported as examples of using BBN and AHP. Differently from the previous applications, this study suggested a method of how to model a BBN and to assign probability information to the BBN model using the results of AHP such that ultimately the model enables prioritizing accident precursors for nuclear accidents.

2. Methodology

2.1. Selection of Four Precursors

2.1.1. Analytic Hierarchy Process (AHP). The Analytic Hierarchy Process (AHP) is a tool for solving multicriteria decision problems. Analytic Hierarchy Process (AHP) proposed by Saaty [19] is very popular and has been applied in wide variety of areas including

(i) planning,

(ii) selecting the best alternative,

(iii) resource allocation and resolving conflicts.

AHP applications are found useful when problems require considerations of both quantitative and qualitative factors. AHP decomposes the problem into small parts in order to facilitate the decision-making in the appraisal task. First, a hierarchy structuring the problem is constructed.

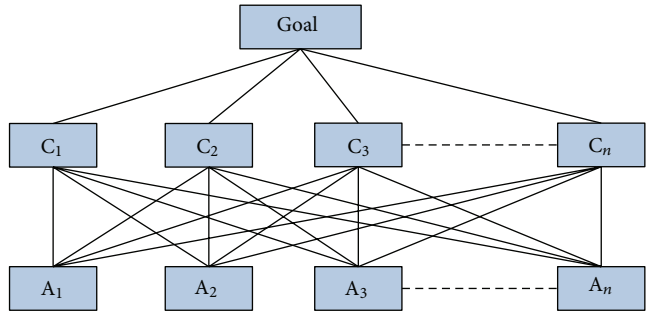

Figure 1: Main structure of AHP in terms of goal, criteria, and alternative.

Table 1: Priority based scale used in AHP.

Fundamental scale	Explanation
1	Equal importance
3	Moderate importance
5	Strong importance
7	Very strong
9	Extreme importance
2, 4, 6, 8	Intermediate levels

The top of the hierarchy represents the goal. Below goal, we have the criteria, subcriteria (if necessary), and alternatives as shown in Figure 1. Although these steps seem very easy to do but how to select criteria in AHP is a question for decision-makers and for experts. In fact, the influences of selected criteria on alternatives and on other external factors which are related to problem have very high impact on decision-making. For instance, if there are 100 criteria, it will not only simplify the problem to select the most appropriate criteria but also reduce the chances of errors.

The appraisal can be constructed top-down or bottom-up but always using pair-wise comparisons. Application of AHP to a decision problem involves four steps [20]:

(i) structuring of the decision problem,

(ii) making pair-wise comparisons and obtaining the judgmental matrix,

(iii) computing local weights and consistency of comparisons,

(iv) aggregation of local weights.

To make comparisons, we need a scale of numbers that indicates how many times more important one element is over another element with respect to the criterion. Table 1 exhibits the scale.

The consistency index (CI) is the deviation of the maximum eigenvalue ($\lambda_{\max}$) from the number of criteria (n) used in the comparison process:

$$\mathrm{CI} = \frac{\lambda_{\max} - n}{n - 1}. \quad (1)$$

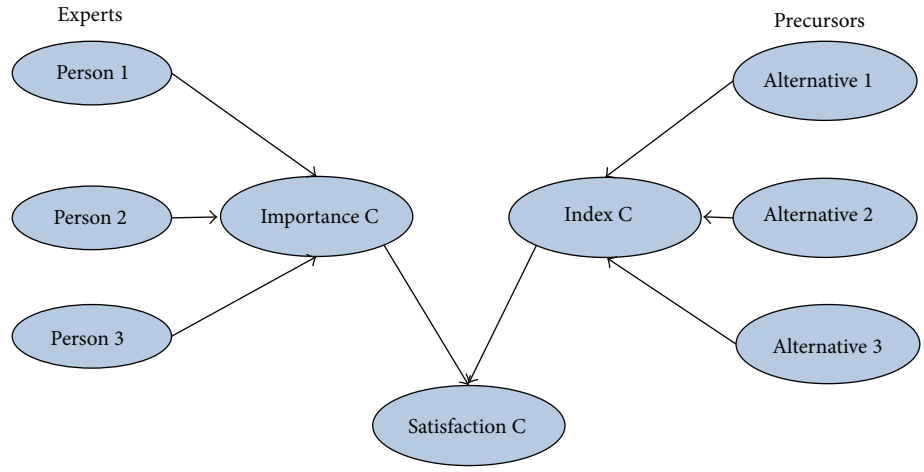

Figure 2: BBN network associated with selection of precursors.

The AHP model provides a feedback to the decision-maker on the consistency of the entered judgments by a measure called consistency ratio (CR):

$$\mathrm{CR} = \frac{\mathrm{CI}}{\mathrm{RI}}. \tag{2}$$

The ratio index (RI) is the average of the consistency index of 500 randomly generated matrices. If the consistency ratio is higher than 10%, it is recommended to revise the comparisons in order to reduce the inconsistency.

2.1.2. Bayesian Belief Networks (BBNs). Bayesian Belief Network (BBN) has become one of the most popular tools to model the phenomena of uncertainty in decision problems (diagnosis, cognitive knowledge, management of project resources, expert system, etc.). BBNs are defined by a directed acyclic graph in which discrete random variables are assigned to each node, together with the conditional dependence on the parent nodes. Root nodes are nodes with no parents, and marginal prior probabilities are assigned to them. The main feature of BBN is that it is possible to include local conditional dependencies into the model, by directly specifying the causes that influence a given effect. It is a graphical model that represents a directed relationship between a set of probabilistic variables. It is a result in probability theory on the Bayes' theorem. This model uses an oriented graph to formalize the uncertainty in the form of a causal graph. In addition, it can help us to make decisions in the event of inaccuracies.

The Bayes' theorem is given by

$$P\left(\frac{A_i}{B}\right) = \frac{P\left(B/A_i\right)P\left(A_i\right)}{\sum_{j=1}^{n} P\left(B/A_j\right)P\left(A_j\right)}. \tag{3}$$

The probability $P(A_i/B)$ is the posterior probability, the term $P(B/A_i)$ is called likelihood, $P(A_i)$ is prior probability, and $1/\sum_{j=1}^{n} P(B/A_j)P(A_j)$ is constant of proportionality which insures that the total probability equals 1. The above equation can also be written as

$$\mathrm{Post}\,(\lambda) \propto \mathrm{Likelihood} \times \mathrm{Prior}\,(\lambda)\,. \tag{4}$$

BN has great practical application in prediction of software reliability, risk informed safety categorization, and modeling uncertainty to find out safety culture and organizational culture in industrial area, and so forth.

2.1.3. Modeling and Selection of Criteria by Using BBN. As discussed earlier that the selection of criteria is one of the important steps in AHP, AHP does not provide help to select criteria and different factors that affect selection of criteria. However, by using BBN, this problem can be solved. During the selection of precursors, there are many conditions and factors which will be divided into two parts as represented in Figure 2. The left hand side of this figure represents the characteristics of experts or person; these may be internal characteristics of experts (e.g., age, gender, profession, region, and behavior) or external characteristics (e.g., facilities, time line, and honorarium). The right hand side of Figure 2 indicates the characteristics of precursors; it also contains internal characteristics (technical and non-technical weakness, workload on staff, lack of training, etc.) and external characteristics (e.g., site choice, climate, weather, and tsunami). The detailed study of these characteristics is essential to select better precursor and to collect best knowledge from experts.

The following terms explain the role of BBN in the selection of criteria.

(i) Expert/person: this is a person who will make selection. This person may belong to any region in the world having any kind of expertise.

(ii) Alternatives: these are the choices available. In our case, these are precursors that play a major role in causing any accident.

(iii) Index of criteria (index C): it is a numerical function that affects all alternatives and represents quality of all alternatives.

(iv) Importance of criteria (importance C): it represents the level of importance of criteria for experts (depends upon characteristics of experts).

(v) Satisfaction of criteria (satisfaction C): it denotes the level of satisfaction of experts to select precursors.

By applying this idea, criteria can be selected by keeping in view the alternatives and experience of experts. Index nodes represent the quality of the alternative for a criterion. To determine the values of these indices in the BBN, values obtained by the AHP method were used, therefore using the same initial data.

Once the characteristics of the person have been entered in the Bayesian network, the importance is set for each criterion. After that, the value of the overall satisfaction is set to the highest value and propagation is done with inference. The first result is the posterior probabilities of the node of alternatives. The connection between three nodes, that is, index, importance, and selection of criteria, can be seen in Figure 2.

2.2. Prioritize the Precursors

2.2.1. Framework. The methodology that this paper focused on is BBN to express the possibility of a consequence using the causal relationship by the combination of causes. Utilizing the nature of BBN, it is possible to evaluate (1) the potential possibility of an accident depending on the prior distribution of the precursors and (2) the priority of precursors in terms of the posterior distribution for an accident.

The BBN model is composed of four precursors and eleven subprecursors decomposed from the precursors. They are ultimately connected to the goal entitled "the possibility of accident including design extended conditions."

Figure 3 shows a framework of the methodology presented in this paper.

At first, we need to enter the prior probabilities in the lowest nodes corresponding to the subprecursors. In general, it is not easy to obtain the prior probabilities because of the nature of the subprecursors which are associated with lack of knowledge and are difficult to be quantified. Due to this circumstance, we performed sensitivity analysis to investigate the change of the goal according to the change of prior probability from assumed distribution. At an initial step, we can assume a uniform distribution for all subprecursors, that is, noninformative distribution. The uniform distribution can be updated depending on the measures taken after an accident because such measures can improve or reinforce the condition of subprecursors. It is also possible to update prior probabilities by expert judgment.

The next step is to input the Node Probability Table (NPT) calculated on the basis of AHP, which is conditional probability or likelihood between a parent node and multiple child nodes. Since all nodes represent qualitative entities, the statistical evaluation of the NPT is also not appropriate. What this paper suggested is how to obtain the weight between child nodes through AHP and to convert them into the NPT.

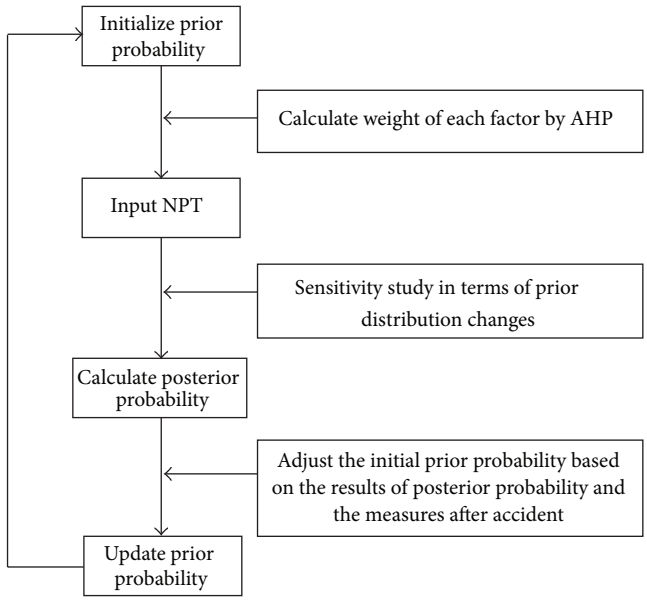

Figure 3: Framework of the BBN model supported by AHP.

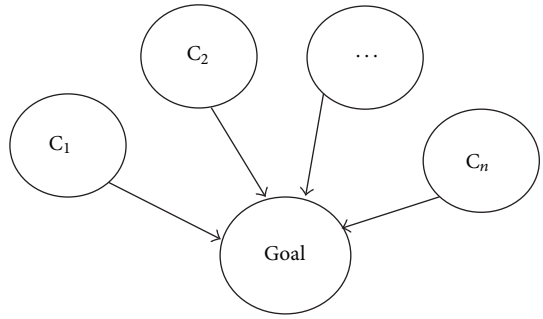

Figure 4: Simple example of a BBN model.

The possibility of the goal is now calculated using the NPT and the prior probabilities assigned to subprecursors on the basis of Bayes' theorem. Furthermore, we are able to check the change in prior probabilities, which is called posterior probabilities and can reestablish priority or ranking among precursors if we assume the occurrence of a goal. If it is made the reinforcement work for the precursor indicated as a critical contributor, its prior probability may be updated. If the quality of the precursor becomes worse, it can be possible to update it accordingly. The entire framework is repeated with the updated prior probabilities.

2.2.2. Generation of Node Probability Tables. Using a hypothetical BBN model shown in Figure 4, the method of applying the results of AHP to make an NPT is described. Because all precursors and subprecursors are selected by the Mutually

Table 2: Pair-wise comparison result of AHP.

Criteria	C_1	C_2	$\cdots$	C_n	Sum
C_1	w_{11}	w_{12}	$\cdots$	w_{1n}	$\sum_{j=1}^{n} w_{1j}$
C_2	w_{21}	w_{22}	$\cdots$	w_{2n}	$\sum_{j=1}^{n} w_{2j}$
$\vdots$	$\vdots$	$\vdots$	$\cdots$	$\vdots$	$\vdots$
C_n	w_{n1}	w_{n2}	$\cdots$	w_{nn}	$\sum_{j=1}^{n} w_{nj}$
Sum	$\sum_{i=1}^{n} w_{i1}$	$\sum_{i=1}^{n} w_{i2}$	$\cdots$	$\sum_{i=1}^{n} w_{in}$	$\sum_{i=1}^{n}\sum_{j=1}^{n} w_{ij}$

Exclusive Collectively Exhaustive (MECE) principle, the BBN model composed of these precursors should have the same structure as Figure 4. Thus, the case that was a single parent node with several child nodes was selected as an example. In Figure 4, the parent node means a goal in the BBN model and N number of child nodes means precursors. Each precursor can have subprecursors and the methodology is equally applied.

The relative weight for each child node is calculated by performing the AHP considering the importance of a child node in terms of the contribution on the possibility of a parent node, and their results are converted into the NPT.

Table 2 shows the results of the pair-wise comparison of AHP. From the results of AHP, the sum of all rows and all columns is calculated. Then, sum of entire row was divided into sum of column. As a result, the relative weight of each child node was obtained through

$$w_k = \frac{\sum_{i=1}^{n} w_{ik}}{\sum_{i=1}^{n}\sum_{j=1}^{n} w_{ij}}, \tag{5}$$

where w_k is the weight of a child node or a precursor, C_k.

Table 3 shows the example of NPT. The distribution of all precursors is discretized into three states, High/Medium/Low. "High" means the condition that a precursor is not managed properly. Getting lower means that the quality of precursor is well managed so that the probability of occurring accident is getting decreased. The goal is also discretized into two states, High/Low. Similarly, "High" stands for the high possibility that an accident occurs, and "Low" corresponds to the opposite condition.

Correction factor, I_k^s, is assigned depending on the states of C_k. Equation (6) calculates the conditional probability or likelihood, L, constituting the NPT:

$$L\left(\text{Goal} = \text{High} \mid C_1 = s_1, C_2 = , \ldots, C_n = s_n\right) = \sum_{k=1}^{n} w_k \times I_k^s. \tag{6}$$

Since w_k represents the degree of contribution that an accident occurrence, the result of (6) is assigned to the "High" state of the goal. In order to obtain the numerical correction factors for three states, we assumed a linear model which has 0.0 at the best condition and 1.0 at the worst condition. This model was divided into three equal parts, and the median value of each part was regarded as calculated as the correction factors. The correction factors are, therefore, expressed as $I_k^{\text{high}} = 0.17$, $I_k^{\text{medium}} = 0.50$, and $I_k^{\text{low}} = 0.83$.

The conditional probability for "Low" is assigned by (7). Even though the sum of conditional probabilities does not necessarily become 1.0, we used (7) for simplification in this study:

$$L\left(\text{Goal} = \text{Low} \mid C_1 = s_1, C_2 = , \ldots, C_n = s_n\right) = 1 - L\left(\text{Goal} = \text{High} \mid C_1 = s_1, C_2 = , \ldots, C_n = s_n\right). \tag{7}$$

3. Results and Discussion

3.1. Selection of Precursors. In AHP and BBN combined method, the purpose of BBN is to select the most suitable criteria or precursors and provide this output into AHP as represented in Figure 5. On the basis of person's characteristics and the impact of all expected alternatives on criteria, BBN chooses a criterion which is satisfied by all aspects.

The persons belonging to different expertise, age, profession, region, and behavior analyze the accident. From Table 4, it can be seen that for each expert there are 29 precursors on the basis of which they need to select the most significant precursors. Each precursor in Table 4 belongs to International Atomic Energy Agency (IAEA) safety standards [21]. These standards have been considered in this study by keeping in view the safety management, technical requirements, plant design, requirements, and safety objectives. It seems very difficult to analyze accident by keeping in view these 29 precursors, but by using BBN only the top four precursors have been selected by considering the expert's judgment as shown in Figure 6.

Figure 7 represents selected precursors that have to be used in AHP. Each precursor has equal weighting of persons' characteristics, that is, 20%, which indicates that experts will have to make prioritization by bearing in mind equal importance of all aspects of criteria. The prioritization in AHP to select the best alternative will be given by keeping in view the experts' experience, profession, age, location, and behavior.

The precursors determined above are weakly linked to each other (mutually exclusive) and contain the causes of a goal comprehensively (collectively exhaustive). More common and fundamental factors which affect all precursors are excluded because it does not meet the purpose of this study, that is, decision-making by distinctive prioritization of precursors. A detailed description of each precursor and its subprecursor is summarized as follows.

(1) Operation: capability that operators can respond to appropriate tasks in timely manner for the following purposes:

(i) O1: prevention,
(ii) O2: mitigation for design basis accidents,

Table 3: Structure of node probability table.

C_n					High					⋯
⋮					⋮					⋮
C_2		High			Medium			Low		⋯
C_1	High	Medium	Low	High	Medium	Low	High	Medium	Low	⋯
Goal = high										⋯
Low										

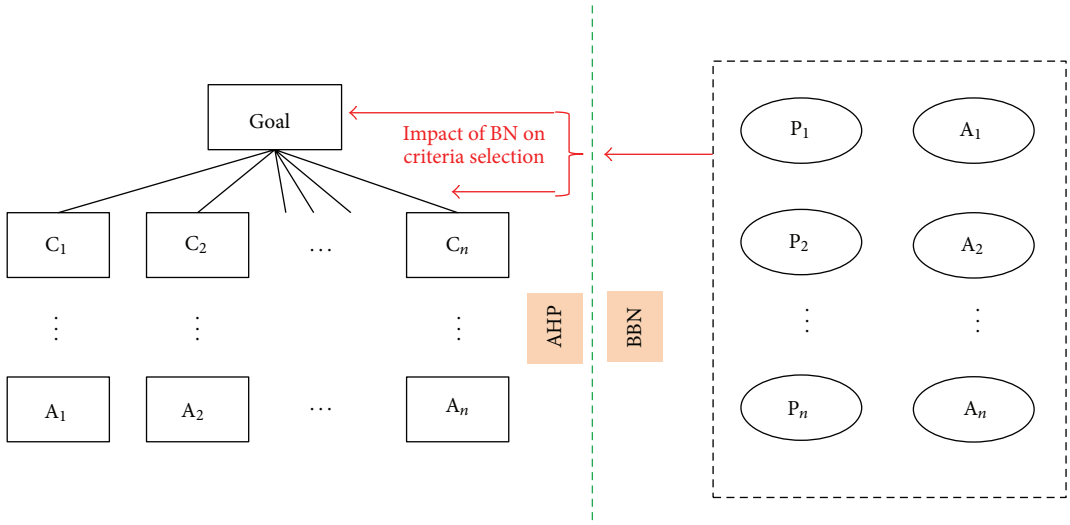

Figure 5: AHP and BBN combined technique.

(iii) O3: mitigation for severe accidents,
(iv) O4: mitigation for design extended conditions.

(2) Maintenance: capability to maintain the availability of safety-related SSC during the whole life-cycle:

(i) M1: procurement,
(ii) M2: field activities (replacement, repair, inspection, test, ...).

(3) Design: capability that designers can provide the defense mechanism for the whole set of postulated accidents:

(i) D1: technical adequacy and comprehensiveness in designing safety provisions (minimize epistemic uncertainty),
(ii) D2: effectiveness of implementing safety provisions (conceptual/detained design, analysis, manufacturing, construction, ...).

(4) Regulation: capability to verify and validate the goodness of the whole above processes:

(i) R1: backfitting—update of up-to-date knowledge and its verification,
(ii) R2: periodic inspections—operation within the licensed scopes,
(iii) R3: licensing—completeness of design basis.

3.2. Results of AHP. AHP was performed to the goal and the precursors, respectively. From Tables 5, 6, 7, 8, and 9, the pairwise comparison matrix and the weight calculated by (5) are presented.

The calculated weights in Tables 5 to 9 are converted to conditional probability by (6) and (7) and this becomes the NPT for the BBN model.

3.3. Sensitivity Analysis of Precursors. In this paper, AgenaRisk was utilized for the development of BBN models [22].

This section examines the sensitivity of the goal according to the prior probability change of each precursor. Initially, the prior probability of the precursors is set to uniform distribution and the probability of the goal is calculated, which is regarded as a reference value. The probability of each precursor is, then, set to low 100% and high 100%, respectively, to check the results of risk reduction (low 100%) and risk achievement (high 100%).

Table 4: List of all expected criteria.

Precursor	Description	Precursor	Description
C_1	Safety management (SM)	C_{16}	Common cause failures (CCF)
C_2	Initiating events (IE)	C_{17}	Auxiliary services (AS)
C_3	Safety assessment (SA)	C_{18}	Equipment outages (EO)
C_4	Availability of facilities (AF)	C_{19}	Organizational aspects (OA)
C_5	Operation (O)	C_{20}	Quality assurance (QA)
C_6	Defense in depth (DiD)	C_{21}	Design (D)
C_7	Accident prevention (AP)	C_{22}	Operator training (OT)
C_8	Radiation protection (RP)	C_{23}	Component survivability (CS)
C_9	Quality management (QM)	C_{24}	Social aspects (SA)
C_{10}	Safety classification (SC)	C_{25}	Emergency diesel generator (EDG)
C_{11}	Maintenance (M)	C_{25}	Protection against disaster (PD)
C_{12}	Political aspects (PA)	C_{26}	Emergency core cooling system (ECCS)
C_{13}	External events (EE)	C_{27}	Regulations (R)
C_{14}	Site characteristics (SC)	C_{28}	Unavailability of safety system (USS)
C_{15}	Control room (CR)	C_{29}	Deficient emergency response (DER)

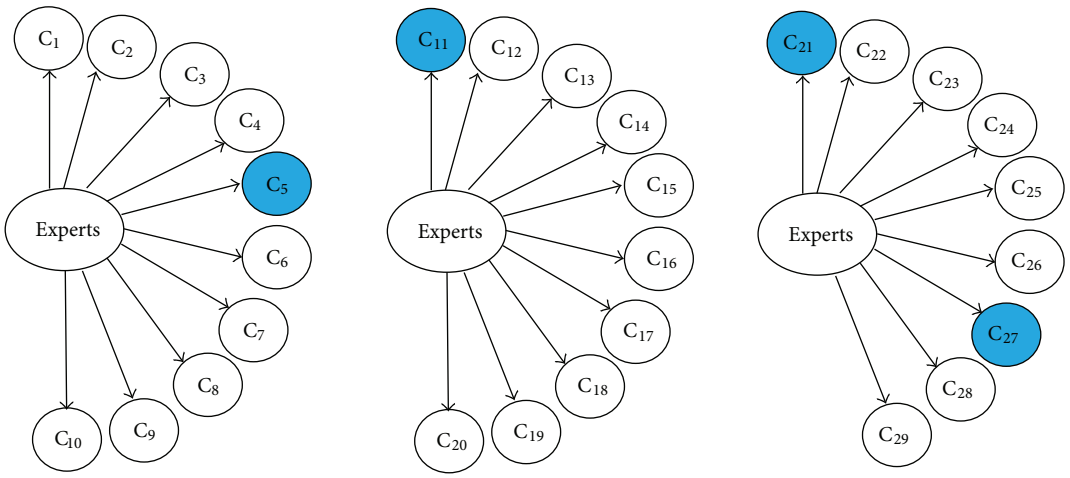

Figure 6: Selection of precursor by using BBN.

Using (8), the results are obtained and showed in Table 10:

$$
\begin{aligned}
S_k^{\text{low}} &= \{E[\text{Goal at } C_k = \text{low } 100\%] \\
&\quad - E[\text{Goal at } C_k = \text{uniform}]\} \\
&\quad \times (\{E[C_k = \text{low } 100\%] - E[C_k = \text{uniform}]\})^{-1}, \\
S_k^{\text{high}} &= \{E[\text{Goal at } C_k = \text{high } 100\%] \\
&\quad - E[\text{Goal at } C_k = \text{uniform}]\} \\
&\quad \times (\{E[C_k = \text{high } 100\%] - E[C_k = \text{uniform}]\})^{-1},
\end{aligned} \tag{8}
$$

where

S_k^{low} and S_k^{high} are sensitivity at low 100% or high 100% conditions,

E[Goal at C_k = low (or high) 100%] is the expectation of the goal when C_k is low or high 100% condition,

E[Goal at C_k = uniform] is the expectation of the goal when C_k is a uniform distribution,

E[C_k = low (or high) 100%] is the expectation of the precursor, C_k, when it is low or high 100% condition,

E[C_k = uniform] is the expectation of the precursor, C_k, when it is a uniform distribution.

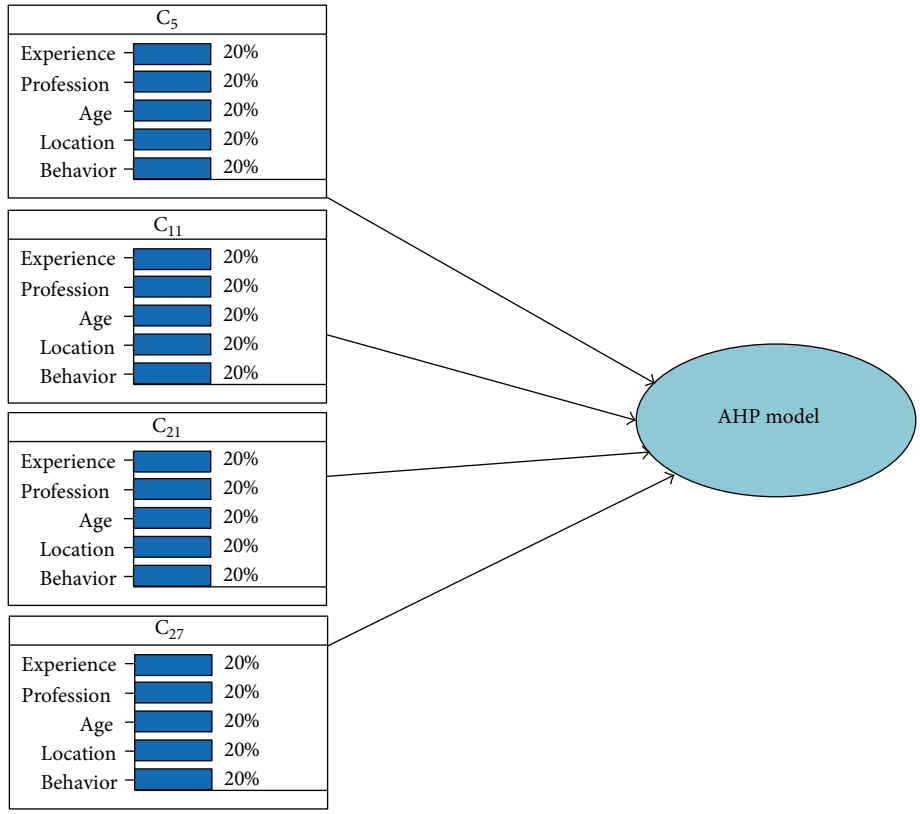

Figure 7: Use of selected criteria into BBN model.

Table 5: The results of pair-wise comparison for Goal.

	Operation	Maintenance	Design	Regulation	Weight (w_k)
Operation	1.00	1.14	3.56	2.00	0.12
Maintenance	0.88	1.00	3.00	2.00	0.16
Design	0.28	0.33	1.00	0.63	0.44
Regulation	0.50	0.50	1.59	1.00	0.28

Table 6: The results of pair-wise comparison for subprecursors of Operation.

Operation	O1	O2	O3	O4	Weight (w_k)
O1	1.00	0.55	0.55	0.42	0.39
O2	1.82	1.00	0.69	0.55	0.26
O3	1.82	1.44	1.00	0.81	0.19
O4	2.38	1.82	1.23	1.00	0.16

Table 7: The results of pair-wise comparison for subprecursors of Maintenance.

Maintenance	M1	M2	Weight (w_k)
M1	1.00	1.26	0.44
M2	0.79	1.00	0.56

Table 8: The results of pair-wise comparison for subprecursors of Design.

Design	D1	D2	Weight (w_k)
D1	1.00	0.87	0.53
D2	1.15	1.00	0.47

Table 9: The results of pair-wise comparison for subprecursors of Regulation.

Regulation	R1	R2	R3	Weight (w_k)
R1	1.00	1.82	2.15	0.20
R2	0.55	1.00	1.00	0.39
R3	0.46	1.00	1.00	0.41

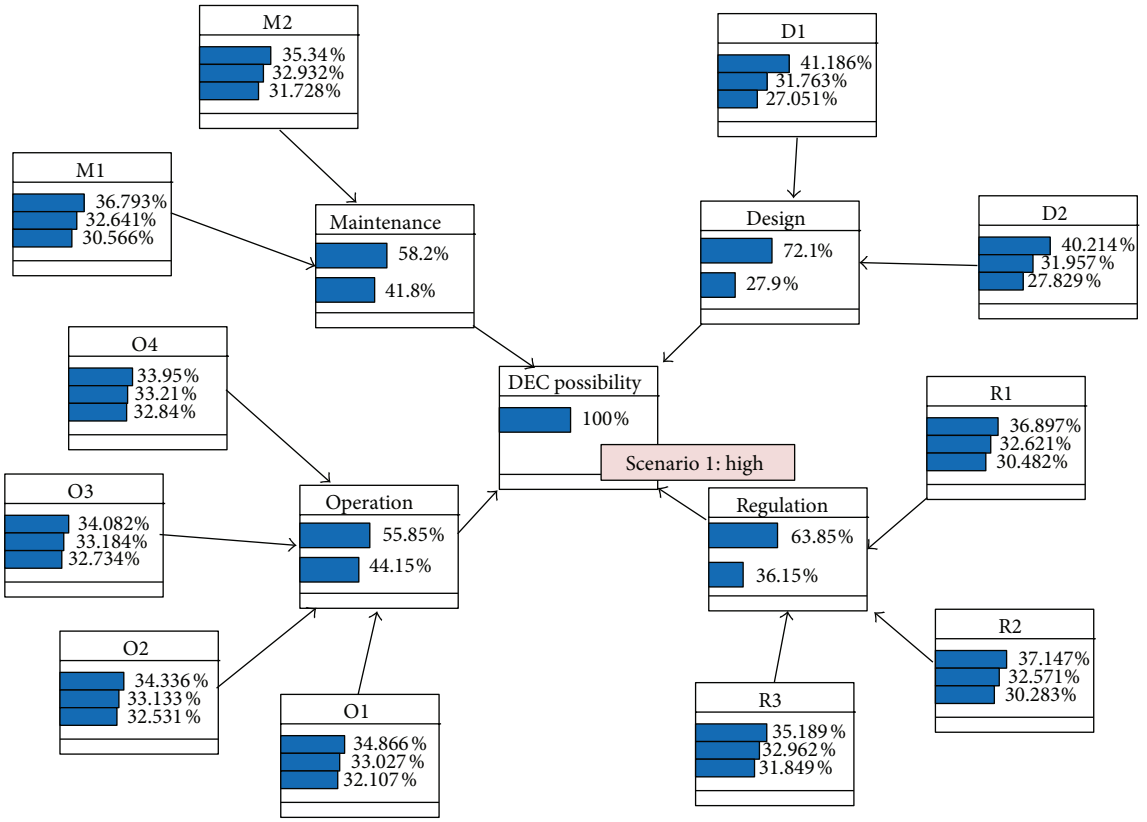

Figure 8: Change of precursors when an accident occurs.

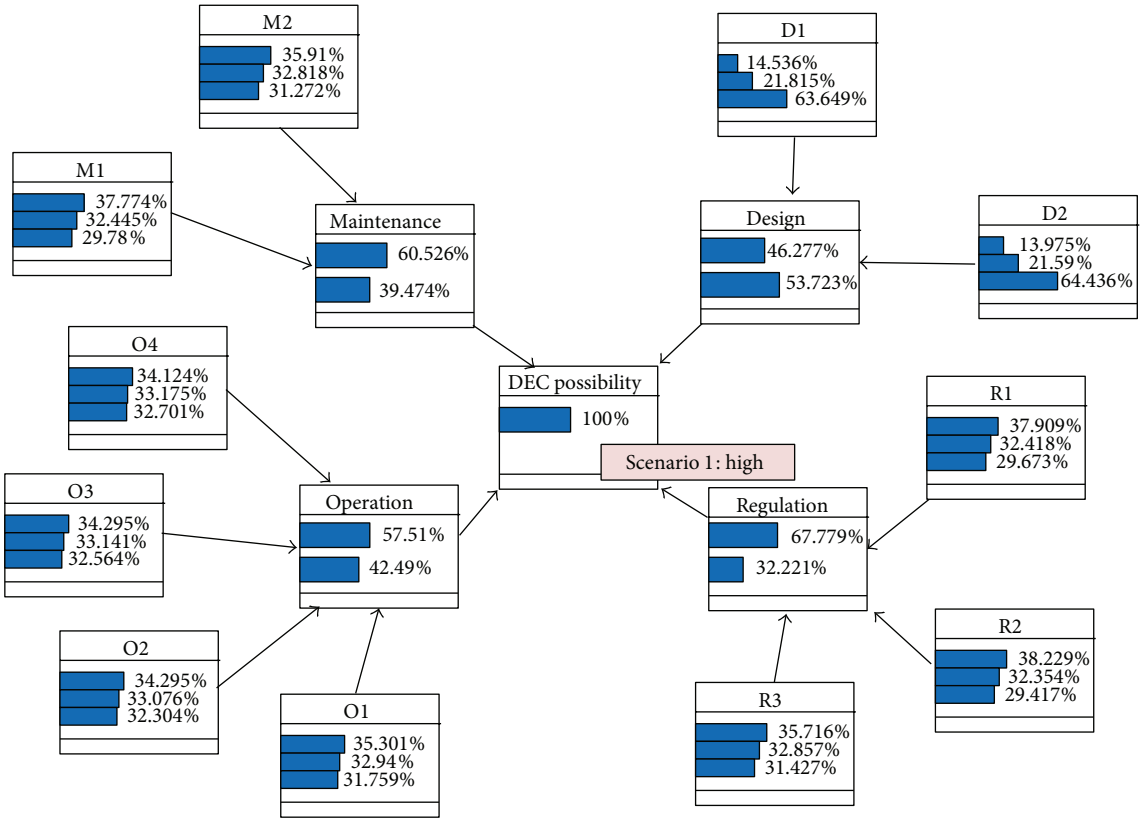

Figure 9: Change of precursors when strengthening D1 and D2.

Table 10: Sensitivity of the goal with the change of prior probabilities.

Precursor	S_k^{high}		S_k^{low}	
	Value	Ranking	Value	Ranking
O1	1.023	8	1.019	8
O2	1.015	9	1.012	9
O3	1.011	10	1.009	10
O4	1.009	11	1.007	11
M1	1.051	5	1.043	5
M2	1.030	6	1.025	6
D1	1.118	1	1.104	1
D2	1.103	2	1.090	2
R1	1.053	4	1.044	4
R2	1.057	3	1.047	3
R3	1.028	7	1.023	7

Table 11: Change of prior probability when the goal is high 100%.

Precursor	R	Ranking
O1	1.013	8
O2	1.009	9
O3	1.007	10
O4	1.006	11
M1	1.031	5
M2	1.018	6
D1	1.071	1
D2	1.062	2
R1	1.032	4
R2	1.034	3
R3	1.017	7

Table 12: Comparison of precursors before and after the update of prior probability.

Precursor	R	Ranking	Initial ranking
O1	1.017	6	8
O2	1.013	7	9
O3	1.008	8	10
O4	1.007	9	11
M1	1.039	3	5
M2	1.023	4	6
D1	0.754	10	1
D2	0.747	11	2
R1	1.041	2	4
R2	1.045	1	3
R3	1.021	5	7

In Table 10, it is turned out that "D1" has higher sensitivity than any other subprecursor, while "O4" has the least contribution to the goal. Since the uniform distribution for subprecursors was initially assumed, the ranking for S_k^{low} and S_k^{high} was identical.

3.4. Calculation of Posterior Probability. In this section, the prioritization of precursors was performed upon the posterior probability assuming that an accident would occur. First, the prioritization of precursors was performed when all precursors have uniform distribution in Figure 8.

The "High" state of the goal was set to 100% so that we can assume that an accident occurs. Assuming this, the posterior probabilites of the subprecursors were calculated and compared with the initial prior probabilities which was a uniform distribution. In order to calculate the expectation, the correction factor was applied to the expectation of the precursor calculation and the second correction factor was applied to the expectation of the goal calculation. The ratio, R_k, is suggested as a metric to provide prioritization among subprecursors can assume an accident occursbution by

$$R_k = \frac{E\left[\mathrm{C}_k \text{ at Goal} = \text{high } 100\%\right]}{E\left[\mathrm{C}_k = \text{uniform}\right]}. \tag{9}$$

The results are shown in Table 11.

From Table 11, the priority of all subprecursors was identically recognized as the result of sensitivity analysis in Table 10 due to the nature of uniform distribution. The derived posterior probability can be the updated prior probability.

From the results, a hypothetical scenario was imagined. Once "D1" and "D2" are identified as the most significant contributors, there is going to be an effort to improve these factors. If this effort is successful, then the prior probability of "D1" and "D2" will be updated to $P(\mathrm{D1} = \text{Low } 100\%)$ and $P(\mathrm{D2} = \text{Low } 100\%)$. In this situation, the posterior probability of each precursor is updated as shown in Figure 9 and Table 12.

New result shows that the priorities of the precursors associated with "Design" become lower than others, which is different from the previous case. In this case, regulation and maintenance factors are relatively importantly evaluated, so it should be reasonable that available resouces are allocated to these factors to take cost-benefitial achievement.

3.5. Case Study. The proposed methodology was intended for general nuclear facilities, but, as a demonstrative case, we applied it to Fukushima accident. The causes of Fukushima accident presented in a lot of accident analysis reports, but, in this paper, the accident analysis report written by Korean Nuclear Society was used for the reference [23].

The lessons of Fukushima accident presented in accident analysis report were summarized in Table 13.

The last column of Table 13 presents the corresponding sub-precursors discussed in this study. Some of lessons learned could not be matched since this did not include safety culture and emergency response preparedness. However, it was found that majority of lessons belong to four precursors.

If the prior probability of each precursor for Fukushima accident is suitably evaluated, the managerial strategy to improve precursors can be possible on the basis of sensitivity analysis and posterior probability.

None of precursors should be dealt with less carefully. However it is also true that we have only limited amount of

Table 13: Lesson learned from Fukushima accident.

Area	Lesson	Precursors
Enhanced safety system and philosophy	(1) Enhance the defense in depth strategy.	R1
	(2) Considering the loss of life and aspect of social crisis in safety goals.	—
	(3) Independence and expertise of regulatory agencies.	—
	(4) Emphasis the responsibility of the operating agency.	—
Enhance the design of safety for the prevention of severe accidents	(1) Review of the design criteria for natural disaster and improve the response capabilities.	M1, R3, D2
	(2) Enhance the diversity and reliability of the power supply system.	D1
	(3) Enhance passive safety system.	R3, D2
	(4) Actively used risk information in the design and operation.	—
	(5) Enhance and reconfirm the safety features of spent fuel storage tank.	D2, R1
Enhanced ability to respond to severe accidents	(1) Prepare realistic ability to respond to assumed severe accident.	O3, D1
	(2) Improvement of procedures including extreme severe accidents response.	O3, O4, R1
	(3) Enhance nuclear plant condition monitoring.	M2
	(4) Fulfill the best manual and accident response by human creativity.	M2, R1
Enhance emergency response system	(1) Enhance emergency response systems.	—
	(2) Emergency response facilities considering the worsening environment.	—
	(3) Reliable radiation monitoring system and rapid radiation impact assessment.	—
	(4) Medical countermeasures against accidents.	—
	(5) Enhance communication system against accidents.	—
	(6) Thorough management of radiation dose.	—
Enhance safe foundation	(1) Emphasize safety culture.	—
	(2) Enhance safety research.	—
	(3) Efforts to promote understanding of radiation.	—

resource to improve them. Particularly the decisions associated with nuclear safety are likely to go along with public atmosphere. While public acceptance is important, technical safety is distinguished from perceptual safety. When we have to focus on some of measures not all, it is expected that a certain quantitative model can help reasonable decision-making.

4. Conclusions

This paper indicated lack of knowledge during the lifetime of plant as basal precursors of nuclear accidents and selected four precursors and their sub-precursors which are detailed constituents.

Such precursors are inherently difficult to be quantified and their priorities are not visible or clear. So, it was impossible to provide numerical information for enhancing nuclear safety. This paper attempted to overcome these shortcomings by using the BBN model, so that the model enables performing sensitivity analysis for precursors and to recognize precursor's priority by updating posterior probability. We needed many of numerical values for qualitative entities to make up the BBN model, so AHP was used as a support tool.

In general, the "Design" was recognized as the most important precursors. However, the possibility of accidents is strongly dependent on culture-specific, country-specific, and plant-specific conditions. They can affect the distribution of prior probability as well as the NPT. Nevertheless, we tried to elaborate this concept in order to draw coincident and relevant conclusions with other studies of Fukushima accident.

We have to agree that there must be argument in choosing numerical values for the BBN model by virtue of AHP because there are still lots of heuristics in this analysis. Furthermore, the accident management, policy, social aspects, and cost-benefit for each precursor are not fully considered yet. However, this model can reduce the intervention of decision-maker's intuition when they have to determine an important direction on nuclear safety. With improving these

issues, it will be expected to provide a decision-making tool to maximize nuclear safety within limited resources.

Conflict of Interests

The authors declare that there is no conflict of interests regarding the publication of this paper.

Acknowledgments

This work has been supported by Research on Risk-Informed Decision-Making by Multi-Variate Reliability Model project funded by Nuclear Safety and Security Commission (NSSC) (Grant no. 1301024-0113-SB110).

References

[1] Q. Wang, X. Chen, and X. Yi-Chong, "Accident like the Fukushima unlikely in a country with effective nuclear regulation: literature review and proposed guidelines," *Renewable and Sustainable Energy Reviews*, vol. 17, pp. 126–146, 2013.

[2] T. N. Srinivasan and T. S. Gopi Rethinaraj, "Fukushima and thereafter: reassessment of risks of nuclear power," *Energy Policy*, vol. 52, pp. 726–736, 2013.

[3] J. J. Bevelacqua, "Applicability of health physics lessons learned from the Three Mile Island Unit 2 accident to the Fukushima Daiichi accident," *Journal of Environmental Radioactivity*, vol. 105, pp. 6–10, 2012.

[4] M. Zubair, S. Park, and G. Heo, "Prioritization of lesson learned from Fukushima accident using AHP," in *Proceedings of the Transactions of the Korean Nuclear Society Spring Meeting*, Gwangju, Korea, May 2013.

[5] The American Nuclear Society special committee on Fukushima, *Fukushima Daiichi ANS Committee Report*, The American Nuclear Society Special Committee on Fukushima, 2012.

[6] "IAEA International Atomic Energy Agency, atoms for peace," Fukushima Daiichi Status Report, October 2011.

[7] "IAEA International Atomic Energy Agency, atoms for peace," Fukushima Daiichi Status Report, August 2012.

[8] "IAEA International Atomic Energy Agency, atoms for peace," Fukushima Daiichi Status Report, November 2012.

[9] "IAEA international fact finding expert mission of the Fukushima Dai-Ichi NPP accident following the great east Japan earthquake and tsunami," IAEA Mission Report, Department of Nuclear Safety and Security, Division of Nuclear Installation Safety, 2011.

[10] M. C. Kim and I. S. Kim, "Decision analysis based on AHP and GTST methodologies with application to CCF-defense strategies," *Nuclear Technology*, vol. 166, no. 3, pp. 283–294, 2009.

[11] A. Ishizaka and A. Labib, "A hybrid and integrated approach to evaluate and prevent disasters," *Journal of the Operational Research Society*, pp. 1–15, 2013.

[12] A. Ahmed, R. Kusumo, S. Savci, B. Kayis, M. Zhou, and Y. B. Khoo, "Application of analytical hierarchy process and Bayesian belief networks for risk analysis," *Complexity International*, vol. 12, pp. 1–10, 2008.

[13] I. Chivatá Cárdenas, S. S. H. Al-jibouri, and J. I. M. Halman, "A Bayesian belief networks approach to risk control in construction projects," in *Proceedings of the 14th International Conference on Computing in Civil and Building Engineering*, Moscow, Russia, June 2012.

[14] D. J. Lee and J. Hwang, "Decision support for selecting exportable nuclear technology using the analytic hierarchy process: a Korean case," *Energy Policy*, vol. 38, no. 1, pp. 161–167, 2010.

[15] G. Yang, W.-J. Huang, and L.-L. Lei, "Using AHP and TOPSIS approaches in nuclear power plant equipment supplier selection," *Key Engineering Materials*, vol. 419-420, pp. 761–764, 2010.

[16] J. S. Ha and P. H. Seong, "A method for risk-informed safety significance categorization using the analytic hierarchy process and Bayesian belief networks," *Reliability Engineering and System Safety*, vol. 83, no. 1, pp. 1–15, 2004.

[17] J. S. Shin, H. S. Son, and G. Heo, "Cyber security risk analysis model composed with activity-quality and architecture model," in *Proceedings of the International Conference on Computer, Networks and Communication Engineering*, pp. 609–612, 2013.

[18] J. S. Shin, H. S. Son, and G. Heo, "Application of Bayesian network methodology for evaluating industrial control system," *Advanced Science and Technology Letters*, vol. 42, pp. 157–161, 2013.

[19] T. L. Saaty, "Risk—its priority and probability: the analytic hierarchy process," *Risk Analysis*, vol. 7, no. 2, pp. 159–172, 1987.

[20] A. Ishizaka and A. Labib, "Selection of new production facilities with the Group Analytic Hierarchy Process Ordering method," *Expert Systems with Applications*, vol. 38, no. 6, pp. 7317–7325, 2011.

[21] "IAEA International Atomic Energy Agency," Safety Standards Series No. NS-R-1, Safety of Nuclear Power Plants Design, Vienna, Austria, 2000.

[22] D. Heckerman, *A Tutorial on Learning with Bayesian Networks*, 1995.

[23] KNS Committee Report on the Fukushima Accident, *Fukushima Nuclear Power Plant Accident Analysis*, Korean Nuclear Society, 2013.